Strong zero Modes in Generalized Spin chains and Topological Quantum Computation

Domenico Pellegrino
M.Sc.

Thesis presented for the degree of

Doctor of Philosophy

to the

National University of Ireland Maynooth

Department of Theoretical Physics

November 2019

Department Head

Prof. Peter Coles

Research advisor

Dr. J. K. Slingerland

In the end she made it...
she spoke as softly as she could...
"Work hard my dear little Ferdinand!" she whispered...
I wasn't afraid of her.
We understood each other deep down...
The fact is that I have worked hard, all in all...

Louis-Ferdinand Céline, *Death on Credit*

Contents

Declaration

I declare that this thesis has not been submitted in whole, or in part, to this or any other university for any other degree and is, except where otherwise stated, the original work of the author.

Domenico Pellegrino, 26 November 2019

Acknowledgements

It is late and I am in my bed; down in Gardiner Street the cars are passing by and I can hear their dull, idle, grumbling. They never stop. Here it is one... now another one.
They light up the ceiling of my bedroom as they go, like scattered shooting stars. I close my eyes and I start thinking. Tomorrow I will finally submit my thesis. I didn't think I could make it. More than once I was on the verge of quitting and only time will tell if I made the right choice by deciding to stay.
So many people assisted me during this strange journey. I would like to list and thank them all.

First of all I should thank Joost Slingerland, my supervisor. He gave me the opportunity to start this difficult, but hopefully rewarding path. I have to thank him for his understanding, readiness and willingness to help me whenever I was in need.
I should thank Graham and Niall, that warmly welcomed me in their research group when I first arrived and allowed me to help them with their work. I am really grateful to them.
I should also warmly thank Stephen and Paul, who shared the office with me and inspired me with countless stimulating and useful discussions.
Obviously I have to thank Aaron and Kevin; with Aaron I shared the joy of some research work and with both I shared many beautiful moments. With great simplicity and true cordiality they accepted me as a friend and all the pints and the cigarettes and the laughs together, helped me to overcome more difficulties and hard times than they might imagine.
I should thank Una, John, Aoife, Darragh, Mikael, Aonghus, Goran, Phil, Babatunde and all the other students, that made the department a great and friendly place to work.
I am also grateful to Monica Harte, Suzie Duffy and Jon-Ivar Skullerud for their hard work and dedication in running the department.
Who else? Well for sure I need to thank Shane, Luke, Ian, all the staff and the professors in DIAS, as they put up with me and provided me with a desk and a nice working place all the times that I stayed there.
I am thankful to all the Italian friends that I met in Dublin, Manfredi, Vincenzo,

Claudio, Damiano, Daniela, Yasir, Franceso and Billy. They made me feel at home every time and made my life in a foreigner country a lot easier.

Who I am missing in my list? I do not know. There are so many people that I met along the way, so many that I cannot even count. Some are still with me, others left me already and ended up who knows where. They're like the characters of a play after that the curtains have closed. You can still hear their voices and see their faces, but they're gone. The lives you shared and your moments together are gone as well; they're wrapped, twined inextricably in space and time, just like you. They're far away, but still so near. If you stretch out your hand, you might almost catch them, like when as a kid I used to pick cherries with my siblings. I can see that. The sun is high and the sky is so blue that you can risk getting lost in it. Marica and Giuseppe are with me. My sister is keeping the bucket down the tree and me and my brother are climbing up, collecting the juicy, fragrant, rubies. My brother is more daring than me and climbs higher on the boughs.
My family is waiting for us. Lunch is almost ready... Here we go. Mom is calling us. We get down the tree and walk towards home. The cicadas, meanwhile, creak their incessant, monotonous song.
As we go back we start play, using the cherries that we picked as earrings, necklaces and bracelets. They are beautiful jewelries and we are two princes and a princess striding along the roads of the citadel. The lizards run away as we go; they go hide under broken bricks and silently spy us from there.
We enter the house and go upstairs. My parents are already sat at the table. My aunt, my uncle and my grandparents are joining us for lunch. The telly is on and it is babbling something that I do not remember, but it's not important. We sit down and start eating, while we talk and laugh about something that I do not remember, because it's not important. My mom smiles and the pasta tastes great, better then ever. I feel safe, I feel home and this is very important...

I wake up. I am still in my room and the cars are still passing by, down in Gardiner Street. They light up the ceiling of my bedroom like idle, scattered, shooting stars. I turn around and you are still sleeping beside me. You're still there, with all your light and your warmth, with all the kindness that you have always given me. To me that have never asked for it. To me that never deserved it. I do not wake you up. Your slumber is important and your dreams are precious like spring dawns.
I need to sleep as well. Tomorrow I will have to submit this thesis. I close my eyes and I feel my consciousness fading away. I let it go. No worries, it will rouse up anew tomorrow morning, like it always did and like will always do, again and again and again and again... till the end.

Abstract

Part of the interest in topological phases of matter stems from their potentially revolutionary technological applications. One of the most exciting possibilities would be the ability to store and manipulate quantum information in topological degrees of freedom. This information would be intrinsically protected from some local error processes and there are now significant efforts being made to harness this property in scalable quantum devices. In this context, we numerically investigate the dynamical evolution of a topological memory that consists of two p-wave superconducting wires separated by a non-topological junction. We consider a closed system and do not consider general types of errors that may arise from the interaction of the system with an external environment. We therefore consider the best case scenario apt to quantum computation and expand upon existing knowledge on the subject. We find that non-adiabatic effects associated with processing and storing quantum information, might be relevant as a source of errors in spite of the topological protection of the quantum qubit. In particular we focus on the primary source of errors (i.e., qubit-loss) and on secondary errors (bit and phase-flip) and provide physical reasoning behind how these types of errors may take place.

Further we consider model for more exotic quantum wires, the so-called Z_N parafermionic clock models that are also expected, in varying degrees, to possess topological protection. We analyze in detail when this protection might take place and provide an iterative construction of the associated zero-energy parafermionic modes. The method, outlined in this thesis, summarizes and generalizes existing methods for constructing zero modes in spin chains and enlightens common surprising features of these types of constructions. This opens up the way for future research on the subject.

Chapter 1

Introduction

Topological phases of matter represent an exciting and fast developing subject of research. Much of the interest in the study of these types of phenomena arise from the fact that they represent a possible promising way towards scalable, fault-tolerant, quantum computation [1, 2].

Roughly speaking the topological properties of the phases of a system can be described in terms of the so called quantized topological invariants. This quantization directly implies that these invariants cannot abruptly jump when we smoothly change the system, for example by means of local perturbations.
In this sense and in what follows we will consider Hamiltonians that are spectrally gapped, local and at zero temperature. The requirement on the gap is needed in order to be able to talk about adiabatic transformations without ambiguities, while the requirement on locality is needed in order to be able to differentiate between systems with different dimensions. The locality condition comes from physical considerations and also from the fact that, if we were not to impose locality, every system could in principle be zero dimensional. The requirement on the temperature implies that we will be mostly interested in the behaviour of the ground state of the system.
These properties allow considering two systems topologically equivalent, if they can be connected via an adiabatic transformation: two gapped ground states are considered in the same phase if there exists an adiabatic interpolation connecting the two Hamiltonians from which they descend, without breaking up locality and without closing the gap [3, 4].

When talking about topological order we further have to make a distinction between intrinsic topological order and non-intrinsic one [5].
Generally, we speak of intrinsic topological order if the system is compatible with the existence of low-energy excitations which are point-like (in two dimensions 2D or above) or line-like (in three dimensions 3D or above). These excitations carry fractional quantum numbers as compared to the microscopic degrees of freedom that enter the Hamiltonian (as, for example, a fractional charge) and are free to move

in the low energy excitation space. An example of this type of topological order is constituted by the toric code [2] and these excitations are usually referred to as (2D) anyons [2, 6].
This definition implies that, strictly speaking, there is no intrinsic topological order in 1D.

Most of the systems without intrinsic topological order need a symmetry in order to enforce topological protection of the topological invariant. By this we mean that, in order to be able to talk about the topological phases of a system, we have to restrict the possible Hamiltonians to those that commute with some set of symmetries and restrict the adiabatic transformations that connect topologically equivalent Hamiltonians to those that act on this same restricted space.
These phases of matter are usually referred to as Symmetry Protected Topological phases (SPT) and contrary to the intrinsic topological ones do not possess long-range entanglement. These phases, almost always, possess topologically protected boundary modes when defined on a manifold with boundary, which are intimately connected to the bulk properties of the system. Often these modes present fractionalized quantum numbers, but are "tied" to the boundary separating different phases, which makes them different from the anyonic excitations that define intrinsic topological order.
The connection between the topological properties of the bulk and the presence of boundary modes sitting at the edge of the system is usually referred to as bulk-boundary correspondence [3, 4, 7].

The SPT phases of systems of free fermions are completely classified and tabulated. This is shown in Table 1.1.

	T	C	S	$d=1$	$d=2$	$d=3$	$d=4$	$d=5$	$d=6$	$d=7$	$d=8$
A	0	0	0	$\varnothing$	$\mathbb{Z}$	$\varnothing$	$\mathbb{Z}$	$\varnothing$	$\mathbb{Z}$	$\varnothing$	$\mathbb{Z}$
AIII	0	0	+1	$\mathbb{Z}$	$\varnothing$	$\mathbb{Z}$	$\varnothing$	$\mathbb{Z}$	$\varnothing$	$\mathbb{Z}$	$\varnothing$
AII	−1	0	0	$\varnothing$	$\mathbb{Z}_2$	$\mathbb{Z}_2$	$\mathbb{Z}$	$\varnothing$	$\varnothing$	$\varnothing$	$\mathbb{Z}$
DIII	−1	+1	+1	$\mathbb{Z}_2$	$\mathbb{Z}_2$	$\mathbb{Z}$	$\varnothing$	$\varnothing$	$\varnothing$	$\mathbb{Z}$	$\varnothing$
D	0	+1	0	$\mathbb{Z}_2$	$\mathbb{Z}$	$\varnothing$	$\varnothing$	$\varnothing$	$\mathbb{Z}$	$\varnothing$	$\mathbb{Z}_2$
BDI	+1	+1	+1	$\mathbb{Z}$	$\varnothing$	$\varnothing$	$\varnothing$	$\mathbb{Z}$	$\varnothing$	$\mathbb{Z}_2$	$\mathbb{Z}_2$
AI	+1	0	0	$\varnothing$	$\varnothing$	$\varnothing$	$\mathbb{Z}$	$\varnothing$	$\mathbb{Z}_2$	$\mathbb{Z}_2$	$\mathbb{Z}$
CI	+1	−1	+1	$\varnothing$	$\varnothing$	$\mathbb{Z}$	$\varnothing$	$\mathbb{Z}_2$	$\mathbb{Z}_2$	$\mathbb{Z}$	$\varnothing$
C	0	−1	0	$\varnothing$	$\mathbb{Z}$	$\varnothing$	$\mathbb{Z}_2$	$\mathbb{Z}_2$	$\mathbb{Z}$	$\varnothing$	$\varnothing$
CII	−1	−1	+1	$\mathbb{Z}$	$\varnothing$	$\mathbb{Z}_2$	$\mathbb{Z}_2$	$\mathbb{Z}$	$\varnothing$	$\varnothing$	$\varnothing$

Table 1.1: Periodic table of topological insulators and superconductors. The second column lists the different possible symmetry classes under T, C and S. These symmetry may be not present, in which case there is a 0, or may be present, in which case we have a ± 1 with respect to the value taken by T^2 and C^2. The first column lists the names given to the different symmetry classes. They come from the Cartan classification of the complete set of the ten large symmetric spaces, of which the quantum mechanical time-evolution e^{itH} is an element. The third part of the table lists the possible topological phases for the different dimensions.

This table considers the symmetry protected classes under time reversal T, charge conjugation C and chiral symmetry $S = TC$. The first two symmetries are realized by antiunitary operators that can square either to +1 or -1. Whenever these symmetries are present and square to +1 (-1), in the respective columns we write +1 (-1). When the symmetry is absent we write 0.
The chiral symmetry S is a unitary operator (as can be checked from its definition) and the behaviour of the theory under it is fixed from the behaviour under T and C, except when $T = 0$ and $C = 0$. In fact the system can be symmetric under S even when it is not symmetric under T and C separately. It is not difficult to convince oneself that there are only 10 possible classes of symmetry and this is known as the Altland-Zirnbauer 10-fold way [8, 9].

The first two rows of the table are called complex classes, while the rest are called real classes. The group of topological phases that a Hamiltonian in a given symmetry class *can* belong to, are listed for the different spatial dimension d (with $\varnothing$ we indicate that the unique possible topological phase is the trivial one). This table is obtained by looking at the homotopy classes of different types of free fermion Hamiltonians using the algebraic properties of the Clifford algebra. In mathematics this goes under the name of K-theory [10][1].

The homotopy groups of the complex classes have a periodicity of 2 in d, while the real classes have a period of 8. This is usually known as Bott periodicity and, for this reason, this table is often referred to as periodic table of topological insulators and superconductors. The classification of SPT phases for interacting fermions is still subject of current research [12, 13].

As we said, in one dimensional systems, the presence of an SPT phase is usually signalled by the appearance of boundary modes at the edge of the system. These modes are generally gapless, or zero energy, and for this reason they are referred to as zero modes. In the Ising/Kitaev chain there are two such modes, that behave like Majorana fermions [14]. This observation has lead to great interest because in the gapped topological phase the two ground states can be used as a qubit space. Transitions between the two different ground states can only happen via processes that add or remove electrons from the system. Since transitions to the excited states are precluded by the gap and since the degrees of freedom are localised at the opposite edges of the system, local noise in the middle of the wire cannot induce transitions between the different ground states. This makes this type of system the ideal candidate for a decoherence-free quantum computer [15].

Even though the potential technological applications of systems in SPT phases regards the properties of the ground state, in the Ising/Kitaev chain, the presence of zero modes has consequences for all the eigenstates of the system. In fact, the

[1]Another approach consists in looking at the theory of Anderson localization of the degrees of freedom at the boundary, and determining which dimensions can host surface states that are not localized for a given symmetry class [11].

existence of operators that commute with Hamiltonian (but do not commute with the fermion parity), implies the existence of a double degeneracy throughout all the spectrum. In this sense, the presence of this type of zero modes constitute an example of eigenstate phase transition [16, 17] and a violation of the Eigenstate Thermalization Hypothesis (ETH) [18, 19]. In order to emphasise this aspect of the story this type of zero modes are usually referred to as "strong zero modes" [20, 21, 22], as opposed to "weak zero modes", which are operators that commute only with the Hamiltonian projected into a low-energy subspace and therefore provide the minimal degeneracy that is generally necessary for a topological phase. The presence of strong zero modes is also responsible for long coherence time for the edge spins [23, 24] and is connected to the problem of prethermalization [25].

In this thesis, we will consider some of the aspects of SPT phases in 1 dimension and we will analyse some of the problems related to the existence of strong zero modes.

An outline of the thesis is as follows.

In Chapter 2 we review the quantum Ising model. We will see that this model can be connected to a system of free fermions hopping on a chain and we will therefore illustrate the concept of symmetry protected topological phases for this specific case. In particular, we will see how the topological phase is connected to the existence of gapless Majorana zero modes at the boundary of the system.

In Chapter 3 we will review more general types of fermionic wires and we will make connections to the experimental realizations of the Kitaev chain, which can be realized as a spinless p-wave superconductor. Subsequently, we will illustrate how to exploit the existence of Majorana zero modes and the resulting degeneracy of the ground state to perform Topological Quantum Computation.

In Chapter 4 we will review the results about numerical analysis conducted on a toy model for a qubit made out of Majorana zero modes. Principally we will consider how non-adiabatic effects of the time evolution of the system can introduce errors in the computational space. Notably, we will consider the problem of qubit loss, phase-flip errors and bit-flip errors and we will show how these types of errors depend on the existence of stray excitations running in the bulk of the system.

In Chapter 5 and 6 we will consider the topological phases of generalized spin chains. In particular we will consider the so called $\mathbb{Z}_N$ quantum clock models, which similarly to the Ising case can be connected to a system of Parafermions living on a chain. We will carefully consider the cases in which parafermionic zero modes exist at the boundary of the system and we will introduce concepts that are relevant when one considers the topological phases of such systems. Specifically, we will introduce the total domain wall angle parity, defined for the bands of the free theory, whose conservation is essential for the existence of the strong zero modes.

In Chapter 7 we will see how to explicitly construct such zero modes and we will

clarify the role played by the total domain wall parity in the existence of zero modes. We will show that the total domain wall parity is connected to the local properties of the terms entering in the expansion of the zero mode in powers of the perturbing parameter.
This construction readily extends to more general spin chains, which share common interesting features with the parafermionic case.

In Chapter 8 we draw our conclusions and indicate some directions for further research.

Regarding the content of the various chapters, the material contained in Chapter 2 and Chapter 3, except when explicitly stated, is introductory review material. The other chapters are based on the following publications, coauthored by the author of this thesis:

[26] A. Conlon, D. Pellegrino, J. K. Slingerland, S. Dooley and G. Kells, **Error generation and propagation in Majorana-based topological qubits**, *Physical Review B*, 100:134307, October 2019.

[27] N. Moran, D. Pellegrino, J. K. Slingerland and G. Kells. **Parafermionic clock models and quantum resonance**. *Physical Review B*, 95:235127, June 2017.

[28] D. Pellegrino, G. Kells, N. Moran and J. K. Slingerland. **Constructing edge zero modes through domain wall angle conservation**. *arXiv e-print*, page arXiv:1908.03459, August 2019 (under publication).

The material contained in [26] is reviewed in Chapter 4. Chapter 5 and Chapter 6 are based upon [27]. Chapter 7, instead, contains a review of [28].

Chapter 2

Ising Model and Majorana Zero Mode

In this section we will introduce concepts that will be relevant for the rest of the thesis. In particular, will introduce the concept of strong zero mode. In reviewing the quantum Ising chain we will follow [21] and we will see how this model connects with the Kitaev chain [14] and with topology.

2.1 Quantum Ising model

The Ising model was first introduced [29] to describe ferromagnetism. In the following we will concentrate on the one dimensional version of the model. We begin by writing down the quantum Hamiltonian of the model. Consider a chain of spin $\frac{1}{2}$ atoms of length L. The Ising Hamiltonian is given by

$$H = -\sum_{i=1}^{L-1} J\sigma_i^z\sigma_{i+i}^z - \sum_{i=1}^{L} f\sigma_i^x \tag{2.1}$$

where σ_i^a are Pauli matrices at site j, J corresponds to the interaction between nearest neighbor spins and f describes an external magnetic field along the x direction. The Hilbert space can be described in terms of the basis

$$|j_1, j_2, \ldots, j_L\rangle \tag{2.2}$$

where $j_i = 0, 1$ is the value of the spin along the z axis at site i. By convention we will suppose that $j_i = 0$ corresponds to spin down and $j_i = 1$ to spin up.

This Hamiltonian has an evident $\mathbb{Z}_2$ symmetry that corresponds to the simultaneous flipping of all the spins on the chain. We can describe this symmetry through the parity operator Q_2

$$Q_2 = \prod_{i=1}^{L} \sigma_i^x \tag{2.3}$$

This model has a phase transition at $T = 0$, which is, therefore, a quantum phase transition [30]. There are no other phase transitions, as it is well known that there are no phase transitions in one dimension for non zero temperature [31]. The critical point is at $J = f$. The ordered phase corresponds to the case $J > f$, while the disordered phase corresponds to $J < f$. This can be easily seen in the extreme cases of large nearest neighbor coupling ($J \gg f$) and large magnetic field ($J \ll f$). In the first case, the ground state is two-fold degenerate and it is constituted by states with all spins up or all spins down $|0, 0, \ldots, 0\rangle$ or $|1, 1, \ldots, 1\rangle$ respectively. In the second case, the ground state is instead unique and the spins are all aligned along the positive x direction.
The magnetization, defined as

$$M = \sum_i \langle \sigma_i^z \rangle \ , \tag{2.4}$$

constitutes the order parameter and can be used to identify the phase transition. In particular, $M = 0$ in the disordered phase and $M \neq 0$ in the ordered phase.

This simple model, used to describe ferromagnets, can be rephrased into a completely different shape and can be used to describe fermions hopping on a chain, which in turn can be used to characterize metals and insulators. This rephrasing can be done through the so called Jordan Wigner transformation [30, 32] we therefore introduce two new operators per site

$$\begin{aligned} c_i &= \frac{1}{2} \left(\prod_{j=1}^{i-1} \sigma_j^x \right) (\sigma_j^z - i\sigma_j^y) \\ c_i^\dagger &= \frac{1}{2} \left(\prod_{j=1}^{i} \sigma_j^x \right) (\sigma_j^z + i\sigma_j^y) \ . \end{aligned} \tag{2.5}$$

It can be easily seen that c_j, $c_j^\dagger$ satisfy the fermionic commutation relation

$$\{c_i, c_j\} = \{c_i^\dagger, c_j^\dagger\} = 0 \qquad \{c_i, c_j^\dagger\} = \delta_{ij} \ . \tag{2.6}$$

and they are therefore fermionic operators that annihilate or create a spinless fermion at site j. We can now invert (2.5) and use these identities to rewrite the Hamiltonian in terms of c_j and $c_j^\dagger$. The substitution gives

$$H = \sum_j -J(c_j^\dagger c_{j+1} + c_{j+1}^\dagger c_j + c_{j+1} c_j + c_j^\dagger c_{j+1}^\dagger) + 2f c_j^\dagger c_j - f \tag{2.7}$$

Taking ideas coming from quantum field theory one can formally define Majorana,

self adjoint operators, as "half" fermions

$$\begin{aligned} a_j &= c_j + c_j^\dagger \\ b_j &= \frac{c_j - c_j^\dagger}{i} \ . \end{aligned} \tag{2.8}$$

Using (2.5) it is straightforward to see that Majorana operators follow the commutation relations

$$\{a_i, a_j\} = \{b_i, b_j\} = 2\delta_{ij} \qquad \{a_i, b_j\} = 0 \ . \tag{2.9}$$

and, in terms of Majorana operators, the Hamiltonian (2.1) takes the form

$$H = iJ \sum_{j=1}^{L-1} b_j a_{j+1} + if \sum_{j=1}^{L} a_j b_j \ . \tag{2.10}$$

Let's now consider the symmetry operator Q_2. The Hamiltonian (2.7) contains terms that do not conserve the fermions number

$$N_F = \sum_{j=1}^{L} c_j^\dagger c_j \ . \tag{2.11}$$

In fact, $c_j c_{j+1}$ and $c_j^\dagger c_{j+1}^\dagger$ do not commute with N_F. Since these operators can only change the number of fermions by 2 units, this means that even though the number operator is not conserved, it is still conserved modulo 2. In terms of the fermionic operators, Q_2 therefore describes conservation of fermionic number modulo 2 and in fermionic terms, Q_2 can be written as

$$Q_2 = \prod_{j=1}^{L} (-i a_j b_j) = (-1)^{N_F} \ . \tag{2.12}$$

For this reason Q_2 is sometimes referred to as the *fermion parity* operator. As a consequence of this $\mathbb{Z}_2$ conserved charge, we have that the spectrum splits into two sectors of distinct parity.

2.2 Strong zero modes

We will now show the presence, in the fermionic model described above, of zero energy modes that characterize the topological order. Let's first define what is meant by a strong zero mode.

A strong zero mode is an operator ψ that commutes with the Hamiltonian in the thermodynamic limit

$$[H, \psi] = O(e^{-\frac{L}{\xi}}) \ , \tag{2.13}$$

where $\xi > 0$ some constant length scale which can also be $+\infty$. This means that

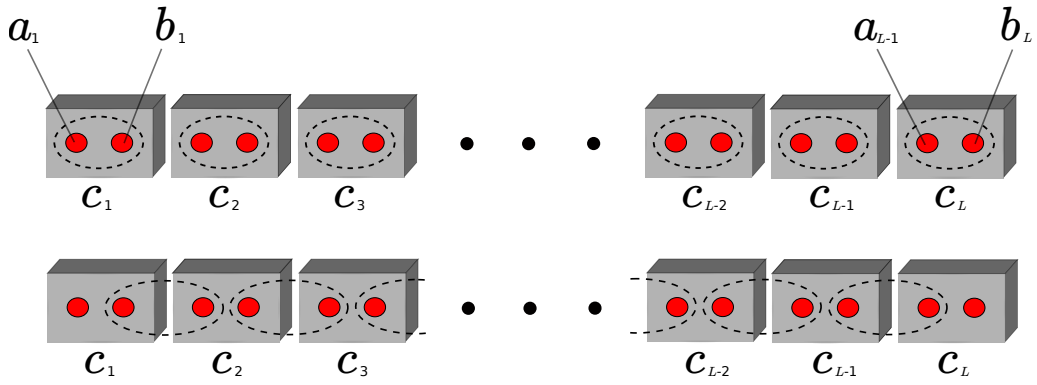

Figure 2.1: The upper figure represents the chain in the completely dimerized, trivial, limit. In dashed lines we represent the interaction between nearest neighbor Majorana operators. The lower figure represents the chain in the opposite topological regime (always in dashed lines we represent the next neighbor interaction). At the end of the chain we can see the two unpaired Majorana.

ψ commutes up to terms that go exponentially to zero in the limit $L \to \infty$. The other relation defining the zero mode regards the relationship between ψ and the symmetry operator Q_2. In particular we require ψ to map a state in a parity sector into a state with opposite parity, that is to say

$$Q_2\psi = -\psi Q_2. \tag{2.14}$$

In order for this operator to exist in the thermodynamic limit, the zero mode has to keep a well defined normalization in the limit $L \to \infty$ (which without loss of generality we can consider to be 1) and we demand that it will be a unitary operator in this limit

$$\psi^\dagger\psi = 1 + O(e^{-\frac{L}{\xi}}) \ . \tag{2.15}$$

Such a zero mode is called an edge zero mode if, additionally, it is localised at the edge of the chain, in the sense that the dependence of ψ on operators that act on sites at distance l from the edge is exponentially small in l.

The existence of a strong zero mode implies that the spectrum of the model is at least doubly degenerate. Suppose in fact $|E\rangle$ to be a state with energy E. Using the definition of a zero mode then we have

$$H\psi|E\rangle = \psi H|E\rangle = E\psi|E\rangle \tag{2.16}$$

and we can be sure that $|E\rangle \neq \psi|E\rangle$, since $|E\rangle$ and $\psi|E\rangle$ have different parities. If this zero mode is confined near the edge of the system the lowest doublet can in principle be used to encode information and to perform topological quantum computation, as we will see in Chapter 3.

The Ising model possesses an edge zero mode, as we will now see by explicit construction. Let's consider the limit $J = 0$ first. In this limit the Hamiltonian

becomes

$$H = if \sum_{j=1}^{L} a_j b_j \ . \tag{2.17}$$

This situation is referred to as the *topologically trivial* limit and this case is depicted in the upper Figure 2.1. The opposite limit is $f = 0$, in which case the Hamiltonian becomes

$$H = iJ \sum_{j=1}^{L-1} b_j a_{j+1}. \tag{2.18}$$

It is evident from H that the operators a_1 and b_L now commute with H. This is trivially true as these operators do not appear in the sum and commute with any bilinear combination of Majorana operators. Moreover

$$a_1^2 = b_L^2 = 1 \tag{2.19}$$

and also

$$a_1 Q_2 = -Q_2 a_1 \qquad b_L Q_2 = -Q_2 b_L. \tag{2.20}$$

This means that these two operators constitute edge zero modes for the system, as they are trivially localised on the edges. This situation is shown in the lower half of Figure 2.1 and is referred to as the *non-trivial topological* limit. Note that, in terms of Pauli matrices, a_1 and b_L are

$$a_1 = \sigma_1^z \qquad b_L = Q_2 \sigma_L^z \tag{2.21}$$

When $J \neq 0$ and $f \neq 0$ the situation is more complicated, but the zero modes still exists as long as $f < J$, as we will now show.
Since we are dealing with free fermions, the zero mode can be easily computed by direct means. It is physically reasonable to expect that in the limit $f \to 0$ the zero modes ψ_1 and ψ_L would reduce to a_1 and b_L respectively. Supposing this to be true we can try to find the zero mode by an iterative construction.

Consider the commutator of (2.10) with a_j and b_j, $1 < j < L$ we have, using (2.9)

$$\begin{aligned} [H, a_j] &= [iJb_{j-1}a_j + ifa_j b_j, a_j] = 2iJb_{j-1} - 2ifb_j \\ [H, b_j] &= [iJb_j a_{j+1} + ifa_j b_j, b_j] = -2iJa_{j+1} + 2ifa_j \end{aligned}$$

and for a_1 and b_L we have

$$\begin{aligned} [H, a_1] &= -2ifb_j \\ [H, b_L] &= 2ifa_L \ . \end{aligned} \tag{2.22}$$

From these relations we can see that it is possible to find terms that, starting from

a_1 and b_L, run deeper into the chain and that gradually remove the b_{j-1} and a_j. Considering the left mode we have

$$\begin{aligned}
&[H, a_1] = -2if b_1 \\
&[H, a_1 + \frac{f}{J} a_2] = -2if \left(\frac{f}{J}\right) b_2 \\
&[H, a_1 + \frac{f}{J} a_2 + \left(\frac{f}{J}\right)^2 a_3] = -2if \left(\frac{f}{J}\right)^2 b_3 \\
&[H, a_1 + \frac{f}{J} a_2 + \left(\frac{f}{J}\right)^2 a_3 + \left(\frac{f}{J}\right)^4 a_4] = -2if \left(\frac{f}{J}\right)^3 b_4 \\
&\dots
\end{aligned}$$

and similarly for b_L. The good candidates for our edge zero modes are therefore given by

$$\psi_{left} = a_1 + \frac{f}{J} a_2 + \ldots + \left(\frac{f}{J}\right)^{L-1} a_L \qquad \psi_{right} = b_L + \frac{f}{J} b_{L-1} + \ldots + \left(\frac{f}{J}\right)^{L-1} b_1 \quad (2.23)$$

and in a chain of length L the commutators with H are

$$[H, \psi_{left}] = -2if \left(\frac{f}{J}\right)^{L-1} b_L \qquad [H, \psi_{right}] = 2if \left(\frac{f}{J}\right)^{L-1} a_1 \ . \quad (2.24)$$

When $f < J$ these operators commute with the Hamiltonian in the limit $L \to \infty$ and are localised on the edges by construction.

Since these operators are made out of linear combinations of a_j and b_j it is also trivially true that

$$Q_2 \psi_{left} = -\psi_{left} Q_2 \qquad Q_2 \psi_{right} = -\psi_{right} Q_2 \ . \quad (2.25)$$

In order to prove that ψ_{left} and ψ_{right} are edge zero modes we only need to prove that they have a finite normalization in the limit $L \to \infty$. For ψ_{left} we have

$$\psi_{left}^\dagger \psi_{left} = \psi_{left}^2$$

because Majorana operators are self adjoint and therefore

$$\psi_{left}^\dagger \psi_{left} = \sum_{j=2}^{2L} \left(\frac{f}{J}\right)^j \sum_{k=1}^{j-1} a_{j-k} a_k \ .$$

Since Majorana operators on different sites anticommute, the only terms that will survive in this sum are the perfect squares, therefore we are left with

$$\psi_{left}^\dagger \psi_{left} = 1 + \left(\frac{f}{J}\right)^2 + \left(\frac{f}{J}\right)^4 + \ldots + \left(\frac{f}{J}\right)^{2(L-1)} = \frac{1 - (\frac{f}{J})^{2L-1}}{1 - \frac{f}{J}} \quad (2.26)$$

which shows that when $f < J$ the normalization of the zero mode is well defined and (2.15) can be satisfied by renormalizing (2.23).

Before continuing our discussion let's stop for a moment to consider what we have done. We started with a spin model presenting a phase transition and we have changed it into another model in which the phase transition of the original one is now signalled by the appearance, persisting throughout the phase, of two zero modes sitting on the edge of the system. Is this still a phase transition? Obviously, the zero modes are present also in the original model but, as we saw earlier in the section, in the Ising model we can describe the phase transition through a local order parameter (the magnetization). Because of the Jordan-Wigner transformation this quantity is now non-local in terms of fermions and this means that the information about the phase transition is somehow "spread" along the wire. From a physical point of view, this means that there is no local order parameter describing the change in the phase of the system and therefore we cannot use the usual Landau-Ginzburg theory to describe it [31]. Since the properties we are considering are not local, the structure of this new phase of matter is largely independent of the local properties of the model. In this sense these types of properties are said to be topological (more correctly they are symmetry protected topological [33]).

2.3 What about Topology?

In this section we will try to give some intuition behind how topology enters into play in what we said before. The following material is loosely based on [7] and we refer there for a more detailed exposition.

Like every solid-state system, the Hamiltonian (2.7) has a boundary part and a bulk part. The bulk part corresponds to the central part of the chain, while the boundary corresponds to the edges. Since the bulk part constitutes the largest part of the system it is reasonable to expect that the physical properties of the system are determined by its behavior. The physics of the bulk states should be largely independent of what happens to the edges and in order to keep the study of the bulk simple, it is natural to use periodic boundary conditions. When the system is periodic, the momentum is a good quantum number and we are allowed to take the Fourier transform, defining operators that create fermions with definite momentum k

$$c_k = \frac{1}{\sqrt{L}} \sum_{j=1}^{L} c_j e^{ikj} \qquad c_k^\dagger = \frac{1}{\sqrt{L}} \sum_{j=1}^{L} c_j^\dagger e^{-ikj} \tag{2.27}$$

with k in the first Brillouin zone. Using this definition and the identity

$$\frac{1}{L} \sum_{j=1}^{L} e^{i(k-k')j} = \delta_{k,k'} \tag{2.28}$$

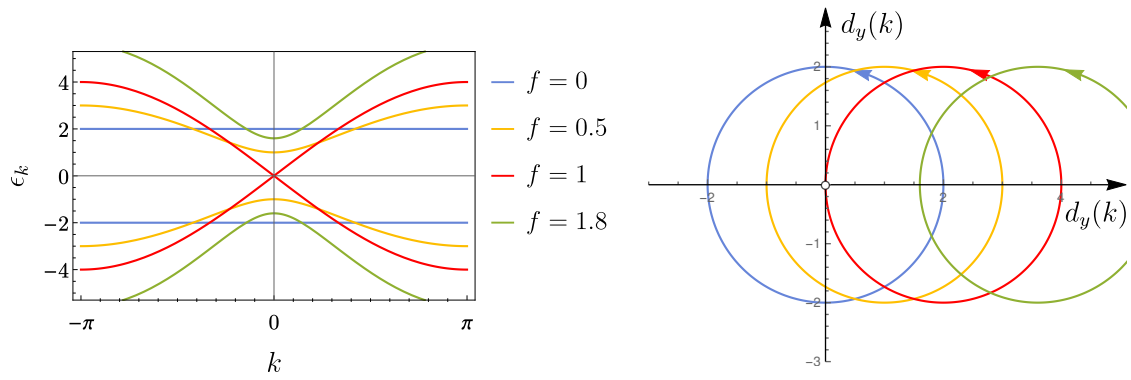

(a) (b)

Figure 2.2: In (a) we show the one particle spectrum $\pm\epsilon_k$ for different values of f and fixed $J = 1$. It can be seen that the gap closes at $f = J$. In Figure (b) we show the $\mathbf{d}$ vector for $k \in [0, 2\pi]$

it can be proved that c_k, $c_k^\dagger$ follow fermionic commutation relations and we can rewrite the Hamiltonian (2.7) as

$$H_{bulk} = \sum_k 2(f - J\cos k)c_k^\dagger c_k - Ji\sin k(c_{-k}c_k + c_{-k}^\dagger c_k^\dagger) - fL \tag{2.29}$$

or, in more concise form

$$H_{bulk} = \frac{1}{2}\sum_k \mathbf{C}_k^\dagger H_k \mathbf{C}_k - fL\ .$$

where $\mathbf{C}_k = \begin{pmatrix} c_k \\ c_{-k}^\dagger \end{pmatrix}$. H_k constitutes the single particle Hamiltonian of the system and in the present case it can be written as

$$H_k = d_z(k)\sigma^z + d_y(k)\sigma^y \tag{2.30}$$

with σ^z and σ^y Pauli matrices (not to be confused with the spin Pauli matrices) and

$$d_z(k) = 2(f - J\cos k) \qquad d_y(k) = 2J\sin k\ . \tag{2.31}$$

In this form we can easily diagonalise H_k and define new variables γ_k by

$$\begin{pmatrix} \gamma_k \\ \gamma_{-k}^\dagger \end{pmatrix} = \mathcal{U}\begin{pmatrix} c_k \\ c_{-k}^\dagger \end{pmatrix} \tag{2.32}$$

where $\mathcal{U}$ is the unitary matrix diagonalising H_k

$$\mathcal{U}^\dagger H_k \mathcal{U} = \begin{pmatrix} \epsilon_k & 0 \\ 0 & -\epsilon_k \end{pmatrix} \tag{2.33}$$

with single particle energies given by

$$\epsilon_k = 2\sqrt{J^2 + f^2 + 2fJ\cos k}\ . \tag{2.34}$$

The matrix $\mathcal{U}$ is usually referred to as a Bogoliubov transformation [30] and it is easy to show that, since it is unitary, γ_k and $\gamma_k^\dagger$ satisfy the usual anticommutation relations. These new fermionic operators are the creation and annihilation operators of the excitations of the system, which are usually referred to as quasiparticles. The many body energy band is determined by a sum of such single particle energies over the allowed k and the gap between the conduction band and the valence band is therefore determined by ϵ_k.

In Figure 2.2(a) we show the behaviour of $\pm\epsilon_k$ for different values of f and fixed J. In particular, we see that the gap closes at $f = J$ and $k = \pi$. This means that while the system is an insulator for $f < J$ it becomes a conductor when $f = J$, as electrons in the valence band can move freely into the conduction band. In particular we note that the dispersion around $k = \pi$ is linear in k. In Figure 2.2(b) we show the behaviour of the vector $\mathbf{d} = (d_z(k), d_y(k))$ as k goes from 0 to 2π. This vector describes a circle of radius $2J$ centered in f. In more general 2 band insulators this curve needs not to be a circle, but would still be a closed curve avoiding the origin, as we imposed periodic boundary conditions. Considering Figure 2.2(b) we can now see that the phases $f < J$ and $f > J$ are topologically distinct. In particular it is impossible to connect continuously the two different regimes without closing the gap.

More physically this means that the qualitative properties of the system are largely independent of the exact shape of $\mathbf{d}(k)$ and that they cannot be changed by local (that is to say continuous) perturbations that do not close the gap. In this sense the phase of the system we are studying is said to be topological.

The topology of the different loops can be characterized by the number times $\mathbf{d}$ winds around the origin as k runs through the Brillouin zone. In the present case this number is 0 for $f > J$, 1 for $f < J$ and undetermined for $f = J$. This winding number is a topological invariant and is called the *Chern number* of the system. The interested reader can find more details about the subject in [4].

Let's now go back to consider the edges of the chain. As we saw, in the topological regime, the system will develop two zero modes localised at the edges. This is indeed a general property of the system and is a manifestation of the non trivial topological properties of the bulk. Zero modes, in fact, are usually localised around the boundaries that separate different phases of the system or at its physical edges. To understand the point consider a linear expansion of H_k around the point where the gap closes

$$H_k \simeq \mu\sigma^z + vk\sigma^y \tag{2.35}$$

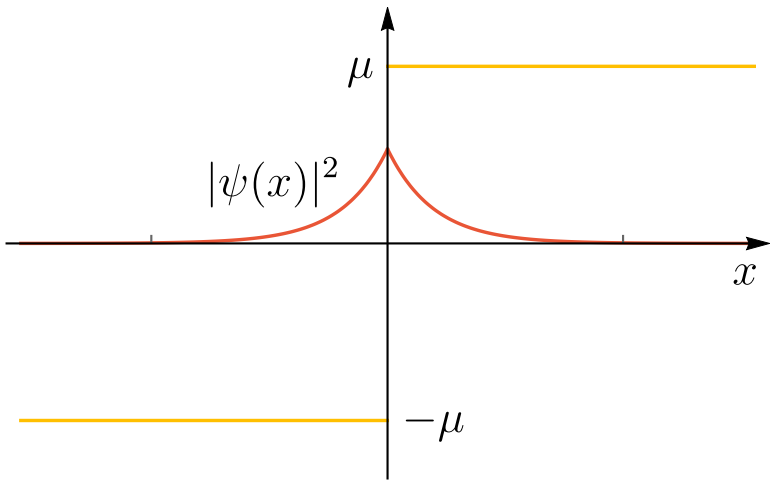

Figure 2.3: In figure we show a plot for $\mu(x)$ and for the solution of the zero mode $\psi(x)$.

where $\mu = 2(f - J)$ and $v = 2fJ$. Let's now suppose that our chain has a boundary delimiting regions where μ picks different signs, delimiting regions with different topological phases, in this sense we will consider μ to be a function of the position x on the chain. In position space we can use (2.35) to write down an effective Hamiltonian in order to consider what happens near the boundary. If we consider the continuous limit this effective Hamiltonian is

$$H_{eff} = \mu(x)\sigma^z - v\sigma^y i\partial_x \ . \tag{2.36}$$

To keep the analysis simple we consider $\mu(x)$ to be

$$\mu(x) = \begin{cases} \mu & x > 0 \\ -\mu & x < 0 \end{cases}$$

where $\mu > 0$. For the following the precise functional form of $\mu(x)$ it is not important, as long as $\mu(x)$ changes sign at $x = 0$. From the previous discussion, we know that at the boundaries there are gapless excitations and we can therefore try to solve

$$H_{eff}\psi(x) = 0 \tag{2.37}$$

which, by substituting H_{eff} becomes

$$\partial_x\psi(x) = \frac{\mu(x)}{v}\sigma^x\psi(x) \tag{2.38}$$

This equation can be easily solved by diagonalising σ^x and the two independent solutions are

$$\exp\left(\pm\frac{1}{v}\int_0^x \mu(x')dx'\right)\begin{pmatrix}1\\ \pm 1\end{pmatrix}$$

since $\mu(x)$ changes sign at the boundary one of the two solutions is normalizable, and we can write

$$\psi(x) = \sqrt{\frac{2m}{v}} \exp\left(-\frac{\mu}{v}|x|\right) \begin{pmatrix} 1 \\ -1 \end{pmatrix} \ . \tag{2.39}$$

Note that if $\mu(x)$ didn't change sign across the boundary we wouldn't get any normalizable solution. Therefore at the interface between two different regimes there is a zero mode that exponentially decays into the chain (see Figure 2.3). Open boundary conditions clearly represent a limiting case of this situation, as they corresponds to taking the limit $\mu \to \infty$ for $x > 0$. In particular this shows how the existence of the zero mode depends on the properties of the bulk. This is a general property of SPT topological systems and it is a consequence of the *bulk-boundary correspondence* we introduced in the previous chapter [7, 4].

Chapter 3

Majorana wires

In this chapter we will review the physical one dimensional systems that are the best candidate to host Majorana zero modes and therefore are supposed to realize the topological phases described in the previous chapter. The following exposition is based upon the material in [34, 35, 36] and [4].

3.1 Majorana femions in 1D wires

We will now consider a generalization of the model introduced in Section 2.1. This constitutes a toy model for spinless, p-wave superconductor on an L-site chain, introduced by Kitaev in his seminal paper on Majorana zero modes [14].

$$H = -\sum_{j=1}^{L-1}(wc_j^\dagger c_{j+1} + |\tilde{\Delta}|e^{i\phi}c_j c_{j+1} + h.c.) - \sum_{j=1}^{L}\tilde{\mu}c_j^\dagger c_j \tag{3.1}$$

As before $c_j^\dagger$, c_j are fermionic creation and annihilation operators. This model reduces to the Ising model when $\tilde{\mu} = -2f$, $w = J$ and $|\tilde{\Delta}|e^{i\phi} = J$.
The parameter $w > 0$ represents the kinetic term, as we will explain in more details in the following. $\tilde{\Delta}$ is the Cooper pairing, responsible for the superconducting phase and $\tilde{\mu}$ represents the chemical potential that determines the Fermi energy.

In order to find the topological phases of the system, we can now again consider the bulk Hamiltonian and perform a Fourier transform to find the spectrum. Repeating what we did in Section 2.3 we find that

$$H_{bulk} = \frac{1}{2}\sum_k \mathbf{C}_k^\dagger H_k \mathbf{C}_k + \tilde{\mu}L \ . \tag{3.2}$$

where $\mathbf{C}_k = \begin{pmatrix} c_k \\ c_{-k}^\dagger \end{pmatrix}$ and similarly to Section 2.3 we have

$$H_k = d_z(k)\sigma^z + d_\phi(k)(\sin\phi\ \sigma^x + \cos\phi\ \sigma^y) \ , \tag{3.3}$$

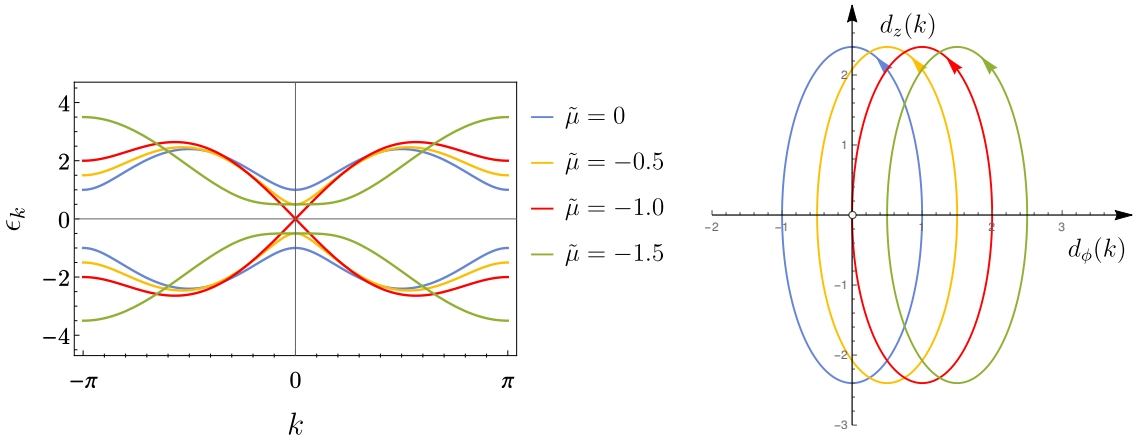

(a) (b)

Figure 3.1: In (a) we show the one particle spectrum $\pm\epsilon_k$ for different values of $\tilde{\mu} < 0$ and fixed $|\tilde{\Delta}| = 1.2$ and $w = 0.5$. It can be seen that the gap closes at $\tilde{\mu} = -2w$. In Figure (b) we show the $\mathbf{d}$ vector for $k \in [0, 2\pi]$

with σ^z, σ^x, σ^y Pauli matrices and

$$d_z(k) = -(\tilde{\mu} + 2w\cos ka) \qquad d_\phi(k) = 2|\tilde{\Delta}|\sin ka \ . \tag{3.4}$$

Note that in the last expressions the dependence on the lattice parameter a was made explicit. Because of the particle hole symmetry the vector $\mathbf{d} = (d_z, d_\phi)$ still lies on the plane as in Section 2.3, but as a result of the phase ϕ, the Pauli matrix σ^y is now rotated around the z-axis

$$\sin\phi\sigma^x + \cos\phi\sigma^y = e^{i\frac{\phi}{2}\sigma^z}\sigma^y e^{-i\frac{\phi}{2}\sigma^z}$$

and the single particle energies are given by

$$\epsilon_k = \pm\sqrt{(\tilde{\mu} + 2w\cos ka)^2 + 4|\tilde{\Delta}|^2\sin^2 ka} \ . \tag{3.5}$$

As we said w represents the kinetic term, therefore the Fermi momentum is determined by the equation

$$-2w\cos(k_F a) = \tilde{\mu} \ . \tag{3.6}$$

It is now easy to see that the system becomes gap-less when $\tilde{\mu} = \pm 2w$. As in the Ising case, these are the boundaries between two phases with different topology. The non-trivial topological phase corresponds to the region $-2w < \tilde{\mu} < 2w$, while the trivial one corresponds to $\tilde{\mu} > 2w$ and $\tilde{\mu} < -2w$. This can be qualitatively understood from the fact that in these last cases we can adiabatically connect the system to the vacuum ($\tilde{\mu} \to -\infty$) or the fully occupied band ($\tilde{\mu} \to +\infty$). More concretely, repeating the analysis of Section 2.3, we can plot the single particle energies of the model and the components of the vector $\mathbf{d}$, from which we can easily

identify the topological and the trivial phases. This is shown in Figure 3.1 for negative values of $\tilde{\mu}$, a similar plot can be obtained for positive ones.

As in the Ising case, for each site we can introduce two Majorana operators:

$$c_j = \frac{1}{2} e^{-i\frac{\phi}{2}} (a_j + i b_j) \qquad c_j^\dagger = \frac{1}{2} e^{i\frac{\phi}{2}} (a_j - i b_j) \tag{3.7}$$

with $a_j^\dagger = a_j$, $b_j^\dagger = b_j$ and

$$\{a_j, b_k\} = 0 \qquad \{a_j, a_k\} = \{b_j, b_k\} = 2\delta_{j,k} \ . \tag{3.8}$$

The introduction of the phase ϕ inside the definition of the Majorana operators is quite convenient as it allows to remove the explicit dependence on ϕ from the Hamiltonian. In terms of Majorana operators the Hamiltonian is in fact

$$H = \sum_{j=1}^{L-1} \frac{i}{2} (w - |\tilde{\Delta}|) b_j a_{j+1} - \sum_{j=1}^{L-1} \frac{i}{2} (w + |\tilde{\Delta}|) a_j b_{j+1} - \sum_{j=1}^{L} \frac{i}{2} \tilde{\mu} a_j b_j - L\tilde{\mu} \ . \tag{3.9}$$

If we consider the special case $\tilde{\mu} = 0$, $w = |\Delta|$ the Hamiltonian becomes

$$H = -i \sum_{j=1}^{L-1} w a_j b_{j+1}$$

and we see that in the topological phase two Majorana operators $a_1 - b_L$ appear at the ends of the chain, as we would expect from the bulk-boundary correspondence. Away from this limit, the Majorana zero modes no longer retain this simple form, but still survive as long as the gap does not close.

Before looking at the connection with possible physical realization of this Hamiltonian, it is useful to consider its continuum limit, which can be obtained by taking $a \to 0$ (and fixing $La = l$). Taking the first order expansion of H_k we have

$$H_k \sim -(\tilde{\mu} + 2w - w a^2 k^2)\sigma^z + 2|\tilde{\Delta}| a k (\sin\phi \sigma^x + \cos\phi \sigma^y) \ . \tag{3.10}$$

We can therefore establish the connection between the physical and the bare quantities by setting

$$\frac{1}{2m} = w a^2 \qquad \mu = \tilde{\mu} + 2w \qquad |\Delta| = 2a|\tilde{\Delta}| \ . \tag{3.11}$$

where m is the effective mass for the electrons.
At low energy and low density, we therefore see that the Hamiltonian H in (3.1) belongs to the universality class of

$$H_{eff} \sim \int dx \ \mathbf{\Psi}(x)^\dagger \left(\frac{p^2}{2m} - \mu \right) \mathbf{\Psi}(x) + \left(|\Delta| e^{i\phi} \mathbf{\Psi}(x) p \mathbf{\Psi}(x) + h.c. \right) \tag{3.12}$$

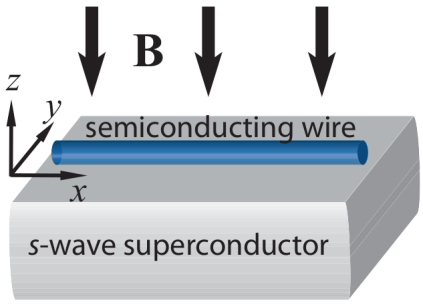

Figure 3.2: Pictorial representation of a spin-orbit coupled semiconductor deposited on an s-wave superconductor. The picture was taken from [34].

with $\mathbf{\Psi}(x)$ real-space creation operator and p momentum operator.

As a final remark note that, not differently from what happened in the Ising case, the Hamiltonian (3.1) commutes with the fermion parity operator

$$Q_2 = \prod_{j=1}^{L}(-ia_j b_j) = (-1)^{N_F} \ , \tag{3.13}$$

which, again, simply counts the number of fermions *mod* 2 (as before N_F stands for the fermion number operator).

In the next section we will see how to realize such an effective Hamiltonian in physical systems.

3.2 Effective spinless p-wave superconductors

Realizing Kitaev's topological superconducting state experimentally requires a spinless one dimensional system, that is one pair of Fermi points p-wave paired at the Fermi energy. Disregarding the difficulties to engineer one dimensional superconducting wires, one major problem comes from the fact that the most common superconductors are s-wave. Nonetheless, this model can be realized as an effective Hamiltonian describing a spin-orbit-coupled semiconducting wire deposited on an s-wave superconductor, with an applied magnetic field (see Figure 3.2). The simplest Hamiltonian describing such a wire is

$$\mathcal{H} = \frac{1}{2}\int dx\ \psi(x)^\dagger H(x)\psi(x)$$

where $\psi(x)$ is the so called Nambu spinor.

$$\psi(x)^\dagger = (\psi_\uparrow(x)^\dagger, \psi_\downarrow(x)^\dagger, \psi_\downarrow(x), -\psi_\uparrow(x))$$

with $\psi_{\uparrow(\downarrow)}(x)$ is the annihilation operator for an electron with spin-up (spin-down) and

$$H(x) = \left(-\frac{\partial_x^2}{2m} - \mu\right)\tau^z - iu\sigma^y\tau^z\partial_x + |\Delta|(\cos(\phi)\tau^x + \sin(\phi)\tau^y) - \frac{g\mu_B B}{2}\sigma^z \ . \quad (3.14)$$

Here m is the effective mass of the electron and μ is the chemical potential. The τs and σs are Pauli matrices and the convention is to use σs when we refer to Pauli matrices acting on spins and τs to indicate Pauli matrices that act on the particle-hole degrees of freedom. The third term with coefficient u, denotes the Rashba spin-orbit coupling [37], while Δ represents the s-wave pairing induced on the wire by proximity effect with the underlying superconductor. The last term corresponds to the Zeeman effect associated with the magnetic field B. Note that it is possible to engineer materials with large g-factors (for example InAs or InSb), so that the effects of the Zeeman energy can be relevant even with a small magnetic field, as a strong one would lead the wire out of the superconducting phase.

Doing a Fourier transform allows us to find the one particle Hamiltonian, which simply reads

$$H_k = \left(\frac{k^2}{2m} - \mu\right)\tau^z + uk\sigma^y\tau^z + |\Delta|(\cos(\phi)\tau^x + \sin(\phi)\tau^y) - \frac{g\mu_B B}{2}\sigma^z \ . \quad (3.15)$$

The single particle energies ϵ_k can be conveniently found by squaring twice H_k[1]. Setting $\xi_k = \frac{k^2}{2m} - \mu$ we get that the single particle energies $\epsilon_\pm(k)$ can be given as

$$\epsilon_\pm(k)^2 = \xi_k^2 + (uk)^2 + |\Delta|^2 + \frac{1}{4}(g\mu_B B)^2 \pm 2\sqrt{\xi_k^2(uk)^2 + \frac{1}{4}(g\mu_B B)^2\xi_k^2 + \frac{1}{4}|\Delta|^2(g\mu_B B)^2} \ .$$

As shown in [36] the topological properties of the system are determined by the gap at $k = 0$[2]. This can be obtained by considering $\epsilon_-(0)$

$$\epsilon_-(0) = \left|\frac{1}{2}g\mu_B B - \sqrt{|\Delta|^2 + \mu^2}\right| \ . \quad (3.16)$$

We therefore see that the gap closes when $(\frac{1}{2}g\mu_B B)^2 = \Delta^2 + \mu^2$, signalling that a

[1]By squaring it the first time we get that H_k^2 is the same as

$$\xi_k^2 + (uk)^2 + |\Delta|^2 + \frac{(g\mu_B B)^2}{4} + 2\xi_k(uk)\sigma^y + \xi_k g\mu_B B\tau^z\sigma^z - |\Delta|(g\mu_B B)(\cos(\phi)\tau^x + \sin(\phi)\tau^y)\sigma^z$$

and squaring the second time yields

$$\left(H_k^2 - \xi_k^2 - (uk)^2 - |\Delta|^2 - \frac{(g\mu_B B)^2}{4}\right)^2 = 4\left(\xi_k^2(uk)^2 + \frac{(g\mu_B B)^2}{4}\xi_k^2 + \frac{|\Delta|^2}{4}(g\mu_B B)^2\right) \ .$$

Since this last equation is invariant under conjugation the formula for $\epsilon_\pm(k)$ follows.

[2]There are two further momenta where the gap can close. They are $k = \pm\pi$, which come as a pair because of particle-hole symmetry. Qualitatively we can expect that the global effects on the winding number coming from these two points cancel out and we do not witness any phase transition. The topological phase transition, therefore, can only take place in correspondence of particle hole symmetric momentum, that is $k = 0$.

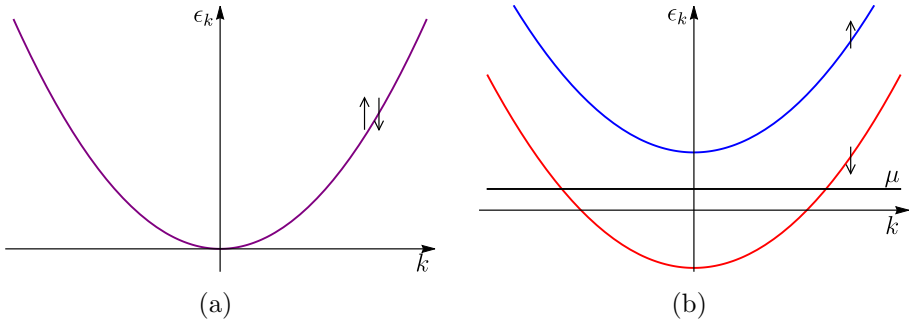

(a) (b)

Figure 3.3: In (a) we show the band structure for ϵ_k for $\mu = 0$ and $B = 0$ ($|\Delta| = u = 0$), with the spin-up and spin-down bands on top of each other. In Figure (b) we show the same for $B < 0$.

topological phase transition is taking place. Since when $B = 0 = u = 0$ the system is just a normal s-wave superconductor[3], we expect that the non-trivial topological phase corresponds to

$$\frac{1}{4}(g\mu_B B)^2 > |\Delta|^2 + \mu^2 \ . \tag{3.17}$$

We will not discuss the general topological phases of this model in detail, and we refer to [36] for further clarification on the subject. In the following we will instead concentrate on the limit of strong Zeeman field $g\mu_B|B| \gg mu^2, |\Delta|$ and we will see how this connects to the spinless p-wave superconductor we mentioned before.
The zeroth order of this limit, gives an Hamiltonian H_k

$$\begin{pmatrix} \frac{k^2}{2m} - \mu - \frac{g\mu_B B}{2} & 0 & 0 & 0 \\ 0 & \frac{k^2}{2m} - \mu + \frac{g\mu_B B}{2} & 0 & 0 \\ 0 & 0 & -\frac{k^2}{2m} + \mu - \frac{g\mu_B B}{2} & 0 \\ 0 & 0 & 0 & -\frac{k^2}{2m} + \mu + \frac{g\mu_B B}{2} \end{pmatrix} \tag{3.18}$$

In Figure 3.3 we show the band structure for $B = 0$ and $B < 0$. As we can see the introduction of the magnetic field separates the spin-up sector from the spin-down sector. If therefore μ lies in this gap, the Fermi surface will consist only of two points as desired. In this limit, the ground state is obtained by filling in all the levels with spin-down electrons, up to the Fermi energy.

At this point we can introduce the effects of the spin-orbit coupling perturbatively in u, and obtain an effective Hamiltonian for the low energy physics of the model. First of all, note that in a perfectly spin-polarized system we could not have spin-singlet Cooper pairing, as this terms always contains a spin-up and a spin-down fermionic operators. The importance of the spin-orbit coupling lies in the fact that it can "tilt" the spins of the lower bands and it can therefore allow such a coupling to take place. In other words, by using first order perturbation theory, we can project all the degrees of freedom into the lower band. Assuming $B < 0$ this can be done

[3]In the case of a normal s-wave superconductor Kramer's theorem prevents the creation of two separated Majorana modes.

by writing

$$\psi_\uparrow(x) \sim -\frac{iu}{g\mu_B B}\partial_x \psi_\downarrow(x) \ . \tag{3.19}$$

If we now set

$$\mathbf{\Psi}(x) \sim \psi_\downarrow(x) \tag{3.20}$$

we get that, up to first order in $um^2/g\mu_B B$, the effective Hamiltonian for the low energy physics of the model is given by

$$H_{eff} \sim \int dx \ \mathbf{\Psi}(x)^\dagger \left(\frac{p^2}{2m} + \mu_{eff}\right) \mathbf{\Psi}(x) + (|\Delta_{eff}| e^{i\phi_{eff}} \mathbf{\Psi}(x) p \mathbf{\Psi}(x) + h.c.) \tag{3.21}$$

with

$$\mu_{eff} = \mu + \frac{1}{2} g\mu_B B \qquad |\Delta_{eff}| = \frac{u}{g\mu_B B}|\Delta| \qquad \phi_{eff} = \phi + \frac{\pi}{2} \ ,$$

which is formally the same as (3.12).

As a final remark, we note that in the opposite limit of small Zeeman field $g\mu_B|B| \ll mu^2$, the Hamiltonian $\mathcal{H}$ is connected to the 1d topological insulators (for more details see [35]).

In the next section we will discuss how it would be possible to exploit the non trivial topology of these models, encoded into the Majorana modes appearing at the end of the chain, to build a quantum memory and, ultimately, a quantum computer.

3.3 Manipulating Majorana qubits

We will now consider ways to manipulate Majorana fermions. Our exposition will closely follow [34].

Suppose that we apply a gate voltage to the system described by (3.15) to adjust the chemical potential μ inside the wire. As we saw the gap at $k = 0$ is given by

$$\epsilon_-(0) = \left| \frac{1}{2} g\mu_B B - \sqrt{|\Delta|^2 + \mu^2} \right| \tag{3.22}$$

and we are in the topological regime when

$$\frac{1}{4}(g\mu_B B)^2 > |\Delta|^2 + \mu^2 \ .$$

If we fix B and Δ we see that by tuning the chemical potential we can drive the system in the topological phase. In particular, when

$$|\mu| < \mu_c = \sqrt{\frac{1}{4}(g\mu_B B)^2 - |\Delta|^2} \tag{3.23}$$

the system is topological and μ_c is the critical value of the chemical potential at which the phase transition takes place. Thus a uniform gate voltage allows the

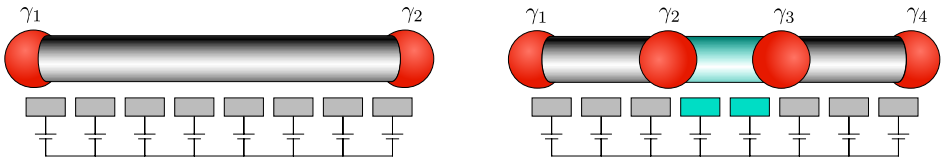

(a) (b)

Figure 3.4: Pictorial representation of the Majorana modes at the end of the superconducting wire. In (a) we show how the tunable voltage gates can be used to create regions with non-trivial topology, where $|\mu| < \mu_c$ (in light blue in the picture). In this way we can also create regions in with trivial topology, where $|\mu| > \mu_c$. The zero modes will delimit the regions with non-trivial topology. This is schematically shown in picture (b).

creation and the removal of Majorana fermions. However, in order to manipulate Majoranas, it would be useful to exert local control over the chemical potential. This can in principle be achieved by tunable gate electrodes coupled to the wire. A schematic illustration is presented in Figure 3.4(a).

As we saw in Section 2.3, zero modes generally lie at the domain walls separating two different phases of the system. Consequently, we see that by locally tuning the chemical potential, we can create multiple pairs of Majorana zero modes along the wire (see Figure 3.4(b)). The ability to locally control the value of the chemical potential, opens up the prospect of dynamically manipulating the zero modes and moving them around on the wire.

Even though for one dimensional systems exchange of particles is strictly speaking not possible, if we consider more general types of wires, like a T-junction, we can imagine being able to dynamically exchange Majoranas at the end of the topological region. This is schematically represented in Figure 3.5.

With this set up we can also exchange Majorana modes separated by a non topological region. This process comprises the creation and annihilation of additional, auxiliary Majorana modes. This is schematically represented in Figure 3.6.

In the next section we will see how Majorana zero modes can be used to encode qubits and how their manipulation can possibly lead to topological quantum computation.

3.3.1 Majorana qubits

In the previous sections we saw that, in certain regimes, spinless p-wave superconductors support Majorana states at the edges of the system. Using Majorana operators instead of fermions is a convenient mathematical artifice, that renders readily identifiable the mechanisms behind the physics that we described. Nonetheless we always have to keep in mind that the physical degrees of freedom of the system are made out of fermionic variables.

Given two Majorana modes γ_1, γ_2 separated by a topological phase, by mimicking

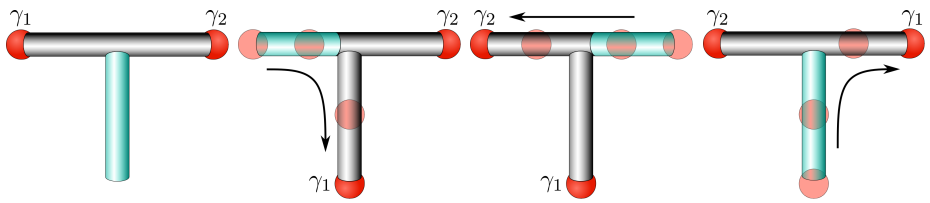

Figure 3.5: From (a) to (d), schematic representation on how to exchange Majorana separated by a topological phase on a T-junction by dynamically tuning the chemical potential using the voltage gates.

our initial definition of Majorana operators, we can write

$$\begin{aligned} c_1^\dagger &= \frac{1}{2}(\gamma_1 - i\gamma_2) \\ c_1 \ &= \frac{1}{2}(\gamma_1 + i\gamma_2) \ , \end{aligned} \tag{3.24}$$

which constitutes fermionic creation and annihilation operators.
These fermionic degrees of freedom cost no energy (in the limit of long chains), as they are made out of zero modes and are delocalised along the chain.

As we saw in Section 3.1 the Hamiltonian of the system conserves the fermion parity Q_2 and the existence of zero modes implies in particular that the ground state is two fold degenerate. We can therefore imagine using the two levels in the ground state of the system to form a qubit in which we would encode some information. In reality, the total fermion parity is a conserved quantity and therefore we can access only one of the two states. This problem can be easily circumvented by considering a system with four Majoranas, like the one depicted in Figure 3.6(a)[4].
Similarly to what we did in equation (3.24) we can define additional fermionic degrees of freedom $c_2^\dagger$, c_2, which will make the ground state four-fold degenerate; opening up the possibility of accessing two states with the same parity. To see how this goes, consider the projection of the parity operator on the ground state manifold

$$Q_2 = (i\gamma_1\gamma_2)(i\gamma_3\gamma_4) = P_1 P_2 \ , \tag{3.25}$$

where we defined the parity operators for the two separate wires

$$P_1 = i\gamma_1\gamma_2 = (1 - 2c_1^\dagger c_1) \qquad P_2 = i\gamma_3\gamma_4 = (1 - 2c_1^\dagger c_1) \ . \tag{3.26}$$

We can identify the four ground states with respect to the occupation number of the fermions c_1 and c_2 (or, equivalently, with respect the parity of the two wires), which means that the four ground states are

[4]Note that in order to create the degenerate state the T-junction geometry is not strictly necessary.

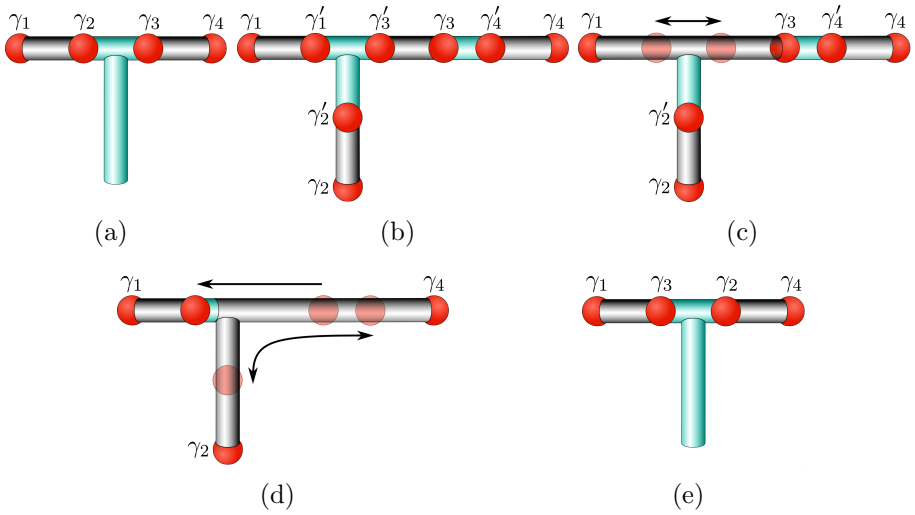

Figure 3.6: From (a) to (e), schematic representation on how to exchange Majorana separated by a non-topological phase on a T-junction by dynamically tuning the chemical potential using the voltage gates. This process requires the creation of auxiliary Majorana modes that are annihilated at the end of the protocol.

$$|00\rangle \qquad |01\rangle \qquad |10\rangle \qquad |11\rangle \ . \tag{3.27}$$

As we said, since the total parity of the system is conserved, depending on the initial conditions, we can access only half of this manifold. Without loss of generality we can assume our qubits to be defined by the even states

$$|\bar{0}\rangle = |00\rangle \qquad |\bar{1}\rangle = |11\rangle \tag{3.28}$$

and we can use Majorana modes to encode information into some superposition of these two states. Nonetheless all this would be useless if we do not have a way to manipulate and access this information. As we saw there are ways in which we can manipulate the positions of the Majorana zero modes along the wire and, in particular, we saw that we can exchange any two of them (on T-junctions). It is therefore meaningful to ask what are the effects of such manipulations on the Majorana qubits.

Suppose therefore that we adiabatically perform one of the braiding processes depicted in Figure 3.5 and Figure 3.6. Since the Majorana are indistinguishable particles all of these transformations have to be cyclic. From the adiabatic theorem, we know that if we act on a non-degenerate state with a cyclic transformation the ground state of the system will acquire a phase that is commonly known as Berry phase [38]. When the state is degenerate the adiabatic evolution is not merely described by a geometric phase associated with a connection (Berry connection), but rather by a unitary transformation associated with a nonabelian vector potential, that acts on the degenerate ground state manifold [39].

Since we are considering the low energy states, the unitary transformation U corresponding to our cyclic adiabatic evolution, should be described in terms of γ_1, γ_2, γ_3, γ_4; which are the only degrees of freedom at hand. We also know that the adiabatic evolution has to preserve the total fermionic parity (as the Hamiltonian does), that is to say

$$[U, Q_2] = 0 \ . \tag{3.29}$$

Let's therefore suppose that we perform the braiding of the Majoranas γ_i and γ_j. It is reasonable to expect that the unitary transformation associated with it U_{ij}, will only depend upon these two operators, as the others are effectively not involved in the transformation. It is not difficult to prove that the unique combination of γ_i and γ_j that commutes with Q_2 is given by $\gamma_i\gamma_j$, since

$$(\gamma_i\gamma_j)^2 = 1 \ . \tag{3.30}$$

The most general unitary transformation that we can think of, hence, takes the form

$$U_{ij} = e^{\beta\gamma_i\gamma_j} = \cos\beta + \sin\beta\gamma_i\gamma_j \ . \tag{3.31}$$

Note that there is no need for the imaginary unit, as the operator $\gamma_i\gamma_j$ is antihermitian.
By acting with our educated guess of U_{ij} on γ_i and γ_j, we get

$$\begin{aligned} U_{ij}\gamma_i U_{ij}^\dagger &= \cos(2\beta)\gamma_i - \sin(2\beta)\gamma_j \\ U_{ij}\gamma_j U_{ij}^\dagger &= \cos(2\beta)\gamma_j + \sin(2\beta)\gamma_i \ . \end{aligned} \tag{3.32}$$

Since at the end of the transformation the zero modes have to be exchanged, we are forced to have $\beta = \pm\frac{\pi}{4}$ and the two different signs distinguish between clock-wise and anticlock-wise exchanges[5].

The action of $i\gamma_i\gamma_j$ in the qubit basis is readily identified and we have

$$\begin{aligned} i\gamma_1\gamma_2 &= i\gamma_3\gamma_4 = -\sigma_z \\ i\gamma_2\gamma_3 &= -\sigma_x \ , \end{aligned} \tag{3.33}$$

leading to the following braiding operators

$$\begin{aligned} U_{12} = U_{34} &= \frac{1}{\sqrt{2}}(1 \pm i\sigma_z) \\ U_{23} &= \frac{1}{\sqrt{2}}(1 \pm i\sigma_x) \ , \end{aligned} \tag{3.34}$$

which constitute a representation for the generators of the Artin braid group B_4.

[5]In Figure 3.5 and Figure 3.6 we only show clock-wise exchange for γ_1, γ_2 and anticlock-wise exchange for γ_2, γ_3. It is not difficult to think of protocols that perform the other exchanges.

This discussion shows that, if we store information into $2n$ Majorana zero modes, we can perform quantum computation on it by braiding them. The next question we should ask is how "powerful" is the quantum computation done with Majoranas. Is it better than what we get from a classical computer?
The set of Pauli matrices acting on n qubits is also known as the Clifford group and the unitary operators that we can build from (3.34) form the normalizer of this group [40]. It is a well known fact [41, 40] that the unitary operators obtained as the normalizer of the Clifford group are not universal quantum gates and that any quantum algorithm performed through them can be efficiently simulated on a classical computer[6].

The advantage of using Majoranas to do quantum computation resides in the fact that, since the degrees of freedom of the system are delocalised on the chain, they are robust against local perturbations that commute with the parity[7]. A quantum computer, or a quantum memory, based on Majorana modes would therefore in principle be unaffected by the problem of decoherence and would not need error correcting codes, which pose a major obstacle to the realization of scalable quantum computers. In this sense the quantum computation performed with Majoranas is said to be topological and it is a specific case of a more general theory that consider quantum computation carried out by braiding anyons [1, 2, 43].

It is important to note that the above discussion holds only for adiabatic exchange of Majorana modes. In the next chapter we will see what kind of errors we can expect to observe if we relax this requirement.
We will now review one of the effects that would in principle allow to experimentally detect the presence Majorana zero modes.

3.4 Detecting Majorana zero modes

In the past years, there has been a great deal of experimental work in order to try to detect the presence of Majorana zero modes in semiconductor-superconductor heterostructures. The majority of these experimental works [44, 45, 46, 47] dealt with the detection of a theoretically predicted peak in the conductance at zero voltage, which is similar to the resonant transmission from scattering theory.
We will not discuss here the problems related to these type of experiments, but we will rather concentrate on another experimental signature of the presence of Majorana zero modes, which is usually referred to as fractional Josephson effect [48, 49, 50]. Importantly this effect can be used to engineer a readout protocol of the Majorana qubit [34], as we will illustrate in the following.

[6]There have been proposals to add noisy gates to this system in order to make the quantum computation universal, for example see [42].

[7]As we saw the operators that commute with the fermionic parity at low energy are of the form $\gamma_i\gamma_j$. If the Majorana are far away from each other, perturbations of this form are supposed to be

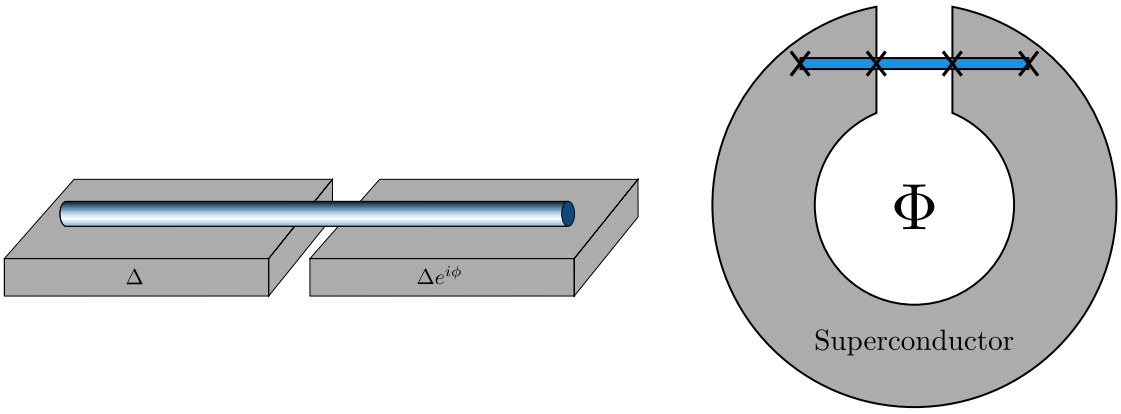

(a) (b)

Figure 3.7: (a) Semiconductor/Superconductor heterostructure. The tunable voltage gates controlling the chemical potential can be placed on top of the nanowire. (b) Top view of the Semiconductor/Superconductor heterostructure embedded into a Superconducting loop. The magnetic flux can be used to control the phase difference ϕ between the two halves of the nanowire. With crosses, we have indicated the positions of the Majoranas zero modes when the system is in the topological phase.

3.4.1 Fractional Josephson effect

Consider a junction of two topological superconductors with two different superconducting gaps, as we schematically show in Figure 3.7(a). Such a configuration can be realized in experiments, for example implementing the design sketched in Figure 3.7(b). The flux Φ in the loop can be used to control the value of the phase ϕ between the two halves of the nanowire.

The presence of the semiconductor between the two regions where the wire is in the superconducting topological phase introduces a tunnelling amplitude between the left electron and the right one. For simplicity let's consider the tunneling Hamiltonian to be

$$H_T = (t c_L^\dagger c_R + t^* c_R^\dagger c_L) \tag{3.35}$$

where t is the tunneling amplitude and c_L, c_R are annihilation operators for the leftmost and rightmost electrons of the wires in the topological phase. In the following we will assume, for simplicity, t to be real and positive.
The same analysis, even if more convoluted, can be conducted using more complicated Hamiltonians [34]. Because of (3.7), we can write (3.35) as

$$H_T = \frac{i}{2}\sin\frac{\phi}{2}(a_L a_R + b_L b_R) + \frac{i}{2}\cos\frac{\phi}{2}(a_L b_R + a_R b_L)\ . \tag{3.36}$$

The presence of this interaction will thus hybridize the two middle zero modes, that will gain a non zero energy. We know that in general the middle zero modes are of

suppressed.

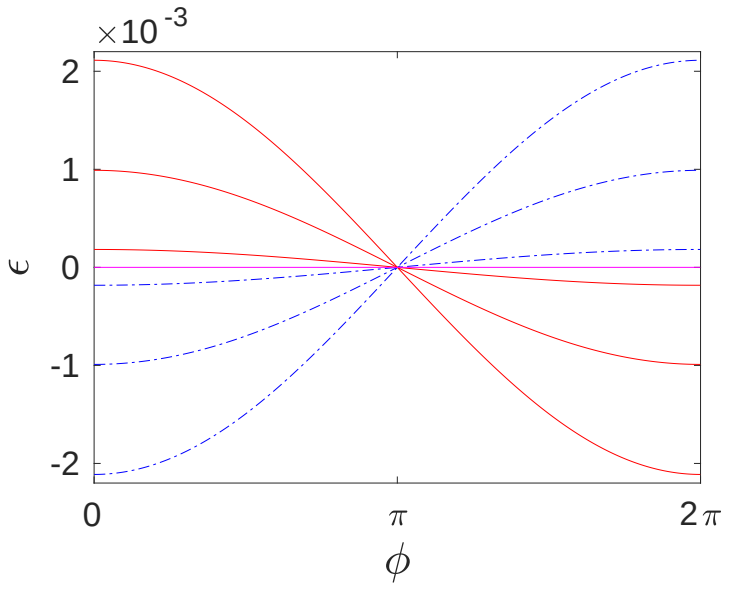

Figure 3.8: Results of numerical simulations on the Kitaev model with a potential barrier separating the two middle Majorana zero modes for different height of the barrier (the wall heights, with the conventions of Chapter 4 are, respectively $\mu_{barrier} = 1.8, 2, 2.5$). As can be intuitively understood the effect gets smaller as we make the barrier higher. In red we show single particle energies associated with the middle zero modes with positive parity, while in dashed blue we show the ones for negative parity. The middle purple line shows the single particle energies associated with the two remaining zero modes. [Other parameters used in the simulation, with conventions that will become clear in the next chapter, are: $m = 0.5$, $a = 0.5$, $\Delta = 0.4$, $L = 200$, and $\mu = 1.0$ (in the topological region). The length of the barrier was set to be 10.]

the form

$$\gamma_L = u_L b_L + \dots \qquad \gamma_R = u_R a_R + \dots \tag{3.37}$$

where $u_{L/R}$ are the real wavefunctions for the zero modes in the left/right wires. The values of $u_{L/R}$ will generally depend on the model details and we saw for the Ising model that they correspond to the normalizations of the zero modes. We see therefore that, up to a first order perturbation expansion, the low energy physics can be described by the effective tunnelling Hamiltonian

$$H_T \approx \frac{t}{2u_L u_R} \cos\frac{\phi}{2} i\gamma_L\gamma_R = \frac{t}{2u_L u_R} \cos\frac{\phi}{2} P \tag{3.38}$$

where we introduced the parity P relative to the middle zero modes, that we encountered in Section 3.3.1.

This means that the quasi-particle energy changes with respect to the occupation number of the middle fermionic degree of freedom built out of the Majoranas, that is

$$\epsilon_\pm = \pm\frac{t}{2u_L u_R} \cos\frac{\phi}{2} \ . \tag{3.39}$$

Hence (see Figure 3.8), for a fixed fermion parity, the spectrum is 4π-periodic rather

than 2π-periodic. Of course, if we consider the whole spectrum irrespective of the parity, then we get back a periodicity of 2π, as it should be because of gauge invariance.

For fixed fermionic parity, this results in a Josephson current I_J that is 4π-periodic, quite unlike the 2π-periodic current of conventional Josephson junctions. This follows from the spectrum as [51]

$$I_J = 2e\frac{d\epsilon_\pm}{d\phi} = \pm\frac{te}{2u_L u_R}\sin\frac{\phi}{2} \ . \tag{3.40}$$

For fixed parity, only one of the subgap states contributes to the current, thus resulting in the 4π periodicity. Note that at $\phi = \pi$ the system becomes degenerate indicating a phase transition. At this point, in fact, the two zero modes are "transparent" and do not couple to each other.

As already said, even though we derived this result for a simple tunneling Hamiltonian, it can be derived also for more general ones. In Figure 3.8 we present the result from numerical simulations on the Kitaev chain, obtained through methods that we will explain in the next chapter. In this figure, we can clearly see the energy of the two middle zero modes following the 4π periodicity that we described. The middle energies are relative to the zero modes not involved in the tunnelling process and therefore stay at zero as we would expect.

3.4.2 Majorana qubit readout

Our discussion on the fractional Josephson effect clarifies that a measurement of the Josephson current coincides, essentially, with a measurement of the parity of the middle Majoranas. This can be used to conceive a readout protocol on the computational space as we will now see. We will follow [34] in the exposition.

The general idea, coming from topological quantum computation [43], is to "fuse" together two of the Majorana zero modes (anyons in the more general framework of TQC) and read the outcome from the Josephson current.
Consider in fact Figure 3.9. We start by creating the Majorana zero modes γ_1, γ_2, γ_3 and γ_4 (Figure 3.9(b)). As we saw we can associate to these zero modes fermionic degrees of freedom

$$c_1 = \frac{1}{2}(\gamma_1 + i\gamma_2) \qquad c_2 = \frac{1}{2}(\gamma_3 + i\gamma_4) \ . \tag{3.41}$$

The definition of these degrees of freedom is not unique, but if the two topological phases are well separated we expect this picture to be the relevant one. Since creating these fermions costs some initial energy[8], we can assume that the system

[8]When we create the zero modes they are not well separated.

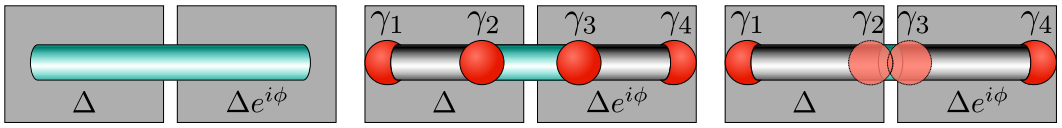

Figure 3.9: From (a) to (c), schematic representation on how to fuse the two middle zero modes.

is in the ground state $|00\rangle$ defined by

$$c_1|00\rangle = c_2|00\rangle = 0 \ . \tag{3.42}$$

We can now bring the Majorana zero modes γ_2 and γ_3 together (Figure 3.9(c)) and, because of this, the middle zero modes will gain a non zero energy. To understand the consequences of this fact, we can perform a basis change by defining

$$c_1' = \frac{1}{2}(\gamma_1 + i\gamma_4) \qquad c_2' = \frac{1}{2}(\gamma_2 + i\gamma_3) \ . \tag{3.43}$$

It can be easily seen that with this definition

$$c_1 = \frac{1}{2}(c_1' + ic_2' + c_1'^{\dagger} + ic_2'^{\dagger}) \tag{3.44}$$

and therefore, using (3.42), it follows that

$$|00\rangle = \frac{1}{\sqrt{2}}\left(|0'0'\rangle - i|1'1'\rangle\right) \ . \tag{3.45}$$

As we saw when we take the two middle zero modes near each other, the two states $|0'0'\rangle$, $|1'1'\rangle$ have energies that differ in sign as in (3.39) depending on the occupancy of the fermion c_2'.
By measuring the Josephson current we will induce a collapse of the wave function with 50% probability in the state $|0'0'\rangle$ and with 50% on the state $|1'1'\rangle$. The sign of the current will determine which ground state the system is in.
In more general wire configurations this effect can be used to perform readout protocols on the qubit space.

Chapter 4

Diabatic errors in Majorana-based qubits

In the previous chapter we saw that, through an adiabatic exchange of Majorana zero modes, it is possible to perform quantum computation. It is important to note that this scenario is feasible only as long as the fermion parity is a rigorously conserved quantity. This is only true for a strictly closed system, since the interactions with some external source of electrons could lead to the possibility of an electron hopping into the system, which would destroy the symmetry protected topological order. In the literature this problem is commonly referred to as quasi-particle poisoning and was explored by different authors [52, 53, 54].

In this chapter we will consider the errors arising, in a closed system, by the non-adiabaticity of the controls exerted over the Majorana zero modes, as any real life experiment will have to deal with some type of diabatic effects. A certain number of these problems were already treated by different authors (see e.g [55, 56, 57]). In this chapter we will review some of the results contained in [26].

4.1 Bogoliubov-de Gennes formalism

Before introducing the subject of this chapter we will review a useful framework that allows to easily solve any two body fermionic Hamiltonian. The methods that we will describe here go under the name of Bogoliubov-de Gennes (BdG) formalism [4, 58]. As we will see this scheme constitutes a generalization of the methods that we employed in the previous chapters, when we computed the single particle energies of the various models that we considered. An important distinction is that the BdG treatment does not need translational invariance to be applicable.
In the following we will consider spinless fermions living on a chain, as we will mainly be interested in this case for the rest of the chapter. It is not difficult to generalize this treatment to consider more general cases (see e. g. [4]).

Consider therefore a general Hamiltonian of the form

$$H = \sum_{\alpha,\beta} c_\alpha^\dagger h_{\alpha\beta} c_\beta + \frac{1}{2} c_\alpha^\dagger \Delta_{\alpha\beta} c_\beta^\dagger + \frac{1}{2} c_\alpha \widetilde{\Delta}_{\alpha\beta} c_\beta \ . \tag{4.1}$$

In order for H to be hermitian, the matrix h obtained from $h_{\alpha\beta}$ is forced to be hermitian and $\widetilde{\Delta}_{\alpha\beta} = \Delta^*_{\beta\alpha}$. Since we are dealing with fermionic operators, the matrix Δ obtained from $\Delta_{\alpha\beta}$ can be chosen to be antisymmetric. If we now set

$$\begin{aligned} c^\dagger &= (c_1^\dagger, \ldots, c_N^\dagger) \\ c \ &= (c_1, \ldots, c_N) \end{aligned} \tag{4.2}$$

H can be conveniently rewritten as

$$H = \frac{1}{2}(c^\dagger, c)\mathcal{H} \begin{pmatrix} c \\ c^\dagger \end{pmatrix} + \frac{1}{2}\mathrm{Tr}(h) \tag{4.3}$$

where

$$\mathcal{H} = \begin{pmatrix} h & \Delta \\ -\Delta^* & -h^* \end{pmatrix} \tag{4.4}$$

is the BdG Hamiltonian of the system. Note that the factor $1/2$ is needed because we have "doubled" the degrees of freedom of the original Hamiltonian.
This doubling procedure has interesting implications on the symmetries of the system. Consider in fact the operator $\mathcal{C} = \tau^x K$, with τ^x a Pauli matrix and K complex conjugation. If we conjugate $\mathcal{H}$ by this operator we have

$$\mathcal{C}\mathcal{H}\mathcal{C}^{-1} = -\mathcal{H} \ . \tag{4.5}$$

This is nothing more than the particle-hole symmetry that we encountered in the previous chapters, which arises, therefore, from the redundancy in our description. As already noted, this implies that the one-particle energies come in pairs with opposite signs.

Because of the hermitian nature of $\mathcal{H}$ and because of particle hole symmetry, we can diagonalise it through a unitary matrix $\mathcal{W}_0$ of the form

$$\mathcal{W}_0 = \begin{pmatrix} U & V^* \\ V & U^* \end{pmatrix} \ , \tag{4.6}$$

where the first half of the columns of $\mathcal{W}_0$ correspond to the positive eigenvalues of $\mathcal{H}$ and the other half to the negative ones. This means that we can define operators $\beta = (\beta_1, \ldots, \beta_N)$ and $\beta^\dagger = (\beta_1^\dagger, \ldots, \beta_N^\dagger)$ such that

$$\begin{pmatrix} \beta \\ \beta^\dagger \end{pmatrix} = \begin{pmatrix} U^\dagger & V^\dagger \\ V^T & U^T \end{pmatrix} \begin{pmatrix} c \\ c^\dagger \end{pmatrix} \ . \tag{4.7}$$

In terms of these operators the original hamiltonian can be written as

$$H = \frac{1}{2}\sum_{n=1}^{N} \epsilon_n \beta_n^\dagger \beta_n - \epsilon_n \beta_n \beta_n^\dagger, \tag{4.8}$$

where ϵ_n are the positive eigenvalues of $\mathcal{H}$. Since $\mathcal{W}_0$ is unitary we have

$$\begin{aligned} UU^\dagger + V^* V^T &= 1 \qquad U^\dagger U + V^\dagger V = 1 \\ U^T V + V^T U &= 0 \qquad UV^\dagger + V^* U^T = 0 \ , \end{aligned} \tag{4.9}$$

and this means that, given any two operators $\beta_m^\dagger$, β_n, they follow

$$\{\beta_m^\dagger, \beta_n\} = \{(V^T c)_m, (V^\dagger c^\dagger)_n\} + \{(U^T c^\dagger)_m, (U^\dagger c)_n\} \ ;$$

where we used the anti-commutation between cs and $c^\dagger$s. Therefore, using again the anti-commutation relations and (4.9), we are left with

$$\{\beta_m^\dagger, \beta_n\} = \sum_k V_{k,m} V_{k,n}^* + U_{k,m} U_{k,n}^* = \delta_{mn} \ .$$

In a similar way, it can be proved that

$$\{\beta_m, \beta_n\} = \{\beta_m^\dagger, \beta_n^\dagger\} = 0 \ .$$

The operators βs and $\beta^\dagger$s are therefore fermionic in nature and can be used to build the Fock space for H. They are usually referred as quasi-particle operators and the eigenvalues of $\mathcal{H}$ constitute the single-particle energies for the spectrum.
Thus we can write

$$H = \sum_{n=1}^{N} \epsilon_n (\beta_n^\dagger \beta_n - \frac{1}{2}) \ . \tag{4.10}$$

The ground state $|\Phi_0\rangle$ of this many-body system shall be considered as the quasi-particle vacuum, because it satisfies

$$\beta_j |\Phi_0\rangle = 0 \qquad j = 1, 2, \ldots, N \ . \tag{4.11}$$

Depending on the structure of H this state can be found in terms of the bare vacuum $|-\rangle$, by acting over it with an adequate number of β_j operators[1]. Up to a reordering

[1]Naively one may think that

$$|\Phi_0\rangle = \prod_{j=1}^{N} \beta_j |-\rangle \ ,$$

but this state often vanishes identically, since it may happen that there is some j for which $\beta_j = \sum_k U_{kj}^* c_k$ (that is $V_{kj}^* = 0$ for all js). For more details see [58].

of the β_j we can therefore write

$$|\Phi_0\rangle = \prod_{k=1}^{M} \beta_k |-\rangle \tag{4.12}$$

with $M \leq N$ such that

$$\beta_j |\Phi_0\rangle = 0 \qquad \forall j > M \ . \tag{4.13}$$

As can be intuitively understood the matrix $\mathcal{W}_0$ that diagonalises the BdG Hamiltonian encodes information about the ground state of the system. This raises the following question: how do we treat, in the same framework, the excited states of the system? The answer to this is very simple. Consider for example the state given by

$$|\Phi_1\rangle = \beta_1^\dagger |\Phi_0\rangle \ . \tag{4.14}$$

Effectively, this one quasi-particle state can be considered as the vacuum of the quasi-particle operators $(\beta'_1, \beta'_2, \ldots, \beta'_{N-1}, \beta'_N)$ defined as

$$\beta'_1 = \beta_1^\dagger \quad \beta'_2 = \beta_2 \quad \ldots \quad \beta'_{N-1} \quad \beta'_N = \beta_N \ . \tag{4.15}$$

This means that, on a practical level, the information about $|\Phi_1\rangle$ can be encoded into a matrix $\mathcal{W}_1$ obtained by exchanging the first column of $\mathcal{W}_0$ with the $N+1$th column or, equivalently

$$U_{l,1} \leftrightarrow V^*_{l,1} \qquad V_{l,1} \leftrightarrow U^*_{l,1} \qquad l = 1, 2, \ldots, N \ . \tag{4.16}$$

This construction can be naturally extended to consider more general cases. For example, we can consider superpositions of different states by rotating the columns of $\mathcal{W}_0$ in the relevant subspaces.

We can now consider the problem of extracting information about the amplitudes contained into these $\mathcal{W}$s matrices. Suppose for example that we would like to compute the overlap between the ground state $|\Phi_0\rangle$ and some other state $|\Phi_1\rangle$ obtained by swapping and rotating the columns of $\mathcal{W}_0$ as explained above.
A fundamental result found by N. Onishi and S. Yoshida [59, 58], establishes the following identity

$$\langle \Phi_1 | \Phi_0 \rangle = \sqrt{\det(U^\dagger U_1 + V^\dagger V_1)} \ . \tag{4.17}$$

This is known as the Onishi formula and can be easily implemented into numerical simulations to allow efficient computation of overlaps.

In the next section we will see where dynamical evolution stands in this BdG picture.

4.1.1 Time-dependent BdG equation

In the following we will often be interested in considering time evolution of the system under a time dependent Hamiltonian. Hence it would be nice to consider this in the same BdG formalism that we used to solve the time independent problems.

Consider therefore a time dependent Hamiltonian $H(t)$ and hence consider $h \equiv h(t)$ and $\Delta \equiv \Delta(t)$. As in the time independent case, we can define a time dependent BdG Hamiltonian

$$\mathcal{H} = \begin{pmatrix} h(t) & \Delta(t) \\ -\Delta(t)^* & -h(t)^* \end{pmatrix} \tag{4.18}$$

Suppose now that we found the quasi-particles operators $\beta_n(0)$ that diagonalise $H(0)$. The time-evolution of the system can be described, in the Heisenberg picture, as

$$\beta_n^{evo}(t) = \mathcal{T} e^{i\int_0^t H(t')dt'} \beta_n(0) \mathcal{T} e^{-i\int_0^t H(t')dt'} \tag{4.19}$$

where $\mathcal{T}$ indicates the time ordering.

As we saw, we can associate a matrix $\mathcal{W}_0(0)$ to the set of quasi-particle operators $\beta_n(0)$ such that

$$\begin{pmatrix} \beta(0) \\ \beta^\dagger(0) \end{pmatrix} = \mathcal{W}_0(0)^\dagger \begin{pmatrix} c \\ c^\dagger \end{pmatrix} \ . \tag{4.20}$$

The time evolution $\mathcal{W}_0(t)$ of $\mathcal{W}_0(0)$, is defined as the matrix such that

$$\begin{pmatrix} \beta^{evo}(t) \\ \beta^{evo}(t)^\dagger \end{pmatrix} = \mathcal{W}_0^{evo}(t)^\dagger \begin{pmatrix} c \\ c^\dagger \end{pmatrix} \ . \tag{4.21}$$

with

$$\mathcal{W}_0^{evo}(t) = \begin{pmatrix} U^{evo}(t) & V^{evo}(t)^* \\ V^{evo}(t) & U^{evo}(t)^* \end{pmatrix} \ . \tag{4.22}$$

Note that this matrix is generally different from the one that diagonalises $\mathcal{H}(t)$, which from now on we will refer to as $\mathcal{W}_0(t)$.

The equation that determines the evolution of $\mathcal{W}_0^{evo}(t)$ is

$$\frac{d}{dt}\mathcal{W}_0^{evo}(t) = -i\mathcal{H}(t)\mathcal{W}_0^{evo}(t) \tag{4.23}$$

as we will now prove.
Consider the Heisenberg equation for the time evolution of $\beta^{evo}(t)$. Strictly speaking the Hamiltonian $H(t)$ do not act on vectors, but with some abuse of notation we can write

$$\frac{d}{dt}\beta^{evo}(t) = i\left[H(t), \beta^{evo}(t)\right] \ . \tag{4.24}$$

where we mean that the commutator acts on each of the components of $\beta^{evo}(t)$. By

taking the derivative of (4.21) we see that

$$\frac{d}{dt}\beta^{evo}(t) = \frac{dU^{evo}(t)^\dagger}{dt}c + \frac{dV^{evo}(t)^\dagger}{dt}c^\dagger \ . \tag{4.25}$$

We can now expand the commutator as

$$\frac{dU^{evo}(t)^\dagger}{dt}c + \frac{dV^{evo}(t)^\dagger}{dt}c^\dagger = i\left[c^\dagger hc + \frac{1}{2}c^\dagger\Delta c^\dagger - \frac{1}{2}c\ \Delta^* c, U^{evo}(t)^* c + V^{evo}(t)^* c^\dagger\right] \ .$$

Using the anti-commutation relations it is straightforward to prove that

$$\frac{dU^{evo}(t)^\dagger}{dt}c + \frac{dV^{evo}(t)^\dagger}{dt}c^\dagger = i\left(U^{evo}(t)^\dagger h - V^{evo}(t)^\dagger\Delta^*\right)c + i\left(U^{evo}(t)^\dagger\Delta - V^{evo}(t)^\dagger h^*\right)c^\dagger \ .$$

Applying the same reasoning to $\beta^\dagger$, gives

$$\frac{dV^{evo}(t)^T}{dt}c + \frac{dU^{evo}(t)^T}{dt}c^\dagger = i\left(V^{evo}(t)^T h - U^{evo}(t)^T\Delta^*\right)c + i\left(V^{evo}(t)^T\Delta - U^{evo}(t)^T h^*\right)c^\dagger \ .$$

Putting all the pieces together gives

$$\frac{d}{dt}\mathcal{W}_0^{evo}(t)^\dagger(t) = i\mathcal{W}_0^{evo}(t)^\dagger\mathcal{H}(t) \ , \tag{4.26}$$

which in turn is the same as (4.23).
The formal solution of equations (4.23,4.26) is well known and can be written as

$$\mathcal{W}_0^{evo}(t) = \mathcal{T}e^{-i\int_0^t \mathcal{H}(t')dt'}\mathcal{W}_0(0) \ . \tag{4.27}$$

The use of the Onishi formula and of (4.27), allows us to track what happens to the underling Fock space without any need to resort to it. In the next section and the following ones, we will put this general framework to work for a specific case.

4.2 The model

The model we will consider is of a generalization of the spinless p-wave superconductor that we saw in Section 3.1 and can be written as

$$H = -\sum_{j=1}^{N-1}(wc_j^\dagger c_{j+1} + \tilde{\Delta}c_j^\dagger c_{j+1}^\dagger + h.c.) - \sum_{j=1}^{N}(\tilde{\mu}_j + \lambda_j)c_j^\dagger c_j \tag{4.28}$$

where, as before, c_j is the fermionic annihilation operator at the j'th lattice site. $\tilde{\mu}_j$ is the lattice chemical potential and w represents the hopping strength between neighboring lattice sites; $\tilde{\Delta} \neq 0$ is the superconducting gap, which in the following we will suppose to be real and constant along all the wire.
Disorder in the chemical potential is introduced using the Gaussian random variable

λ_j for which mean and variance are respectively

$$\langle \lambda_j \rangle = 0 \qquad \langle \lambda_i \lambda_j \rangle = \alpha \delta_{ij}/a \tag{4.29}$$

and a is the lattice spacing.

The chemical potential $\tilde{\mu}_j$ can vary across the wire and will be used to control the boundaries between topological regions (where $|\tilde{\mu}_j| < 2|w|$) and non-topological regions (where $|\tilde{\mu}_j| > 2|w|$). As we saw in Section 2.3, Majorana bound states are localised at the boundaries between topological and non-topological regions in the wire.

The continuum limit of the chain can be obtained by taking the total number of lattice sites $N \to \infty$ and the lattice spacing $a \to 0$, with the length of the wire $L = Na$ kept constant.
In this limit, repeating the argument we gave at the end of Section 3.1, it can be shown that the lattice Hamiltonian (4.28) becomes

$$H = \int_0^L dx \mathbf{\Psi}^\dagger(x)[(-\partial_x^2/2m - \mu(x) - \lambda(x))\sigma_z + \Delta \partial_x \sigma_x]\mathbf{\Psi}(x) \ , \tag{4.30}$$

where $\mathbf{\Psi}^\dagger(x) = (c^\dagger(x)\, c(x))$ and the effective parameters m, μ, Δ and λ are related to the bare quantities as

$$m = 1/(2wa^2) \qquad \mu(x) = \tilde{\mu}_{x/a} + 2w \qquad \Delta = 2a\tilde{\Delta} \qquad \lambda(x) = \lambda_{x/a} \ . \tag{4.31}$$

The boundary wall separating a topological and non-topological regions, at a position x_{wall} along the wire, here and in the following, will be modelled by a sigmoid function for the chemical potential

$$\mu(x) = \mu_{NT} + \frac{\mu_T - \mu_{NT}}{1 + e^{-(x - x_{\text{wall}})/\sigma}} \ , \tag{4.32}$$

where σ characterises the steepness of the wall and $\mu_{T(NT)}$ is the chemical potential in the non-trivial topological region (trivial topological region). See Fig. 4.1 for an illustration. For convenience, in Eq. (4.32) we use the continuous label x instead of the discrete label j [i.e., $\tilde{\mu}_j \to \mu(x)$], although the lattice sites always appear at the discrete positions $x = ja$, where a is the lattice spacing and $j = 1, ..., N$ is an integer.

Multiple walls along the wire are modelled by adding sigmoid functions at various positions ($x_{\text{wall}}^{(2)}$, $x_{\text{wall}}^{(3)}$, etc.) along the wire, with an appropriate normalisation, to give the desired value of the chemical potential between any two walls. In the two-wire scenario described in Section 4.5 and in Fig. 4.1, we choose the normalisation such that the chemical potential at the outer boundary walls is $\mu = 20w$, and at the middle wall is $\mu = 2.5w$ (unless otherwise stated).

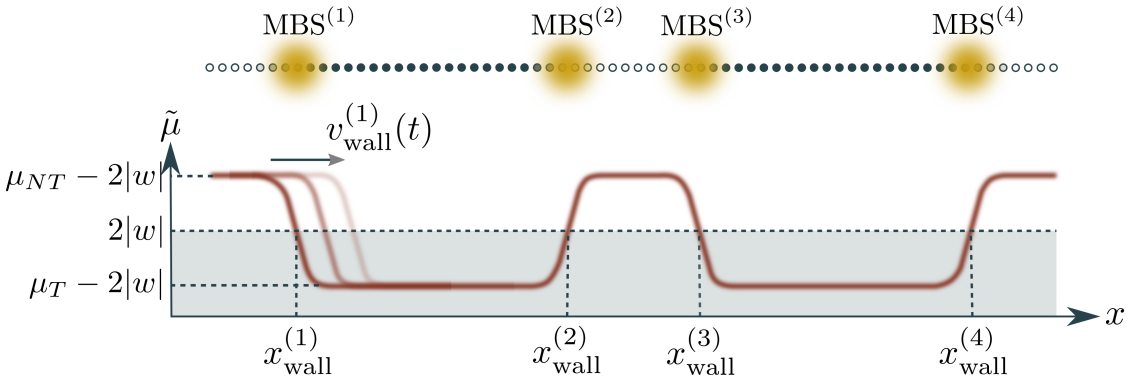

Figure 4.1: Top: A schematic illustration of the Kitaev chain used in the following. Majorana bound states (MBS) are localised at the boundaries between topological and non-topological regions. Bottom: The chain is in a topological phase in regions where $|\mu| < 2|w|$ (the shaded area) and in a non-topological phase in regions where $|\mu| > 2|w|$. The MBS at $x^{(i)}_{\text{wall}}$ is manipulated by moving the boundary wall with a velocity profile $v^{(i)}_{\text{wall}}(t) = dx^{(i)}_{\text{wall}}(t)/dt$.

It will be useful for what follows, to define the Fermi momentum and the Fermi velocity as

$$k_F = \sqrt{2m\mu_T} \qquad v_F = \frac{k_F}{m} \,. \tag{4.33}$$

which are the usual definition restricted to the topological phase. The gap energy and the finite localization length due to disorder will be defined as

$$E_{\text{gap}} = \Delta k_F \qquad l = \frac{v_F^2}{\alpha} \,. \tag{4.34}$$

The Hamiltonian (4.28) falls into the BdG framework that we described in the previous section, therefore its solution can be obtained through the methods developed there. In particular, this set-up will allow us to dynamically evolve the system by considering a time dependence of $x^{(i)}_{\text{wall}}(t)$. This will result in a time dependent chemical potential and, consequently, a time dependent Hamiltonian.
More explicitly, given a time dependent $H(t)$, we can write it as

$$H(t) = \sum_{n=1}^{N} \epsilon_n(t)(\beta_n^\dagger(t)\beta_n(t) - 1/2) \tag{4.35}$$

where the BdG transformations are

$$\begin{aligned} \beta_n(t) &= \sum_j U_{j,n}(t)c_j + V^*_{j,n}(t)c_j^\dagger, \\ \beta_n^\dagger(t) &= \sum_j U^*_{j,n}(t)c_j^\dagger + V_{j,n}(t)c_j, \end{aligned} \tag{4.36}$$

Here and in the following, we will assume that the positive single particle spectrum is labeled in increasing order $\epsilon_0 \leq ... \leq \epsilon_{N-1}$. Pairs of Majorana bound states, if

well separated, are associated with zero energy modes ($\epsilon_0 \approx 0$, $-\epsilon_0 \approx 0$,... etc.). If there are m such zero modes $\{\beta_j\}_{j=0}^m$, then there are 2^m degenerate ground states $(\beta_0^\dagger)^{l_0}...(\beta_m^\dagger)^{l_m}|\Phi_0\rangle$, where $l_j \in \{0,1\}$ and $|\Phi_0\rangle$ is the quasi-particle vacuum described in Section 4.1.

4.3 Dynamics of the topological qubit

As we said our aim is to study possible sources of errors on the Majorana qubit. In Section 3.3.1 we saw that, in order to have a Majorana qubit, we need to consider four Majorana zero modes. This is implemented in our model with four boundary walls at the positions $x_{\text{wall}}^{(1)}$, $x_{\text{wall}}^{(2)}$, $x_{\text{wall}}^{(3)}$, $x_{\text{wall}}^{(4)}$. We again refer to Fig. 4.1 for a pictorial representation.
The qubit space is then encoded in either the global even or odd parity subspace of the associated 4-fold degenerate ground state space

$$|\Phi_0\rangle \qquad \beta_0^\dagger|\Phi_0\rangle \qquad \beta_1^\dagger|\Phi_0\rangle \qquad \beta_0^\dagger\beta_1^\dagger|\Phi_0\rangle \ .$$

We will choose our logical qubit to be spanned by the ground states of the even-parity sector

$$|\bar{0}\rangle \equiv |\Phi_0\rangle \qquad |\bar{1}\rangle \equiv \beta_0^\dagger\beta_1^\dagger|\Phi_0\rangle. \tag{4.37}$$

Since the Hamiltonian $H(t)$ can be time-dependent, the spectrum $\epsilon_n(t)$, the normal mode operators $\beta_n(t)$, and the degenerate ground states $\{|\bar{0}(t)\rangle, |\bar{1}(t)\rangle\}$ can also be time-dependent[2].

Suppose therefore that at the initial time $t = 0$, the system is in the superposition state

$$|\psi(0)\rangle = \alpha_0|\bar{0}(0)\rangle + \alpha_1|\bar{1}(0)\rangle \ , \tag{4.38}$$

with $|\bar{0}(0)\rangle$ and $|\bar{1}(0)\rangle$ are ground states of the Hamiltonian $H(t)$ at time $t = 0$. At a later time the system has evolved to the state

$$|\psi(t)\rangle = \mathcal{T}e^{-i\int_0^t H(t')dt'}|\psi(0)\rangle \ . \tag{4.39}$$

If the boundary walls, and hence the Hamiltonian $H(t)$, are changed very slowly, then by the adiabatic theorem [38, 39], in the ideal case, the system at a later time

[2]We note that the notation here could lead to the misconception that the qubit-space is identified with the occupation numbers of the zero modes alone. This would in turn imply that fidelity measures of the qubit-space can be computed by performing a partial trace over the bulk-eigenmodes. In the following we will take the view that readout protocols that can distinguish fermionic and vacuum channels (see for example [60]) must, in some guise, project to the actual energy eigenstates and, as such, should also be able to detect errors that come from states where the occupation numbers of some bulk modes, together with one or both zero modes, have been flipped.

t will remain in a superposition of the instantaneous ground states ($|\bar{0}(t)\rangle$, $|\bar{1}(t)\rangle$, which constitute the computational basis),

$$|\psi_{\text{ideal}}(t)\rangle = \alpha_0|\bar{0}(t)\rangle + \alpha_1|\bar{1}(t)\rangle \ , \tag{4.40}$$

with the same amplitudes as the initial state. This is the key feature of topological computation: if we assume adiabaticity, the only way to rotate within the ground state space is to braid MBS around each other and we regard $|\psi_{\text{ideal}}(t)\rangle$ as the ideal, error-free evolution.

Deviations from adiabaticity will lead to excitation of the bulk modes, corresponding to qubit loss. We quantify the qubit-loss by the probability P_{loss} that the system is not in one of our instantaneous qubit states:

$$P_{\text{loss}}(t) = 1 - |\langle\psi(t)|\bar{0}(t)\rangle|^2 - |\langle\psi(t)|\bar{1}(t)\rangle|^2 \ ; \tag{4.41}$$

therefore $P_{\text{loss}} = 0$ if there is no qubit-loss and $P_{\text{loss}} = 1$ if the qubit is completely lost.

Since qubit loss corresponds to energy excitations, qubit-loss errors can, in principle, be detected by projective measurements of energy. More damaging are the undetectable errors resulting from the bulk excitations returning to the ground state. We consider two types of qubit error: bit-flips and phase-flips.

A bit-flip error occurs if the system returns to the qubit space in the state

$$|\psi_{\text{bit}}(t)\rangle = \alpha_0|\bar{1}(t)\rangle + \alpha_1|\bar{0}(t)\rangle \ , \tag{4.42}$$

i.e. with the qubit basis states exchanged ($|\bar{1}(t)\rangle \leftrightarrow |\bar{0}(t)\rangle$). We quantify the bit-flip error with the probability:

$$P_{\text{bit}}(t) = |\langle\psi(t)|\psi_{\text{bit}}(t)\rangle|^2 \ . \tag{4.43}$$

In the following study of this type of error (Section 4.5.1), to not over complicate the discussion, we will generally choose $\alpha_0 = 0$ and thus the bit-flip error will simply be given as

$$P_{\text{bit}}(t) = |\langle\psi(t)|\bar{1}(t)\rangle|^2 \ . \tag{4.44}$$

A Phase-flip error occurs if the system returns to the qubit state

$$|\psi_{\text{phase}}(t)\rangle = \alpha_0|\bar{0}(t)\rangle - \alpha_1|\bar{1}(t)\rangle \ , \tag{4.45}$$

so with a changed sign in correspondence of $|\bar{1}\rangle$. We quantify this type of error with the probability:

$$P_{\text{phase}}(t) = |\langle\psi(t)|\psi_{\text{phase}}(t)\rangle|^2 \ . \tag{4.46}$$

In the following discussions of phase-flip error (see Section 4.5.2) we will choose $\alpha_0 = \alpha_1 = 1$, which means, more explicitly

$$|\psi(0)\rangle \equiv \frac{1}{\sqrt{2}}(|\bar{0}\rangle + |\bar{1}\rangle) \tag{4.47}$$

and

$$|\psi_{\text{phase}}(t)\rangle \equiv \frac{1}{\sqrt{2}}(|\bar{0}(t)\rangle - |\bar{1}(t)\rangle) \ . \tag{4.48}$$

As already mentioned, all the overlaps will be numerically evaluated using the Onishi formula.

4.4 Qubit loss in single wall movements

In this section we will discuss how simple movement protocols of the external walls affect $P_{\text{loss}}(t)$, but first we will review the concept of critical velocity

4.4.1 Critical velocity and propagating excitations

It is well known [55, 56, 61] that, when considering non-adiabatic effects on the Kitaev model, the concept of critical velocity emerges. Roughly speaking this velocity corresponds to a threshold velocity of the wall movement, above which it is not possible to reach the adiabatic limit.

To understand how this goes, consider the movement with velocity $v(t)$ of one of the walls separating the topological phase from the non-topological phase. At least locally we can consider the effects of this movement by transforming to a frame that moves at velocity $v(t)$. This transformation is implemented by the translation operator

$$W(t) = \exp\{-i\hat{P}\int_0^t v(t')dt'\} \ ,$$

where $\hat{P}$ is the momentum operator. The Hamiltonian in the moving frame, compatible with the time dependent Schrödinger equation, is given by

$$H'(t) = W(t)H(t)W(t)^\dagger + i\frac{dW(t)}{dt}W^\dagger(t) = H(0) + \hat{P}v(t) \ , \tag{4.49}$$

where the first term is $H(0)$ because we are supposing that time dependence in $H(t)$ enters only through a spatial translation by a distance $\int_0^t v(t')dt'$.
If we consider the Kitaev chain the additional term $\hat{P}v(t)$, with periodic boundary conditions, can be written as

$$\hat{P}v(t) = \sum_{j=1}^{N-1} \frac{v(t)}{i2a}(c_j^\dagger c_{j+1} - c_j^\dagger c_{j-1}) \ . \tag{4.50}$$

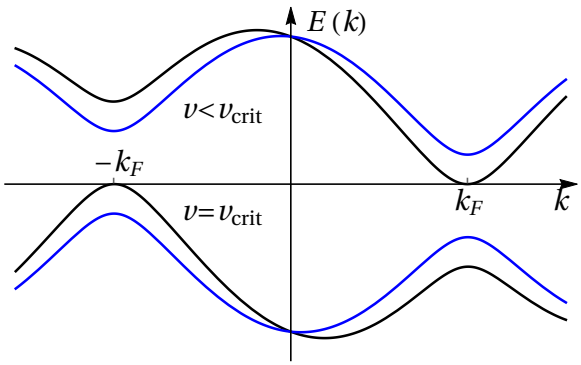

Figure 4.2: Bulk single particle energies of the instantaneous Hamiltonian in the "moving frame" $v < v_{crit}$ (blue) and $v = v_{crit}$ (black), where the gap is closed.

This means that the bulk, single particle energies for a Kitaev chain (plotted in Fig. 4.2) is given by[3]

$$\epsilon(k) = \pm\sqrt{(-\tilde{\mu} - 2w\cos(ka))^2 + 4\tilde{\Delta}^2\sin^2(ka)} + \frac{v(t)}{a}\sin(ka)\ . \tag{4.51}$$

Remembering that $\tilde{\Delta} = \frac{\Delta}{2a}$, it can be seen that for $v < |\Delta|$ the spectrum is gapped (so long as $\mu \neq 0$ and $\Delta \neq 0$). However, when $v \geq |\Delta|$ the spectrum becomes gapless at approximately either the positive or negative Fermi momentum.
This argument suggests that the behaviour of the system for $v < |\Delta|$ and $v \geq \Delta$ is completely different and that there is a critical velocity $v_{crit} = \Delta$ separating the normal regime from the one in which the movement of the wall always ends up producing excitations, irrespective of how slowly we accelerate it[4].

The moving frame picture also allows estimating the group velocity of the excitations produced by the wall movement when $v < v_{crit}$.
Consider in fact Figure 4.2 and suppose that the wall movement, through some diabatic effect, manages to excite some quasiparticle in the excited states. In the ground state of the system all the one particle states with $\epsilon < 0$ are occupied. For a sub-critical velocity $v < v_{\text{crit}}$, the occupied one-particle state with the highest energy is at $k \approx -k_F$, while the lowest energy unoccupied one-particle state is at $k \approx k_F$. The smallest energy excitation between states has, therefore, a momentum of $2k_F$. The excitations are composed of quasi-particles and quasi-holes (quasi-holes will eventually be reflected at the wall) and this means that the excitations produced by the non-adiabatic effects travel with a velocity peaked approximately around v_F.

[3]In momentum space the Hamiltonian becomes

$$H = \sum (c_k^\dagger c_{-k}) H_k \begin{pmatrix} c_k \\ c_k^\dagger \end{pmatrix}$$

with

$$H_k = (\tilde{\mu} - 2w\cos ka)\sigma^z + 2\tilde{\Delta}\sin k\sigma^y + \frac{v(t)}{a}\sin k\ ,$$

from which the single particle spectrum simply follows by diagonalisation.

[4]Note that this is the same as what happens in superfluids.

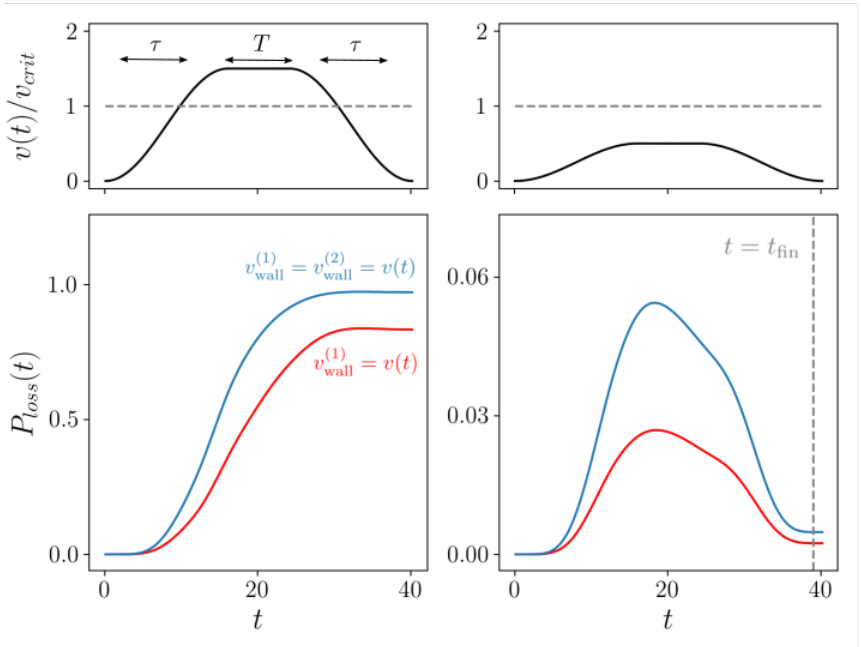

Figure 4.3: Qubit-loss for $v_{\max} > v_{\text{crit}}$ (left panel) and $v_{\max} < v_{\text{crit}}$ (right panel). The corresponding wall velocity profiles are plotted above. We see that the final qubit loss is larger for two moving walls than for a single moving wall (blue lines vs. red lines) (Plotted for $\Delta = 0.4$).[Other parameters: $a = 0.5$, $m = 0.5$, $L = 200$, $\mu_T = 1.0$.]

We will discuss this further in Section 4.5.1.

4.4.2 Qubit loss in a Majorana transport protocol

In order to put our intuition to a test, consider the transport of the first Majorana zero modes constituting the qubit at wall 1, between two different positions on the wire. To model this transport, we consider a velocity profile of the form

$$v^{(1)}_{\text{wall}}(t) = \begin{cases} v_{\max} \frac{1-\cos\left(\frac{\pi}{\tau}t\right)}{2} & 0 \leq t \leq \tau \\ v_{\max} & \tau \leq t \leq \tau + T \\ v_{\max} \frac{1-\cos\left(\frac{\pi}{\tau}(t-T)\right)}{2} & \tau + T \leq t \leq 2\tau + T \\ 0 & \text{otherwise .} \end{cases} \tag{4.52}$$

I. e. we accelerate the wall from zero velocity to a maximum velocity $v_{\max}$ and keep moving it with a constant velocity for a period T, before decelerating the wall back to zero velocity (see Fig. 4.3, top panels). A large τ corresponds to a slow acceleration of the wall, while a $\tau = 0$ corresponds to a sudden movement.

The difference between the $v < v_{\text{crit}}$ regime and the $v > v_{\text{crit}}$ regime, is revealed by comparing the left and right panels in Fig. 4.3. We see that at some time t_{fin} after the wall movement has ended, the final qubit-loss $P_{\text{loss}}(t_{\text{fin}})$ is small if $v_{\max} < v_{\text{crit}}$, but can be close to 1 if $v_{\max} > v_{\text{crit}}$. Note that in the $v < v_{\text{crit}}$ regime, the motion is

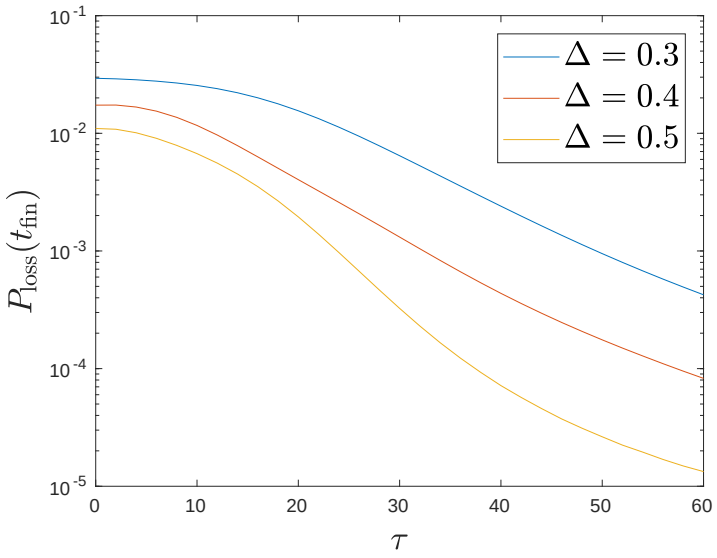

Figure 4.4: The final qubit-loss at some time t_{fin} after the walls have come to rest, plotted as a function of $\tau = 1/\omega$ (for $v_{\mathrm{max}} = 0.1$ and $T = 30$). [Other parameters: in all figures, $a = 0.5$, $m = 0.5$, $L = 200$, $\mu_T = 1.0$.]

by no means adiabatic (except at very low velocity) and there is considerable qubit loss during the wall's motion in the acceleration phase, however the system returns to the ground state manifold as the wall is slowed down. This means that the wall can be moved far faster than what would be naively thought, without incurring in a permanent qubit loss. This has also been noted in earlier works on this subject [56, 55] and it is linked to the notion of super-adiabaticity, where the motion can be considered adiabatic in a moving frame (see e.g Ref. [62]). From now on we will refer to this regime as super-adiabatic.

Along the same lines, it makes sense to also consider the motion of two boundary walls (the two leftmost walls at $x^{(1)}_{\mathrm{wall}}$ and $x^{(2)}_{\mathrm{wall}}$), both by identical velocity profiles $v^{(1)}_{\mathrm{wall}}(t) = v^{(2)}_{\mathrm{wall}}(t)$ given as in Eq. (4.52), so that the two walls are moving in sync and that the length of the wire remains constant, see e.g. Ref [55]. The numerical results shown in Fig. 4.3 show that there is no advantage to coordinated wall movement, compared to a single moving wall. Indeed in the right panel of Fig. 4.3 we see that for $v_{\mathrm{max}} < v_{\mathrm{crit}}$ the qubit-loss is approximately a factor of two higher than for a single moving boundary wall, and that this factor persists throughout the movement protocol.

In order to investigate the dependence of the qubit-loss on the wall acceleration, in Fig. 4.4 we plot the final qubit-loss $P_{\mathrm{loss}}(t_{\mathrm{fin}})$ as a function of τ in the subcritical ($v < v_{\mathrm{crit}}$) regime. For large τ, corresponding to slow wall acceleration, we see that the qubit-loss follows an exponential decay (in agreement with the results of Ref. [55]). However, the behaviour is different in the region where $\tau \to 0$, corresponding to sudden movement of the wall. In this limit, the qubit-loss reaches its maximum value (for a given $v_{\mathrm{max}} < v_{\mathrm{crit}}$). Since the qubit-loss saturates at a small value as the

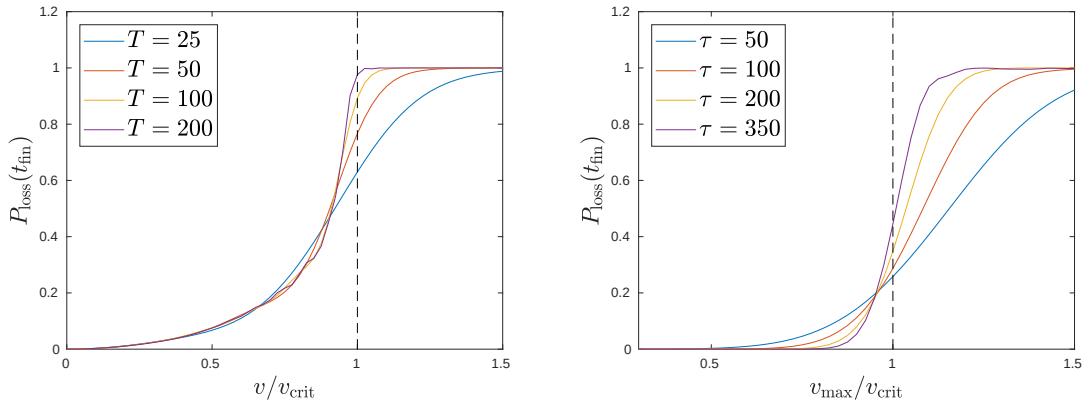

(a) (b)

Figure 4.5: (a) The final qubit-loss in the limit of sudden wall acceleration ($\tau \to 0$). As T gets large we see a sharp distinction emerge between the $v_{\text{max}} > v_{\text{crit}}$ and $v_{\text{max}} < v_{\text{crit}}$ regimes (here, $v_{\text{crit}} = |\Delta| = 0.2$). (b) Final P_{loss} for different τ and the length of the time the system continues moving at v_{max}, $T = 0$. As we can see, also in this case there are two different behaviours of the system depending on whether $v_{\text{max}}/v_{\text{crit}}$ is greater or lesser than 1. This graph is produced with $\Delta = 0.4$. [Other parameters: in both figures, $a = 0.5$, $m = 0.5$, $L = 200$, $\mu = 1.0$ (in the topological region)].

acceleration is increased, we conclude that there is no critical acceleration analogous to the critical velocity in this set-up.

In Figure 4.5(a) we plot the qubit-loss as a function of v_{max} in the limit of sudden movement ($\tau \to 0$). As the time T spent at the maximum velocity increases, we see a sharp distinction emerging between the $v_{\text{max}} > v_{\text{crit}}$ and $v_{\text{max}} < v_{\text{crit}}$ regimes: for $v_{\text{max}} > v_{\text{crit}}$ the qubit-loss approaches unity and all the information is lost into bulk states, while for $v_{\text{max}} < v_{\text{crit}}$ we have $P_{\text{loss}}(t_{\text{fin}}) < 1$.

In Figure 4.5(b) we show the qubit-loss for $T = 0$ and increasing τ plotted against different v_{max}. It can be seen that for larger and larger τ the qubit-loss tends closer and closer to a step function. This shows that our intuition behind the critical velocity is correct, as it means that for $v_{\text{max}} < v_{\text{crit}}$ we can in principle reach the adiabatic limit by accelerating slow enough and that this is generally not possible for $v_{\text{max}} > v_{\text{crit}}$. In this regime, the system inevitably loses some information into excitations of the bulk.

Energy corrections and effective mass

When the system comes to a complete stop the non-adiabaticity of the protocol translates into a $P_{\text{loss}}(t_{\text{fin}})$ that is not exactly zero. The accumulated deviations from the super-adiabatic regime result in a final resting energy above that of the ground state.

During a super-adiabatic protocol, the instantaneous energy loss can be related

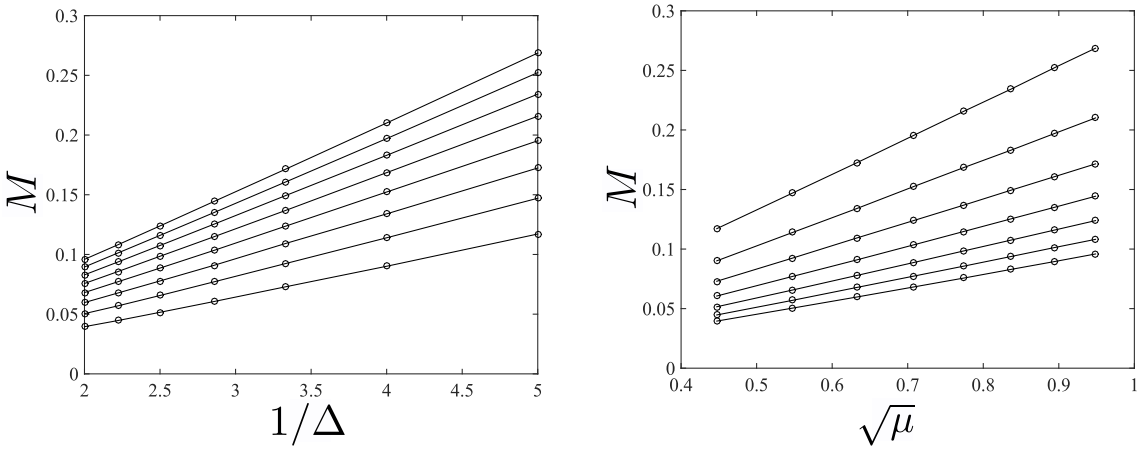

(a) (b)

Figure 4.6: The effective mass scales as (a) $M \propto 1/\Delta$ and (b) $M \propto \sqrt{\mu} \propto k_F$. This allows us to relate the topological gap and the effective wall mass as $E_{\rm gap} \propto k_F^2/2M$.

to a kinetic energy with an effective mass

$$M \propto k_F^2/E_{\rm gap} = k_F/\Delta \ . \tag{4.53}$$

To confirm this in the hard-wall limit we work in the moving frame picture and estimate the energy increase with respect to the static ground-state energy as:

$$E(t) = \frac{1}{2}\mathrm{Tr}_+(\mathcal{W}_0^{evo}(t)^\dagger H(0)\mathcal{W}_0^{evo}(t) - \mathcal{W}_0(t)^\dagger H(0)\mathcal{W}_0(t)) \tag{4.54}$$

where the subscript + on the trace means we only use positive energy modes ($[U^T, V^T]^T$) and $\mathcal{W}_0^{evo}(t)$, $\mathcal{W}_0(t)$ are defined as in Section 4.1.1. In general, we find that if the motion is super-adiabatic then

$$E(t) \approx \frac{M}{2}\gamma(t)v(t)^2. \tag{4.55}$$

where $\gamma(t) = 1/\sqrt{1 - v(t)^2/\Delta^2}$. The effective rest mass is plotted as a function of Δ and μ in Figure 4.6(a),(b). The scaling allows us to relate the topological gap $E_{\rm gap} \propto k_F^2/2M$.

In Figure 4.7 we show a comparative plot between $E(t)$ and $\frac{M}{2}\gamma(t)v(t)^2$. The value of the effective mass is obtained by the least square method.

4.4.3 Qubit-loss due to an oscillating wall

We will now consider the qubit loss $P_{\rm loss}$ due to the motion of a single boundary wall, the wall at position $x_{\rm wall}^{(1)}$, with an oscillating velocity profile of the form:

$$v_{\rm wall}^{(1)}(t) = v_{\rm max}\sin(\omega t). \tag{4.56}$$

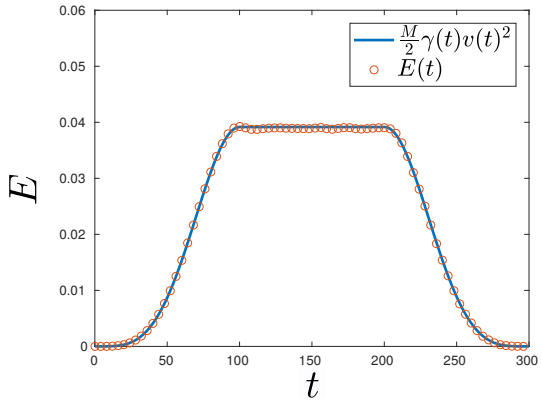

Figure 4.7: the solid line represents the curve $\frac{M}{2}\gamma(t)v(t)^2$. The empty circles represent the value of $E(t)$ obtained through (4.55). The value of $M \approx 1.69$ was obtained by fitting the two curves. Other parameters were $L = 100$, $\Delta = 0.4$, $\mu = 1$, $a = 0.5$ and $m = 0.5$. The velocity profile was chosen as in (4.52), with $\tau = 50$, $T = 100$ and $v_{\max} = 0.2$.

Since the wall is continuously moving, it is appropriate to calculate the time-averaged rate of qubit-loss

$$\langle dP_{\text{loss}}/dt\rangle = \frac{1}{t'' - t'}\int_{t'}^{t''} dt(dP_{\text{loss}}(t)/dt) \ , \tag{4.57}$$

over some interval $t'' - t' = n\pi/\omega$ spanning some periods of the oscillation. The colour map in Fig. 4.8(a) shows $\langle dP_{\text{loss}}/dt\rangle$ as a function of the wall motion parameters ω and $v_{\max}$. We can identify several features. First, when $v_{\max} = 0$ or when $\omega = 0$ the qubit-loss rate is zero, as expected, since the wall is static in this case. For small values of $v_{\max}$ the qubit-loss rate is small irrespective of the value of ω. This is the adiabatic regime where the wavefunction of the system closely follows the ground state of the instantaneous Hamiltonian. However, for velocities larger than the critical velocity $v_{\text{crit}} = |\Delta|$ the qubit-loss rate is large, even for small frequencies ω. This is consistent with the results of Ref. [56, 55].
In the same figure we see that the rate of qubit-loss is highest when the wall oscillation frequency ω is close to the gap energy $E_{\text{gap}} = \Delta k_F$. This is verified in Figure 4.8(b), where we plot a cross-section of Fig. 4.8(a) at a fixed sub-critical value of $v_{\max}$, for different values of the superconducting gap Δ (and hence different values of the gap $E_{\text{gap}} = \Delta k_F$). Figure 4.8(b) also shows that for $\omega \gg E_{\text{gap}}$, the qubit-loss rate decreases quickly.

While the frequency $\omega_{\max}$ at which we have maximum qubit-loss rate grows with Δ, the actual qubit-loss rate $\langle dP_{\text{loss}}/dt\rangle_{\max}$ decreases (see insets of Figure 4.8(b)). This decrease can be partially put down to the fact that the overall rate of qubit loss depends on the oscillation amplitude. For our choice of parameterisation given in (4.56) we have

$$x^{(1)}_{\text{wall}}(t) = x^{(1)}_{\text{wall}}(0) + \frac{v_{\max}}{\omega}(1 - \cos\omega t) \tag{4.58}$$

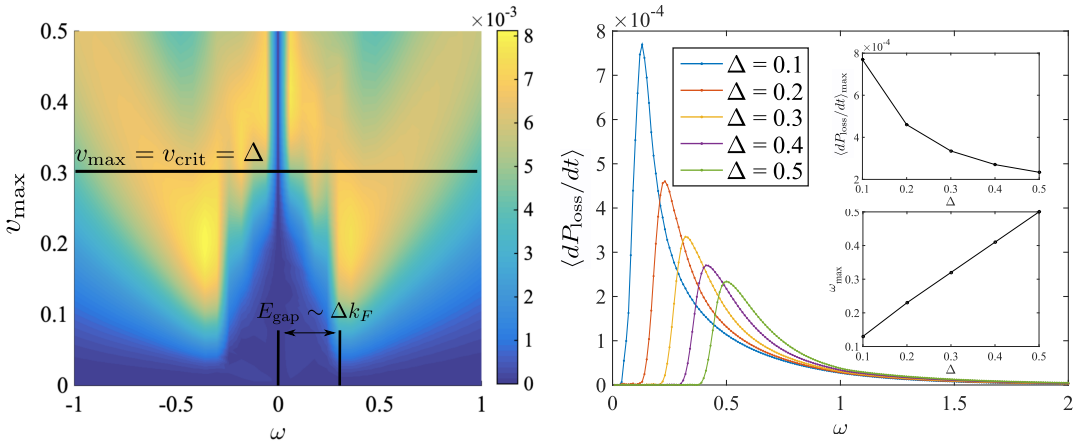

(a) (b)

Figure 4.8: (a) The time-averaged qubit-loss, as a function of the wall velocity parameters $v_{\max}$ and ω. The horizontal black line shows the critical velocity $v_{\text{crit}} = |\Delta| = 0.3$. To generate this figure we used $L = 200, a = 1, m = 0.5, v(t) = v_{\max} \sin(\omega t)$, and $\mu = 0.5$. The boundary potentials, in this case, were set to be essentially infinite ($\mu_{\text{boundary}} = -2000$) and the wall gradient with $\sigma = 1$ as in the parameterisation (4.32). (b) A cross section of (a) at $v_{\max} = 0.02$. We see that the maximum qubit-loss rate occurs when the frequency is close to E_{gap}, but where the maximum value decays as $1/E_{\text{gap}}$. The low frequency regime corresponds to the super-adiabatic limit and so we typically see very low rates of qubit loss error. Crucially, because the maximum resonant frequency scales with E_{gap}, in the high frequency regime, increasing the topological order parameter can make the system more susceptible to errors.

and thus, for fixed maximum velocity, we have a smaller oscillation amplitude at higher frequencies.

For fixed frequencies larger than the gap (see e.g., $\omega \approx 0.6$ in Figure 4.8(b)), we see that the rate of qubit-loss increases as Δ is increased. This is in contrast to the situation in the low frequency adiabatic regime, where increasing Δ (and hence increasing gap E_{gap}) decreases the rate of qubit-loss. Thus while it makes sense to try to maximise the topological gap to counteract low-frequency noise and/or errors associated with a deliberate motion of the topological boundary, the situation is more complicated if the range of perturbing frequencies extends above the frequency corresponding to the bulk gap.

In the next chapter we will address the problem of undetectable qubit errors.

4.5 Undetectable qubit errors

In this section we will analyse the bit-flip errors and phase-flip errors, which are undetectable within the common paradigm for quantum computation. These errors can be in principle corrected by means of quantum detecting/correcting codes, a scenario which topological schemes are supposed to avoid.

4.5.1 Bit-flip errors

In the previous section we saw that the movement of the boundary wall can lead to qubit-loss that can be recovered, to some extent, when $v < v_{\text{crit}}$. This raises the question: can the system return to the qubit space with an error?

First we note that, in general, we expect to generate excitations that are local because of the local nature of the perturbation. These local excitations can then propagate through the wire over time.

To investigate this, we consider a single wall (at the position $x^{(1)}_{\text{wall}}$) oscillating sinusoidally with a velocity profile

$$v^{(1)}_{\text{wall}}(t) = v_{\max} \sin(\omega t). \tag{4.59}$$

similar results can be obtained with the shuttling movement protocol given by Eq. (4.52).

In Fig. 4.9(a) we plot the deviations from the ideal particle density

$$\Omega_j(t) = \langle \Phi_0(t) | c_j^\dagger c_j | \Phi_0(t) \rangle - \langle \Psi_{\text{ideal}}(t) | c_j^\dagger c_j | \Psi_{\text{ideal}}(t) \rangle \tag{4.60}$$

as a function of time t and the position j along the wire. The plot clearly shows a particle density wave that propagates across the wire; the velocity of the propagating wave can be read off from the plot and is found to be approximately equal to the Fermi velocity v_F. This agrees with the intuition that we built in Section 4.4.1, where we saw that excitations with $2k_F$ momentum are favoured energetically.

We can now envision a mechanism for the occurrence of bit-flip errors. The excitations generated at a moving wall can travel across the wire and tunnel through non-topological regions in the wire, carrying information between Majorana zero modes. The resulting interaction between the mode and the Majoranas can, in principle, induce bit-flip errors in the topological qubit.

It is important to note that, in order for the Majorana zero modes to interact with the incoming density wave packet, one of the walls on the other side of the system must also be in motion. If this is not the case, since the density wave packet will be composed of eigenstates of the static Hamiltonian, it will not be able to dissipate at the wall, and it will simply be reflected or transmitted without any chance for the excitation to decay back into the degenerate ground state.

This is verified numerically in Fig. 4.9(b), where we show the bit-flip error P_{bit} due to the oscillation of boundary walls (the walls that are moving are indicated in curly brackets in the legend). We see that there is no bit-flip error if a single wall is moved and all other walls remain static, however, if two walls are moved, bit-flip errors P_{bit} appear abruptly after some delay. The times at which the bit-flip errors begin to appear can be estimated as the time taken for the propagating wave to

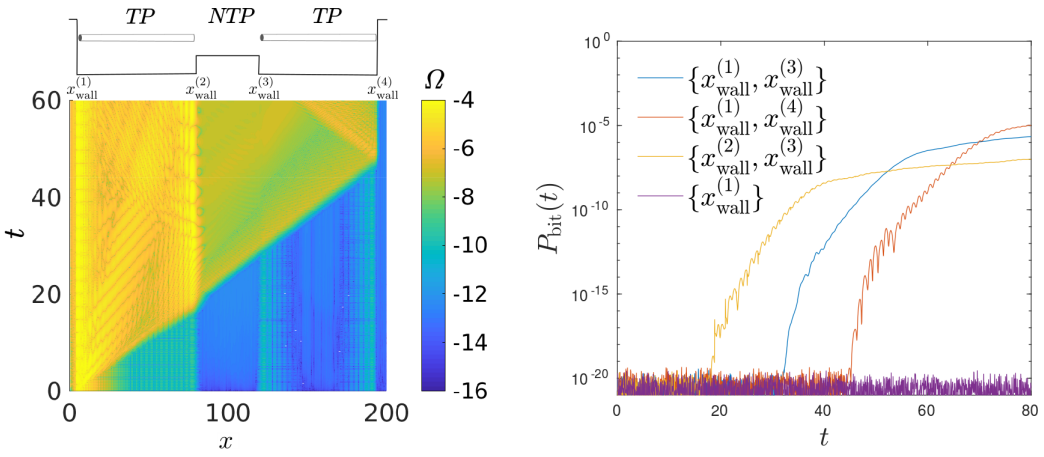

Figure 4.9: (a) The density wave packet generated by a *single* moving wall at $x^{(1)}_{\rm wall}$ travels at a velocity approximately equal to v_F. We can see the wave tunnelling through the non-topological barrier separating the topological phases (barrier height $\mu_{\rm barrier} = -2.5$). Here, $v_{\rm max} = 0.3$, and $\omega = 3$. (b) The bit-flip error $P_{\rm bit}$ increases suddenly as the excitation produced by the movement of one wall hits another moving wall (legend shows which walls are in motion). The time at which the error begins to increase can be estimated as approximately $t \approx |x^{(i)}_{\rm wall} - x^{(j)}_{\rm wall}|/v_F$ where $|x^{(i)}_{\rm wall} - x^{(j)}_{\rm wall}|$ is the distance between the two moving walls. [Other parameters for both figures: $m = 0.5$, $a = 0.5$, $\Delta = 0.4$, $L = 200$, and $\mu = 1.0$ (in the topological region).]

reach the other moving wall, i.e., as

$$t \approx \frac{|x^{(i)}_{\rm wall} - x^{(j)}_{\rm wall}|}{v_F} \ ,$$

where $|x^{(i)}_{\rm wall} - x^{(j)}_{\rm wall}|$ is the distance between the two moving walls. In particular the sudden jumps in $P_{\rm bit}$, at times compatible with our analysis on the velocity of stray excitations, provide strong evidence that the same stray excitations are responsible for the measured bit-flip error.

Effects of disorder

The central result of this section, so far, is that bit-flip error can occur in a two wire setup if there is a process whereby a quasi-particle is excited in one wire, tunnels through the middle barrier to the other wire, and then decays back to the ground state manifold. In order to avoid such a process, one straightforward approach would be to increase the barrier between the wires to prevent inter-wire tunneling. However, within the general schemes to manipulate quantum information using wire networks (see for example Ref. [34]), one often needs to bring neighboring Majoranas together, a process which would render the barrier more transparent and potentially would also excite more propagating quasi-particles.

Another solution to prevent quasi-particle propagation is to introduce some dis-

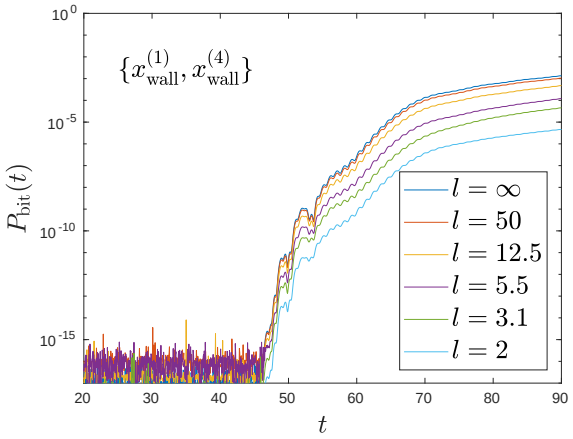

Figure 4.10: Bit-flip error is suppressed by adding disorder in the middle of the left-hand wire. Here, the disordered region is of length ~ 40, and a shorter localisation length l corresponds to increased disorder. We use $v_{\mathrm{max}}/v_{\mathrm{crit}} = 0.75$, the middle barrier height is $\mu_{\mathrm{barrier}} = -2.5$, $\sigma = 2$ and the data is averaged over 20 disorder realizations. [Other parameters used for the figure: $m = 0.5$, $a = 0.5$, $\Delta = 0.4$, $L = 200$, and $\mu = 1.0$ (in the topological region).]

order into the wires themselves. We will consider this scenario with some care.
At first, we might naively try to introduce disorder throughout all the wire. However there are downsides to doing this. In static scenarios, in fact, disorder decreases the gap between the ground state and the bulk excitation spectrum, increasing the bound-state decay length [63, 64, 65] and this results in a topological space that is less resilient to qubit-loss. Moreover, it has been shown [56] that moving the confining potential over a disordered region results in a dramatically lower critical velocity, thus severely hampering the rate at which quantum gates can be mechanically performed. An effective compromise is to deliberately disorder only the central wire regions. This allows for an effective critical velocity of the wire ends that is equal to the p-wave order parameter Δ, while also providing a region where bulk excitations are prevented from propagating and reducing the probability that the excitations originating at one wall can tunnel to another wire. This approach still allows for low barrier transparency and so the original schemes [34] for braiding and rotating Majorana pairs can be performed as usual.

In Fig. 4.10 we present the results of our numerical simulations, where disorder has been introduced in the middle of the left-hand wire. As earlier, we simulate a scenario where there is an oscillation of two walls at positions $x^{(1)}_{\mathrm{wall}}$ and $x^{(4)}_{\mathrm{wall}}$ in different wires. The figure shows the decrease in the probability of bit-flip error as we decrease the localization length l in the disordered region. This indicates that, as the disorder is increased, the wave associated with excitations, accrued at the boundaries, cannot propagate through the wire, hence reducing the probability of bit-flip error.

4.5.2 Phase-flip errors

In a two wire setup, phase-flip error can occur in precisely the same way as bit-flip error: excitations originating in one wire tunnel into the other wire and relax to the ground state. However there is another process through which phase error can occur, which importantly does not involve tunneling between wires.
This mechanism relies on the fact that the energy splittings between states in the bulk are not necessarily the same as the splittings between the ground states. In systems that experience continual qubit-loss this can lead to a small but systematic phase error being returned to the qubit space, when excitations interact back with the moving Majorana zero mode.

A necessary feature here is that pairs of bulk excitations that differ in the occupation of the edge modes have slightly different energies. In non-interacting systems, this can only happen when the Majorana zero modes overlap and therefore there is a splitting between the ground states as well. In this case the time evolution generates a Rabi oscillation between the two ground states $|\psi_\pm\rangle = \frac{1}{\sqrt{2}}(|\bar{0}\rangle \pm |\bar{1}\rangle)$.
The rate of oscillation is such that

$$|\langle\psi_-(t)|\psi_+(t)\rangle| = \sin\frac{\delta(t)}{2} \ . \tag{4.61}$$

with

$$\delta(t) = \int_0^t [E_1(t') - E_0(t')]dt' \ , \tag{4.62}$$

where we have introduced the energies of the two ground states. Since this phase depends on the difference in energy between the ground states, it is related to the the decay length of the Majorana edge states.
In Ref. [55] it was noted that since the decay length of the bound states takes on a relativistic-like correction in moving frames. This rate of rotation within the ground state space can in addition depend on velocity of the system as well.

The correction to the phase oscillation that we study here depends on the presence of a continual qubit-loss/gain channel between the ground state and excited states. If this is the case then energy mismatches between bulk eigenstate pairs will lead to a systematic deviation from the "natural" Rabi oscillation.
To analyze this deviation, we first recall that throughout this manuscript we take the view that parts of the state which leave the ground state space are detectable. Therefore we are interested only in the phase rotation within the ground-state manifold. This means that we need to calculate the conditional probability of having a phase-flip, given that the time-evolved state is projected into the ground state manifold. This probability is given by

$$R(t) = \frac{P_{\text{phase}}(t)}{1 - P_{\text{loss}}(t)} = \frac{|\langle\psi(t)|\psi_-(t)\rangle|^2}{|\langle\psi(t)|\psi_-(t)\rangle|^2 + |\langle\psi(t)|\psi_+(t)\rangle|^2}. \tag{4.63}$$

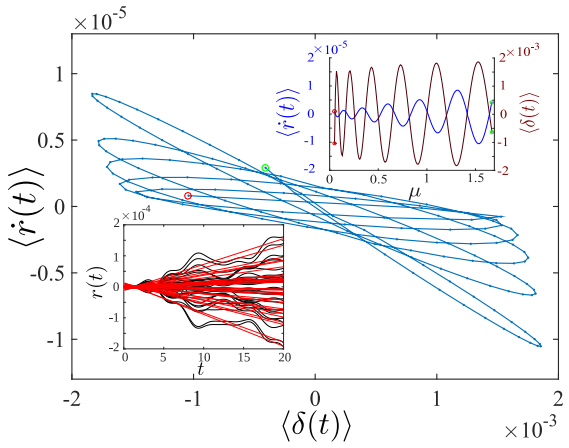

Figure 4.11: Main figure and upper inset: Qubit-loss induced deviation from the natural phase oscillation tends to act in the opposite direction to the natural oscillation. The red dots indicate $\mu = 0.03$ and the green $\mu = 1.68$. Lower inset: The deviation $r(t) = \phi(t) - \delta(t)$ (black) and the slopes of the fitted red lines give $\langle \dot{r}(t) \rangle$. To generate this figure two wires of lengths 45 and 40 were used with an essentially infinite barrier between them. The continuum order parameter was set to $\Delta = 0.4$ in the left wire and $\Delta = 0.8$ in the right. The effective electron mass was set to $m = 0.5$ and a lattice constant of $a = 0.5$ was used. The velocity of the left-hand boundary of the left wire was moved according to $v(t) = 0.1 \sin(2t)$

From here we can calculate the phase rotation angle within the ground-state manifold as

$$\phi(t) = 2 \sin^{-1} \sqrt{R(t)}, \tag{4.64}$$

and then calculate the difference from the natural rotation angle $\delta(t)$ as

$$r(t) = \phi(t) - \delta(t) \tag{4.65}$$

In Figure 4.11 we plot the behaviour of dr/dt as a function of the chemical potential μ and the natural phase oscillation due to the small even splitting in both wires. We see that the rate of this phase deviation opposes the mean splitting between the even-odd pairs $\langle \delta(t) \rangle$ that drives the natural phase oscillation. The mechanism that we describe here relies on there being differences in energies between bulk even-odd eigenpairs. In a non-interacting system this is necessarily due to a splitting of the edge modes (making them no longer perfect zero modes). This then also implies that there is a splitting between ground states and, as a result, a natural non-topological rotation within the qubit space. This process can be counteracted by making the wire longer, as this will reduce the overlap between the edge modes. The situation is different in interacting systems because in the presence of interaction, the many-particle energy spectrum can no longer be described in terms of single particle modes. One thus expects that there may not be an even-odd degeneracy for bulk states when interactions are strong, even though the ground state degeneracy is robust due to its topological nature. Indeed there is significant evidence that the

even-odd symmetry within higher energy eigenpairs breaks down in regions where bands with different fermion numbers are energetically similar [66, 67]. It may therefore be possible that phase errors similar to the one described here are possible in the presence of non-adiabaticity and interactions, even though the ground state is essentially degenerate.

Chapter 5

Generalized Spin Chains and Parafermions

As we saw in the previous section looking at the Ising model in fermionic language gives us a new way of understanding its phase transition. In particular since the fermionic quantities are non-local in terms of spin quantities, the transition in the fermionic language cannot be described by any local order parameters and we cannot use Landau-Ginzburg theory. We saw that these types of transitions are topological in nature, since they are largely independent of the local structure of the model.
In this sense it is worth looking into a simple generalization of the Ising model, in order to see if also in this case we can understand the phase transitions of this model in topological terms. The simplest generalization consists in considering a chain with $N > 2$ spins values with a $\mathbb{Z}_N$ symmetry operators. These models are known as Potts models [68, 69] and their quantum version as quantum chiral Potts models [70, 71, 72]. A great deal of work has been done in order to characterize the thermodynamic phases of these systems [73, 74, 75, 76, 77], which have shown an even richer range of possibilities than the Ising model.

As we will see in this chapter, similarly to what happens in the Ising case and using a generalization of the Jordan Wigner transformation, the degrees of freedom of these models can be transformed into non local quantities which are a generalization of Majorana modes, usually known as parafermions [78].
The topological behaviour of these models is still not completely clear and the purpose of this and the following sections will be to clarify some of its aspects. In particular we will consider the existence of zero modes in the quantum clock model. The material contained in this chapter is based on [27].

5.1 The quantum Clock Model

In the following, we will be mainly interested in the $\mathbb{Z}_N$ quantum clock Hamiltonian as given in [79, 22]. The Hamiltonian defining the model can be written in the form

$H = H_0 + fV$ and

$$\begin{aligned} H_0 &= -\sum_{k=1}^{L-1} e^{i\theta}\sigma_k^\dagger\sigma_{k+1} + e^{-i\theta}\sigma_k\sigma_{k+1}^\dagger \\ V &= -\sum_{k=1}^{L} e^{i\phi}\tau_k + e^{-i\phi}\tau_k^\dagger \end{aligned} \tag{5.1}$$

the σ and τ matrices are defined as

$$\sigma = \omega^{i-1}\delta_{ij} \qquad \tau = \delta_{i+1,j(\text{mod } N)} \tag{5.2}$$

and ω is a root of the unity

$$\omega = e^{\frac{2\pi i}{N}} \ .$$

It can be directly checked that

$$\sigma^N = \tau^N = 1$$

The Hilbert space is spanned by vectors of the form

$$|\mathbf{i}\rangle = |i_1, i_2, \ldots, i_L\rangle \tag{5.3}$$

where $i_k \in \mathbb{Z}_N$ represents the values of the "clocks" at each site and we will call this the *spin representation*. For $N = 2$ the model correspond to the transverse Ising model and the matrices σ, τ correspond to the Pauli matrices σ^z, σ^x. In the case $N = 3$ we have instead

$$\sigma = \begin{pmatrix} 1 & 0 & 0 \\ 0 & \omega & 0 \\ 0 & 0 & \omega^2 \end{pmatrix} \qquad \tau = \begin{pmatrix} 0 & 1 & 0 \\ 0 & 0 & 1 \\ 1 & 0 & 0 \end{pmatrix} \tag{5.4}$$

and for general N

$$\sigma = \begin{pmatrix} 1 & 0 & 0 & \cdots & 0 \\ 0 & \omega & 0 & \cdots & 0 \\ \vdots & & \ddots & & \vdots \\ 0 & 0 & \cdots & \omega^{N-2} & 0 \\ 0 & 0 & \cdots & 0 & \omega^{N-1} \end{pmatrix} \quad \tau = \begin{pmatrix} 0 & 1 & 0 & \cdots & 0 \\ 0 & 0 & 1 & \cdots & 0 \\ \vdots & & & \ddots & \vdots \\ 0 & 0 & \cdots & 0 & 1 \\ 1 & 0 & \cdots & 0 & 0 \end{pmatrix} \tag{5.5}$$

The commutation relations between σ and τ matrices are

$$\tau_k\sigma_j = \omega^{\delta_{k,j}}\sigma_j\tau_k \tag{5.6}$$

These models are a generalization of the Ising model and are known as chiral Potts models [70, 71, 72].

As we saw, in the Ising model, a prominent role is played by the parity operator, which in fermionic language is an operator that counts the number of fermions modulo 2. The following operator generalizes the fermion parity operator of the Ising model and will play a similar role to it in the following

$$Q_N = \prod_{k=1}^{L} \tau_k. \tag{5.7}$$

This operator moves the clock at each site one unit back and commutes with the Hamiltonian, as can be directly checked. The spectrum of the Hamiltonian thus splits into N sectors, identified by the three eigenvalues of Q_N.

Using a non-local transformation introduced by Fradkin and Kadanoff [78], analogous to the Jordan–Wigner transformation, we can rewrite the spin model in terms of parafermionic variables. Parafermionic operators are defined as follows,

$$\gamma_{2k-1} = \sigma_k \prod_{j<k} \tau_j \qquad \gamma_{2k} = \omega \sigma_k \prod_{j \leq k} \tau_j$$

and satisfy the relations

$$\gamma_k \gamma_j = \omega^{\mathrm{sign}(k-j)} \gamma_j \gamma_k \qquad \gamma_i^N = 1 \ . \tag{5.8}$$

These operators can be considered as the creation/annihilation operators for parafermionic excitations. As in the Ising case, using these relations, we can rewrite the clock Hamiltonian in terms of the parafermionic operators

$$\begin{aligned} H_0 &= -J\omega e^{i\theta} \sum_{k=1}^{L-1} \gamma_{2k}^\dagger \gamma_{2k+1} + h.c. \\ V &= -f\omega e^{i\phi} \sum_{k=1}^{L} \gamma_{2k-1}^\dagger \gamma_{2k} + h.c. \end{aligned} \tag{5.9}$$

and the parity operator becomes

$$Q_N = \omega^{-L} \prod_{k=1}^{L} \gamma_{2k-1}^\dagger \gamma_{2k} \ .$$

In general we can see that

$$Q_N \gamma_j = \omega \gamma_j Q_N \ . \tag{5.10}$$

In the exact same way as the Ising case, there exist two parafermionic operators, localised on the edges, that commute with H_0, namely γ_1 and γ_{2L}, as they do not appear in the sum and commute with all the other terms. In spin terms they are

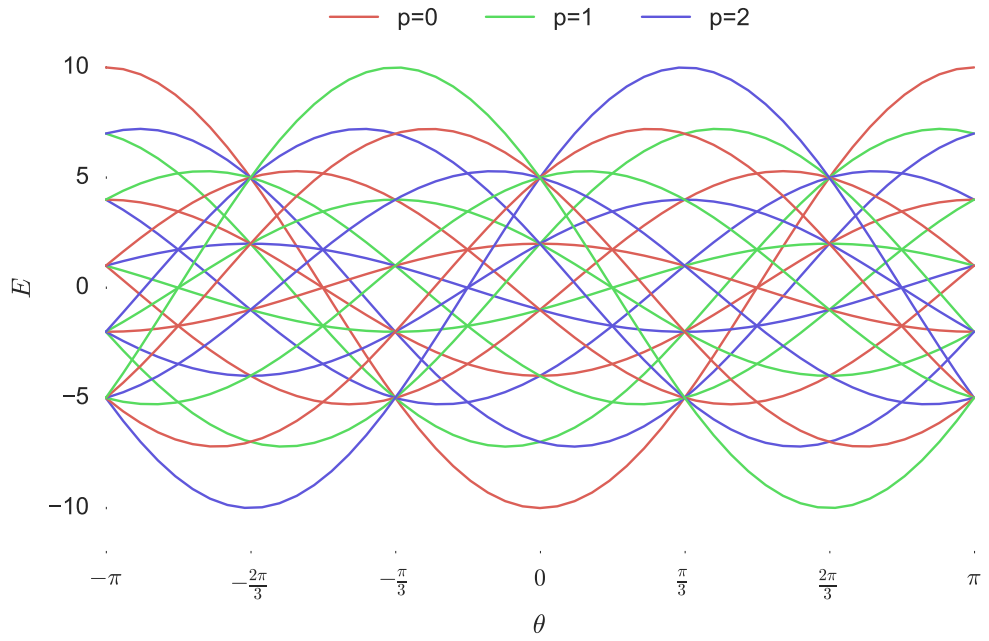

Figure 5.1: Spectrum of H_0 for $L = 6$. The different colors represent the different total domain wall parities (see Section 5.1.2).

given by

$$\gamma_1 = \sigma_1 \qquad \gamma_{2L} = \omega \sigma_L Q_N \ . \tag{5.11}$$

5.1.1 Free spectrum

In terms of the basis written above H_0 is in diagonal form and its spectrum, for a given state $|\mathbf{i}\rangle = |i_1, i_2, \ldots, i_L\rangle$ in the spin representation is given by

$$E_{i_1,i_2,\ldots,i_L} = \sum_{k=1}^{L-1} \epsilon_{i_{k+1}-i_k} = n_0\epsilon_0 + n_1\epsilon_1 + \ldots + n_{N-1}\epsilon_{N-1} \tag{5.12}$$

where

$$\epsilon_m = -2\cos\left(\frac{2\pi m}{N} + \theta\right) \tag{5.13}$$

and n_m counts the number of domain walls of type m in the state (5.3). We say that there is a domain wall of type m between sites $k+1$ and k when $i_{k+1} - i_k = m$. In particular, the absence of a domain wall is the same as a domain wall of type 0. The typical energy bands of H_0 for different values of θ are shown in Fig. 5.1 for $N = 3$.

The energy of the free model is therefore determined by the set of tuples of type $(n_0, n_1, \ldots, n_{N-1})$ such that

$$n_0 + n_1 + \ldots + n_{L-1} = L - 1 \tag{5.14}$$

Note that the spectrum of H_0 is the same in each Q_N-sector, so that three copies of each band exist, with different values of Q_N. This degeneracy may be split through the action of V and as we know this is related to the existence of a zero mode, in the sense that if a zero mode exists the degeneracy persists up to exponentially small corrections in the length of the system.

In the next chapter we will see that the degeneracy generally does not split except possibly when different bands cross. It is therefore meaningful to carefully consider when this happens.

5.1.2 Resonance points

As can be seen in Figure 5.1, in the free spectrum, it may occur that there are θ-values at which bands with different tuples $(n_0, n_1, \ldots, n_{N-1})$ have the same energy. From now on we will refer to these special points of the free spectrum as *resonance points*. As we will see in the following, these points play a fundamental role when we consider the problem of the existence of edge zero modes. It is then of interest to ask for which θ values these resonance points occur, and whether they are dense on the θ-axis in the limit $L \to \infty$.

Let us consider two bands, labelled by tuples $\vec{a}$ and $\vec{b}$ where a_j gives the number of domain-walls of type j for the first band, etc. We write $\vec{c} = \vec{a} - \vec{b}$, and note that $\vec{c}$ satisfies the following constraint

$$\sum_j^{N-1} c_j = 0 \tag{5.15}$$

From (5.12), we see that the bands labelled by $\vec{a}$ and $\vec{b}$, are degenerate precisely when

$$\cos(\theta) \sum_j^{N-1} c_j \cos(\frac{2\pi j}{N}) = \sin(\theta) \sum_j^{N-1} c_j \sin(\frac{2\pi j}{N}) \tag{5.16}$$

Assuming that both sides of this equation are nonzero, we find that the bands are degenerate at θ values which satisfy

$$\tan(\theta) = \frac{\sum_j^{N-1} c_j \cos(\frac{2\pi j}{N})}{\sum_j^{N-1} c_j \sin(\frac{2\pi j}{N})} \tag{5.17}$$

and hence the bands cross twice over the full range of possible θ values. Alternatively, it may be that both sides of (5.16) are zero. In this case the bands are degenerate for all θ and we can write

$$\sum_{j=0}^{N-1} c_j \omega^j = 0. \tag{5.18}$$

When N is a prime number, it is easy to see that this can never be satisfied together

with (5.15) and $\vec{a} \neq \vec{b}$.To see why this is true consider the polynomial

$$\Phi_N(x) = 1 + x + \ldots + x^{N-1} = \prod_{j=1}^{N-1}(x - \omega^j) \tag{5.19}$$

From this decomposition it is clear that

$$\Phi_N(\omega) = 0 \tag{5.20}$$

When N is prime Φ_N, corresponds with the cyclotomic polynomial of order N, that is the unique monic, irreducible polynomial over $\mathbb{Z}$ (and $\mathbb{Q}$), such that (5.20) holds true and $\deg(\Phi_N)$ is the smallest possible. Suppose now that there exists a vector of integers $\vec{c}$ such that (5.18) is true as well. Let's introduce the polynomial

$$p(x) = \sum_{j=0}^{N-1} c_j x^j \ . \tag{5.21}$$

The condition (5.18) means in particular that $p(1) = 0$, that is

$$p(x) = (x-1)(\bar{c}_0 + \bar{c}_1 x + \ldots + \bar{c}_{N-2} x^{N-2}) \tag{5.22}$$

with $\{\bar{c}_j\}$ still integers, as can be easily seen by induction. Since $p(\omega) = 0$ we have that $\bar{c}_0 + \bar{c}_1\omega + \ldots + \bar{c}_{N-2}\omega^{N-2} = 0$. If $\bar{c}_{N-2} = 1$ we could conclude, but in general (using (5.20)) we have

$$(\bar{c}_0 + 1) + (\bar{c}_1 + 1)\omega + \ldots + (\bar{c}_{N-2} + 1)\omega^{N-2} + \omega^{N-1} = 0 \tag{5.23}$$

and this contradicts the fact that (5.19) is the unique *monic* polynomial of degree $N-1$, irreducible over $\mathbb{Z}$ and such that ω is one of its roots. Hence there are no bands which are everywhere degenerate for N prime.

Let's now prove that if N is composite it is possible to find bands that are everywhere degenerate. Suppose $N = ef$ then it suffices to consider e coefficients $\{d_j\} \in \mathbb{Z}_n$ such that

$$\sum_{j=0}^{e-1} d_j = 0 \tag{5.24}$$

then we have

$$\sum_{j=0}^{e-1} d_j \sum_{k=0}^{f-1} \omega^{ek+j} = 0 \tag{5.25}$$

in fact $(\omega^e)^f = 1$ and therefore

$$\sum_{k=0}^{f-1} \omega^{ek+j} = \omega^j \sum_{k=0}^{f-1} \omega^{ek} = 0 \qquad \forall\ 0 \leq j < e \tag{5.26}$$

Equation (5.25) can be recast in the form (5.18) and the sum of all the coefficients vanishes because of (5.24).

This discussion characterizes the points where the bands are degenerate. We can further distinguish resonance points by a symmetry of H_0, that will be of great importance in the following. We will name this symmetry P and it can be written as

$$P = \sigma_1^\dagger \sigma_L. \tag{5.27}$$

From now on we will refer to this quantity as the total domain wall parity. Writing $P = e^{\frac{i2\pi p}{N}}$, we get

$$p = i_L - i_1 = \sum_{j=1}^{L-1} i_{j+1} - i_j = \sum_{k=1}^{N-1} k n_k \tag{5.28}$$

so all states in the H_0-band labeled by $(n_0, n_1, \ldots, n_{N-1})$ have total domain wall parity given by p. We note that there are special values of θ at which the total domain wall parity is conserved even though different bands cross. One of these special points for the $N = 3$ model is found at $\theta = \frac{\pi}{6}$, which also corresponds to the super-integrable point of the model when $\phi = \frac{\pi}{6}$ [71, 70]. This is illustrated in Figure 5.1. We will see in Section 6.2.1 that strong zero modes may only occur at any given θ if either there are no bands crossing at this value of θ, or alternatively, if any bands that cross have the same value of p (taken modulo N).

5.1.3 Resonance points in the thermodynamic limit

We can now deal with the question of whether resonance points occur arbitrarily near any particular value of θ. This is clearly not the case for finite L, but as L grows, ever more resonance points appear and in the limit $L \to \infty$ they do form a dense set on the θ-axis, for all $N > 2$. To see this, we first note that the two solutions to Eq. (5.17) are in fact given by

$$\theta = \frac{\pi}{2} - \arg\left(\sum_j c_j \omega^j\right) \pmod{\pi}. \tag{5.29}$$

It is clear that we can make the linear combination $\sum_j c_j \omega^j$ take any fixed argument α, to arbitrary accuracy, if we are allowed to take the coefficients c_j as large as we want. However a complication is once again the condition that $\sum_j c_j = 0$. We can circumvent this as follows. First of all note that we can choose any two powers of ω, for example ω and $\omega^0 = 1$ as a basis for the complex plane over the reals. We can then take a point z with $\arg(z) = \alpha$ in the complex plane and write

$$z = a + b\omega \tag{5.30}$$

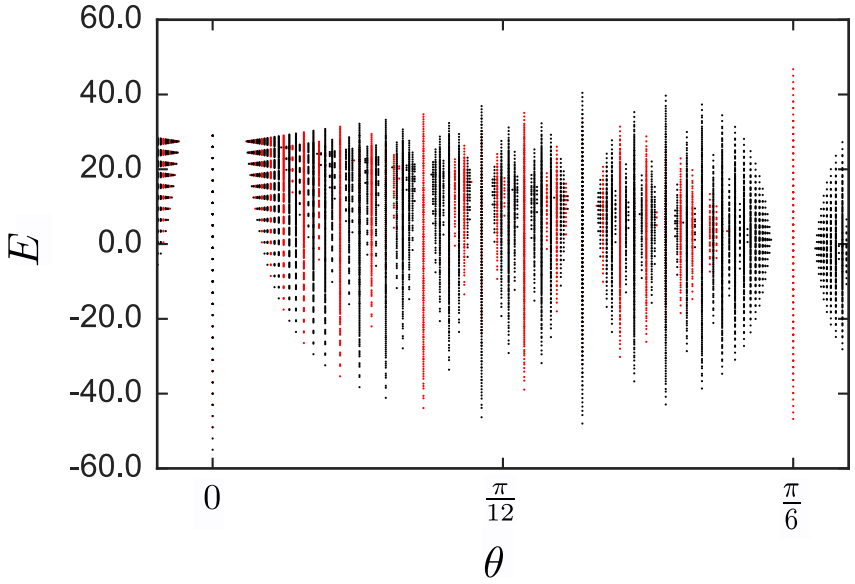

Figure 5.2: All resonance points in the unperturbed spectrum of an $N = 3$ system of length $L = 30$. The red dots indicate resonance points where the total domain wall angle p of the crossing bands is equal [27].

with $a, b \in \mathbb{R}$. The coefficients a, b can be therefore arbitrarily well approximated by rationals $a', b' \in \mathbb{Q}$, as $\mathbb{Q}$ is dense in $\mathbb{R}$. In particular, for any chosen ϵ, we can find $Z = a' + b'\omega$ such that

$$|\arg(Z) - \alpha| < \epsilon. \tag{5.31}$$

We can now write $a' = \frac{a_1}{a_2}$ and $b' = \frac{b_1}{b_2}$ for integers a_1, a_2, b_1, b_2 and consider

$$Na_2b_2Z = Na_2b_2(\frac{a_1}{a_2} + \frac{b_1}{b_2}\omega) - (a_1b_2 + a_2b_1)(\sum_{j=0}^{N-1}\omega^j). \tag{5.32}$$

as the second term on the right is identically zero. We now have that $Z \neq 0$ and Na_2b_2Z is of the form $\sum_j c_j\omega^j$ with $c_j \in \mathbb{Z}$. More importantly, it is also true that $\sum_j c_j = 0$ and

$$\arg(Na_2b_2Z) = \arg(Z). \tag{5.33}$$

This means we can indeed get within any ϵ of our chosen argument α using a judicious choice of coefficients c_j. Hence the resonance points are dense on the θ axis in the limit $L \to \infty$.

As an illustration of how the θ axis is eventually covered by resonance points, we show all resonance points in a $N = 3$ chain of length $L = 30$ in Fig. 5.2. This figure shows that while the resonance points are eventually dense on the axis, there are notable gaps without any resonances even at large finite sizes, surrounding the most prominent resonances. Also, higher order resonance points tend to appear at high energy, meaning that if only states with energy below a given bound are considered, there may be appreciable regions of the θ-axis where no resonance effects

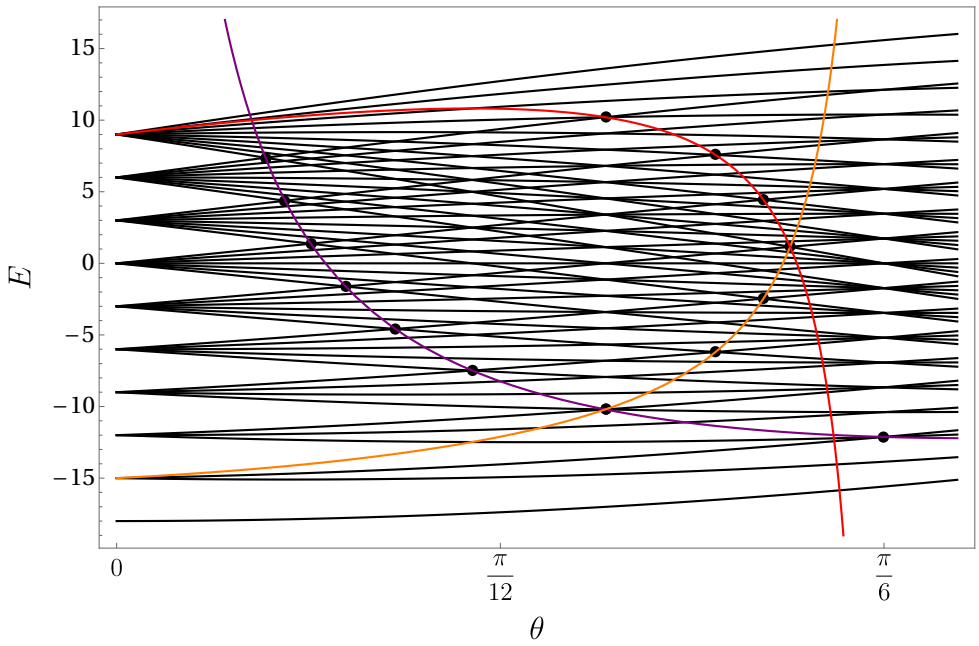

Figure 5.3: Free spectrum for a chain of length L=10.

are observed.

Given the above discussion, it is interesting to analyse how the distance between two resonance points goes to zero. As a study case we will consider the resonance at $\theta = 0, \frac{\pi}{6}$ for $N = 3$. Consider therefore Fig. 5.3. The different curves represent the set of the first crossings that appear near $\theta = 0$ and $\theta = \frac{\pi}{6}$. The analytic form of these curves can be found by considering the type of domain walls that come in contact at the resonance. First of all, note that for $\theta = 0$ the different bands can be distinguished by the number of n_0 domain walls. Therefore the eigenstates in the bottom band have $n_0 = L - 1$, eigenstates in the second band have $n_0 = L - 2$ and so on. Near $\theta = 0$ we have from (5.13)

$$\epsilon_m \approx -2 + 2\sin\left(\frac{2\pi m}{3}\right)\ \theta \tag{5.34}$$

This means in particular that $\epsilon_1 > \epsilon_2$ for small enough θ. Thus we can exactly distinguish the types of bands that are generated from $\theta = 0$ by the number of domain wall n_2 and n_1. For example, the first resonance points near $\theta = 0$ are determined by equating the energies of the tuples $(L-1-k, 0, k)$ and $(L-2-k, k+1, 0)$ for $2 \leq k \leq L-1$. Using (5.12) we find that at the crossings θ_k^0 is given by

$$\theta_k^0 = \arctan\left(\frac{\sqrt{3}}{2k-1}\right) \qquad 2 \leq k \leq L-1 \tag{5.35}$$

The first curve, which delimits the region of the parameter space near $\theta = 0$ where there are no crossings, is obtained by writing k in terms of θ_k into the energy and

extending by continuity to all θ

$$E(\theta) = -2\left(L - \frac{3+\sqrt{3}\cot(\theta))}{2}\right)\cos(\theta) - \left(1+\sqrt{3}\cot(\theta)\right)\cos\left(\frac{4\pi}{3}+\theta\right) \quad (5.36)$$

The top resonance point is given by θ_L^0, and in the limit of large L we have

$$\theta_L^0 \sim \frac{1}{L} \quad (5.37)$$

A similar analysis can be conducted for the other crossings. In particular for $\theta = \frac{\pi}{6}$ we find that the meeting point of the curves delimiting the region where the zero mode exists (red and yellow curves in Figure 5.3) is given by

$$\theta_L^{\frac{\pi}{6}} = \arctan\left(\frac{\sqrt{3}(L-2)}{3L-2}\right) \quad (5.38)$$

and again, for large L, we have

$$\theta_L^{\frac{\pi}{6}} - \frac{\pi}{6} \sim \frac{1}{L} \quad (5.39)$$

The presence of a region that scales like $\frac{1}{L}$ near crossings in which we can find the zero modes is a general property of the free spectrum as for other resonances we need to solve a similar set of equations. For a different, more rigorous argument we refer to [27].

5.2 Dihedral symmetry

When the angle ϕ is a multiple of $\frac{2\pi}{N}$, the models we study have an enlarged group of symmetries, isomorphic to D_N, the symmetry group of a regular polygon with N sides. The $\mathbb{Z}_N$ generated by Q_N is included in this D_N as the group of rotations of the polygon.

We now present the D_N symmetry explicitly[1]. First of all, recall that the dihedral group D_N is generated by two elements a and b subject to the relations

$$a^N = b^2 = (ab)^2 = e \quad (5.40)$$

where e is the group identity. Here, q can be viewed as a rotation over an angle $\frac{2\pi}{N}$ and r as a reflection acting on the regular N-gon (see Fig). The group has a total of $2N$ elements, the rotations q^j and the reflections $q^j r$, with $j \in \{0, ..., N-1\}$.
We now introduce an operator R, such that $R^2 = (Q_N R)^2 = I$, which together with

[1]Our presentation of the D_N symmetry group here is in accordance with the results given by Motruk, Berg and Pollmann[80] and generalizes some of their findings.

Q_N (from (5.7)) generates a D_N symmetry. First we define η to be the operator that transforms each clock value as

$$\eta|s\rangle = |N-s\rangle \tag{5.41}$$

with $\eta|0\rangle = |0\rangle$. Note that η corresponds to the complex conjugation of the eigenvalues of σ. We see that $\eta^2 = 1$ and that the following exchange relations with τ and σ hold

$$\sigma\eta = \eta\sigma^\dagger \qquad \tau\eta = \eta\tau^\dagger \tag{5.42}$$

We can now define

$$R_0 = \prod_{k=1}^{L} \eta_k. \tag{5.43}$$

This satisfies $(R_0)^2 = I$, $(R_0 Q_N)^2 = 1$ and

$$R_0 H(\theta,\phi) = H(-\theta,-\phi)R_0. \tag{5.44}$$

We note that R_0 and Q_N generate a D_N group together, but R_0 is only a symmetry if $\theta = \phi = 0$. In order to solve this issue consider the operator F, which reverses the clock chain, more explicitly,

$$F|i_1, i_2, ..., i_L\rangle = |i_L, ..., i_2, i_1\rangle \tag{5.45}$$

Note that $F^2 = 1$ and $FQ_N = Q_N F$. Combining R_0 with the operator F we obtain the generator of D_N, $R = R_0 F$ which is a symmetry for all θ as long as $\phi = 0$. From the definition it is then clear that

$$R^2 = (RQ_N)^2 = I \tag{5.46}$$

and $RH(\theta,\phi) = H(\theta,-\phi)R$, which in particular gives

$$[H(\theta,0), R] = 0. \tag{5.47}$$

We see that we have D_N-symmetry at $\phi = 0$ and in fact, $\mathbb{Z}_2 \times D_N$ symmetry if $\phi = \theta = 0$, as we have F as an additional commuting symmetry when $\theta = 0$.

Since D_N is a non-Abelian group, its presence causes degeneracies in the spectrum. To see why this is true, first note that from (5.46) we have $Q_N R = RQ_N^{-1}$. This means that if $|\psi\rangle$ is an eigenstate of H and of Q_N with eigenvalues E and ω^q) respectively then $R|\psi\rangle$ is an eigenstate of H and Q_N, in fact

$$\begin{aligned} HR|\psi\rangle &= RH|\psi\rangle = E|\psi\rangle \\ Q_N R|\psi\rangle &= RQ_N^{-1}|\psi\rangle = \omega^{-q} R|\psi\rangle \end{aligned}$$

As a result all eigenstates of Q_N with eigenvalues $\omega^q \neq \omega^{-q}$ are at least doubly degenerate. Only states with eigenvalues of Q_N being ± 1 have a chance of being nondegenerate.
Generically only states within a given irreducible representation of D_N will be degenerate[2]. Since D_N has only one dimensional and two dimensional irreducible representations for all N we see that the D_N symmetry only causes doublets and not higher multiplets of degenerate states (or bands) to appear. With exact diagonalisation it can be seen that the D_N doublets are split when $\phi \neq 0$, so it is not possible to extend the D_N symmetry to this regime.

Roughly speaking this unexpected symmetry comes essentially from the addition of the hermitian conjugate to the Hamiltonian of the free parafermion [81]. It can be seen that R exchanges this Hamiltonian with its hermitian conjugate, resulting thus in a symmetry of $H(\theta, 0)$, which is a sum of the two.

[2]In principle there might be some additional degeneracy due to some other symmetry that we did not consider, however we can exclude this by analysing the system with exact diagonalisation.

Chapter 6

Parafermionic Strong Zero Modes

In this chapter we will carefully consider the existence of strong zero modes in the clock models. We will start by reviewing some of the results shown in [27]. We will first show some general features of the problem using perturbation theory and then we will consider the specific case $N = 4$, that is exactly solvable (in some particular regimes that we will explain in detail).

6.1 Parafermionic strong zero modes and the domain wall picture

As in the Ising case, also for the quantum clock model we can define strong zero modes. In the same way as before a strong zero mode is an operator ψ such that

- $[H, \psi] = O(e^{-\frac{L}{\xi}})$
- $Q_N \psi = \omega \psi Q_N$
- $\psi^\dagger \psi = 1 + O(e^{-\frac{L}{\xi}})$,

where as before ξ is some positive constant that can also be $+\infty$ and $\omega = e^{i\frac{2\pi}{N}}$. The first and the last relations are the same as the ones for the Ising case, while the second one reduces to the Ising case when $N = 2$. The zero mode is said to be an edge zero mode if it is localised on the edge of the system, in the same sense as before. In the following we will also usually consider the more restrictive condition

$$\psi^N = 1 + O(e^{-\frac{L}{\xi}}), \tag{6.1}$$

since we want the strong zero mode to describe a parafermionic degree of freedom sitting on the edge.

As we pointed out in the previous chapter the free Hamiltonian H_0 has two zero modes at the edges of the system. For convenience, we restate here the form taken by the edge zero modes

$$\gamma_1 = \sigma_1 \qquad \gamma_{2L} = \omega \sigma_L Q_N. \tag{6.2}$$

Just as in the Ising case, it is natural to ask whether such zero modes can survive the introduction of the interaction V.

As we saw, the existence of strong zero modes implies degeneracies throughout the spectrum. Since the operator Q_N generates a representation of $\mathbb{Z}_N$, this degeneracy will involve bands with different eigenvalues of Q_N and the existence of strong zero modes will result in an N-fold degeneracy of energy bands. A way to rule out the existence of strong zero modes, is therefore to consider when bands in different q-sectors develop splittings. In this sense it is meaningful to consider perturbation theory between different sectors of the spectrum.

With this aim in mind, we will now introduce the domain-wall representation, where one focuses on the differences between clock values on neighbouring sites, rather than the clock values themselves. This picture allows us to directly write down the Hamiltonian in each q-sector. We find that by doing this there are only two terms in the Hamiltonian which depend on the particular q-sector. Better still, both of these act at the right end of the chain. This makes the domain-wall representation very convenient for numerical calculations and a natural setting for perturbative expansions.

First of all note that the states in the spin representation are not eigenstates of the symmetry operator Q_N. The eigenstates can be easily constructed by considering

$$|\mathbf{i}\rangle_q^S = \frac{1}{\sqrt{N}} \sum_{j=0}^{N-1} \omega^{-jq} Q_N^j |\mathbf{i}\rangle \tag{6.3}$$

where $\frac{1}{\sqrt{N}}$ ensures that these states are normalized to 1. By acting with Q_N it can be easily verified that

$$Q_N |\mathbf{i}\rangle_q^S = \frac{1}{\sqrt{N}} \sum_{j=0}^{N-1} \omega^{-jq} Q_N^{j+1} |\mathbf{i}\rangle^S = \omega^q |\mathbf{i}\rangle_q^S$$

and therefore these states constitute the basis in which both Q_N and H_0 are in diagonal form. We can now define states in the domain wall picture in each q-sector. First we define operators α and β given by

$$\begin{aligned} \alpha_k &= \prod_{j=1}^{k} \tau_j \\ \beta_k &= \sigma_k^\dagger \sigma_{k+1} \end{aligned} \tag{6.4}$$

These operators have the same matrix representations as operators τ and σ respectively, except that they act on the domain-wall basis. In terms of these operators

τ_k can be written as

$$\tau_k = \begin{cases} \alpha_1 & k = 1 \\ \alpha_{k-1}^\dagger \alpha_k & 1 < k < L \\ Q_N^\dagger \alpha_{L-1}^\dagger & k = L \end{cases} \tag{6.5}$$

and the Hamiltonian (5.1) is now given by

$$H_0 = -Je^{i\theta} \sum_{k=1}^{L-1} \beta_k + h.c \tag{6.6}$$

$$V = -fe^{i\phi} \left(\alpha_1 + \sum_{k=1}^{L-2} \alpha_k^\dagger \alpha_{k+1} + Q_N^\dagger \alpha_{L-1}^\dagger \right) + h.c. \tag{6.7}$$

Note that in this form all q-dependence appears only in V, on the terms $-fe^{i\phi} Q_N^\dagger \alpha_{L-1}^\dagger$ and $-fe^{-i\phi} \alpha_{L-1} Q_N$, which act on the end of the chain.

Since Q_N commutes with H (and with α_{L-1} and $\alpha_{L-1}^\dagger$), this Hamiltonian is block diagonal, and we can write the Hamiltonian in each q-sector by replacing Q_N with the appropriate eigenvalue,

$$H_0^q = -Je^{i\theta} \sum_{k=1}^{L-1} \beta_k + h.c \tag{6.8}$$

$$V^q = -e^{i\phi} \left(\alpha_1 + \sum_{k=1}^{L-2} \alpha_k^\dagger \alpha_{k+1} + \omega^q \alpha_{L-1}^\dagger \right) + h.c. \tag{6.9}$$

and $(\alpha_k^\dagger)^d$ can be interpreted as an operator that creates a domain-wall of type d at site k. We are now ready to introduce the domain wall representation

$$|\mathbf{d}\rangle_q^D = |d_{k_1}, d_{k_2}, \ldots, d_{k_m}\rangle \ ,$$

where $k_1 < k_2 < \ldots < k_m$ and m defines the number of domain walls different from 0. d_{k_l} represent the value of the k_lth domain wall

$$d_{k_l} = i_{k_l+1} - i_{k_l} \tag{6.10}$$

and we can write

$$|\mathbf{d}\rangle_q^D = \prod_{l=1}^{m} (\alpha_{k_l}^\dagger)^{d_{k_l}} |0, 0 \ldots 0\rangle_q^S \ . \tag{6.11}$$

As an example, for $L = 4$ and $N = 3$, we write

$$|1_2 2_3\rangle_q^D = (\alpha_2^\dagger)^1 (\alpha_3^\dagger)^2 |\emptyset\rangle_q = \frac{1}{\sqrt{3}} \left(|0010\rangle + \omega^{-q} |1121\rangle + \omega^{-2q} |2202\rangle \right) \tag{6.12}$$

While this way of writing the states is reminiscent of second quantization, one should

remember that the "vacuum states" $|0,0...0\rangle_q^S$ are not annihilated by the domain-wall annihilation operators and also that

$$[\alpha_k, \alpha_j^\dagger] = 0, \tag{6.13}$$

so the domain-wall creation operators are not the usual creation operators of bosonic or fermionic Fock space. There have been attempts to formulate a Fock space for parafermions, notably the work of Cobanera and Ortiz [82].

6.2 Perturbation Theory

In the previous chapter we explored in detail the appearance and characterisation of resonance points in the unperturbed spectrum. The reason we are so interested in resonance points is that the behaviour of the perturbative series depends very much on whether one is on or off resonance. We will show that at the off-resonant points q-sector dependent contributions only occur at an order of perturbation theory that scales with the length of the system. On the other hand, when we perform the perturbative expansions at resonant points (where bands of different domain-wall type and number cross), we typically see that there are q-sector dependent terms which split the degeneracy at an order that does not scale with L. In this section we examine these perturbative series at both resonant and off-resonant points.

Our approach is to employ the Rayleigh-Schrodinger degenerate perturbative method pioneered by Bloch [83, 84, 85]. In this approach, one generates effective Hamiltonians acting within a degenerate band of the unperturbed system, which can be diagonalised to approximate the true eigenvalues of the full system. We outline the method in detail in Appendix A. Here we simply state the effective Hamiltonians $H_q^{\text{eff}(0)}$, $H_q^{\text{eff}(1)}$ and $H_q^{\text{eff}(2)}$ for the Bloch expansion in the $Q_N = q$ sector for a given band, where (0), (1) and (2) indicate the orders of the expansion

$$\begin{aligned} H_q^{\text{eff}(0)} &= P_0 H_0 P_0 \\ H_q^{\text{eff}(1)} &= P_0 H_0 P_0 + f P_0 V^q P_0 \\ H_q^{\text{eff}(2)} &= P_0 H_0 P_0 + f P_0 V^q P_0 + f^2 \left(P_0 V^q \frac{Q_0}{E_0 - H_0} V^q P_0 \right). \end{aligned} \tag{6.14}$$

In these expressions, P_0 is the projector onto the band[1], $Q_0 = 1 - P_0$ is its complement, while E_0 is the unperturbed energy of the band, as given by Eq. (5.12). As we already noted, there are only two terms in V^q that actually depend on q, the terms proportional to α_{L-1} and $\alpha_{L-1}^\dagger$. Only terms in the perturbative expansion which contain these terms can lead to an energy splitting between q-sectors. It is

[1]Note that if there are crossing between bands, as it happens at resonance, P_0 is the projector onto all the crossing bands together.

also important to note that both these terms break the total domain wall parity, defined in (5.28).

6.2.1 Perturbation at resonant and off-resonant θ

In order to understand why at resonant points the system will generally develop splitting we consider the simplest resonance point, which appears at $\theta = 0$. For notational convenience we will consider only the case of $N = 3$.
Consider therefore the two first excited bands that come into contact at $\theta = 0$. These bands contain only one non-trivial domain wall. We can order the basis elements for these bands as:

$$|1_{L-1}\rangle_q^D, |1_{L-2}\rangle_q^D, ..., |1_1\rangle_q^D, |2_1\rangle_q^D, ..., |2_{L-2}\rangle_q^D, |2_{L-1}\rangle_q^D \tag{6.15}$$

using (6.14) we see that the relevant matrix elements are given by

$$\begin{aligned} {}_q^D\langle 1_j|\alpha_j^\dagger\alpha_{j+1}|1_{j+1}\rangle_q^D = 1 \qquad {}_q^D\langle 1_{L-1}|\alpha_{L-1}|2_{L-1}\rangle_q^D = 1 \\ {}_q^D\langle 2_{j+1}|\alpha_{j+1}^\dagger\alpha_j|2_j\rangle_q^D = 1 \qquad {}_q^D\langle 2_{L-1}|\alpha_{L-1}^\dagger|1_{L-1}\rangle_q^D = 1 \end{aligned} \tag{6.16}$$

we thus have that the effective Hamiltonian to the first order can be written in this basis, up to a constant term equal to E_0, as a $L' = 2L - 2$ Toeplitz matrix

$$H_q^{eff(1)} \approx -f \begin{pmatrix} 0 & e^{-i\phi} & 0 & \dots & 0 & e^{i\phi}\omega^q \\ e^{i\phi} & 0 & e^{-i\phi} & \dots & 0 & 0 \\ 0 & e^{i\phi} & & & : & : \\ : & : & & & e^{-i\phi} & 0 \\ 0 & 0 & \dots & e^{i\phi} & 0 & e^{-i\phi} \\ e^{-i\phi}\omega^{-q} & 0 & \dots & 0 & e^{i\phi} & 0 \end{pmatrix}. \tag{6.17}$$

This matrix can be easily diagonalised by considering eigenvectors of the type

$$\begin{aligned} |v_k^q\rangle = &\omega^{-\frac{q}{L'}}\Big(e^{i\frac{2\pi k}{L'}}|1_{L-1}\rangle_q^D + e^{i2\frac{2\pi k}{L'}}|1_{L-2}\rangle_q^D + \ldots + e^{i(L-1)\frac{2\pi k}{L'}}|1_1\rangle_q^D + \\ &e^{iL\frac{2\pi k}{L'}}|2_1\rangle_q^D + e^{i(L+1)\frac{2\pi k}{L'}}|2_2\rangle_q^D + \ldots + e^{iL'\frac{2\pi k}{L'}}|2_{L-1}\rangle_q^D\Big). \end{aligned} \tag{6.18}$$

Imposing the condition

$$H_q^{eff(1)}|v_k^q\rangle = E_q(k)|v_k^q\rangle \tag{6.19}$$

we find that the relevant equations to solve the system are

$$\begin{cases} \omega^{-\frac{q}{L'}}e^{ik}e^{-i\phi} + \omega^{\frac{q}{L'}}e^{-ik}e^{i\phi} = E_q(k) \\ \omega^{-\frac{q}{L'}}e^{ik}e^{-i\phi} + \omega^{\frac{q}{L'}}e^{i(L'-1)k}e^{i\phi} = E_q(k) \end{cases}$$

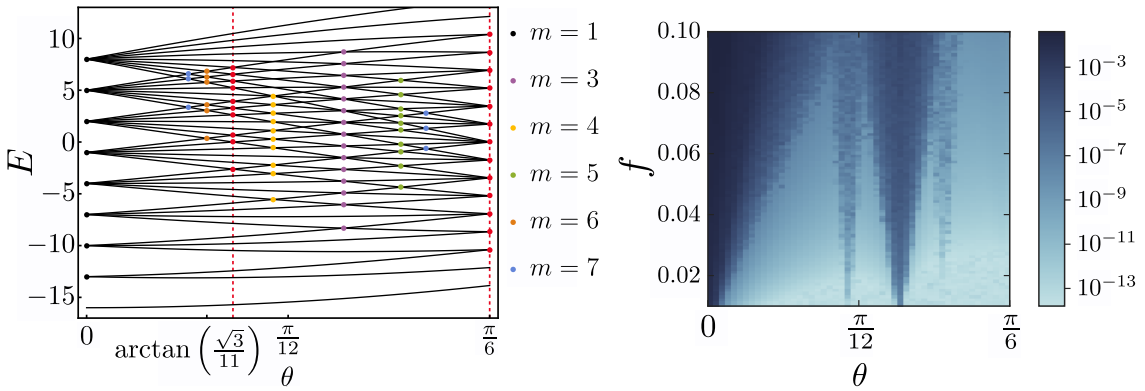

(a) (b)

Figure 6.1: In (a) we show the free spectrum for $L = 9$, $N = 3$. In red we plot resonance points where total domain wall parity is conserved. With m we indicate the order of the crossings. In (b) we plot the maximum energy splitting between the $q = 0$ and $q = 1$ sectors for a chain of length $L = 9$ with $N = 3$ and $\phi = 0$. Results obtained using exact diagonalisation where each data point corresponds to the maximal difference between all 6561 eigenvalues in the $q = 0$ and $q = 1$ sectors.

and this gives

$$E_q(k) = E_0 + 2\cos\left(\frac{2\pi}{L'}\left(k + \frac{q}{3}\right) - \phi\right) \qquad k = 0, 1, \ldots, L' - 2, L' - 1\ . \tag{6.20}$$

Note that when $\phi = 0$, upon sending $k \to L' - 1 - k$ and reordering, the spectrum of the sectors $q = 1$ and $q = 2$ are the same. This degeneracy is a result of the dihedral symmetry that we exposed in Section 5.2 (in the present case this is trivially true, as for $\phi = 0$ the matrices in (6.17) for $q = 1$ and $q = 2$ are the conjugate transpose of each other). The degeneracy between the $q = 1, 2$ sectors and the sector $q = 0$ is instead completely lifted at first order in perturbation theory and this is generally true for $\phi \neq 0$ between sectors $q = 1$, $q = 2$ as well. This argument shows that the zero mode is not stable under perturbation at the resonance point $\theta = 0$ and this agrees with the analysis of [22]. We stress again that the terms responsible for the breaking of the degeneracy, change the total domain wall parity of the bands.

The case for general resonance points is obviously more involved, as we need to consider bands with different numbers of domain walls that cross at a fixed θ. Nonetheless, our numerical analysis shows that the main features of the mechanism can be grasped already at this level. In figure 6.1(b) we show the maximal energy difference between bands at $q = 0$ and at $q = 1$ for $N = 3$ and $L = 9$, $\phi = 0$. In each q-sector the energy levels have been ordered and we have plotted the maximal absolute difference between eigenvalues at the same position in this ordering. We can see that the splitting increases near the resonance points.

It is clear from figure 6.1(b) that the largest splitting between sectors occurs around the $\theta = 0$ point. This can be attributed to the first order processes occurring there. For larger f, we see other branches of splittings emerge. These can be

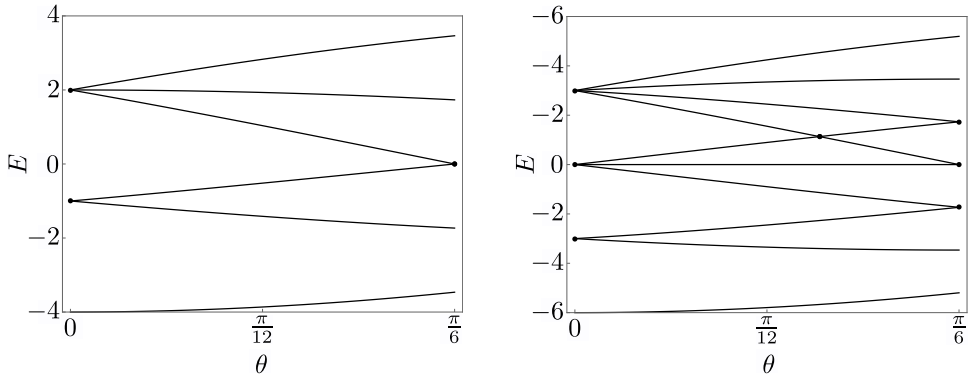

Figure 6.2: In (a) the free spectrum for $L = 3$. In (b) the free spectrum for $L = 4$. Note that in this case a new resonance point appears at $\theta = \arctan\left(\frac{\sqrt{3}}{5}\right)$. The splitting between different sectors in correspondence with this resonance point will therefore be of order $m = 3$.

attributed to third, fourth and fifth order processes occurring at the other resonance points, as indicated in figure 6.1(a). We will see in chapter 7 that the order m at which the splitting occurs, corresponds to

$$m = L_\theta - 1$$

where L_θ is the length of the chain in which the resonance points at a certain θ first appears when we consider chains of increasing length. This is illustrated in Figure 6.2, where the free spectrum for a chain of length 3 and a chain of length 4 are shown.

While in principle for $\theta = \frac{\pi}{6}$ we would expect a splitting between sectors at order $m = 2$, this is not the case and the same seems to be true away from resonance points (especially at low f). This happens because in these cases the domain-wall parity is conserved throughout the bands of the free spectrum. We will examine this situation in more detail in chapter 7, where we will show that in such cases it is possible to construct a strong zero mode. Some splitting does appear at larger f even away from resonances, but this can be ascribed to finite size effects which allow for q-dependent perturbative processes at order f^L and these effects overshadow the higher order resonance points.

To consider more carefully the details of the perturbation theory at off-resonant points and at $\theta = \frac{\pi}{6}$ we can perform the perturbative expansion numerically and estimate the maximal energy splitting between sectors with $q = 1$ and $q = 0$. The results of this analysis are shown in Figure 6.3 and Figure 6.2.1.

In figure 6.3 we show the maximal difference between the perturbative energy estimates for states in the $q = 0$ and $q = 1$ sectors of the first excited band at off-resonant θ. We note that the difference is nonzero from the third order onward, but decreases with increasing order $n \geq 3$ and is always small enough to be explained as an error

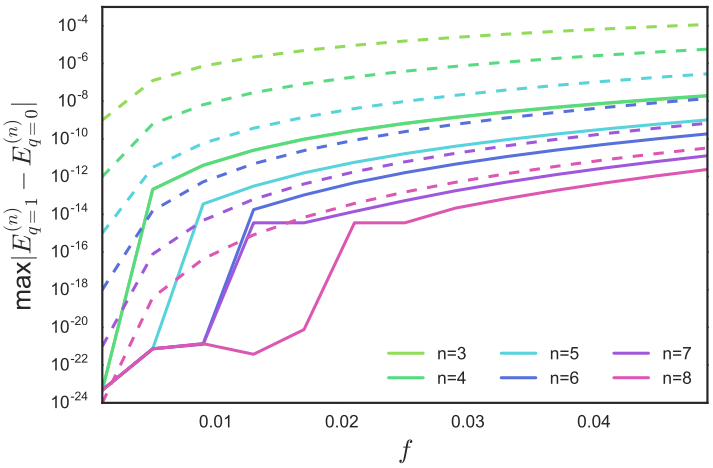

Figure 6.3: The maximum differences between $q = 1$ and $q = 0$ sectors of the estimates from n^{th} order degenerate perturbation theory for a range of values of the perturbing parameter f. This is for the first excited band above the ground state, for a chain of length $L = 11$ with $N = 3$ and with chiral parameter $\theta = 0.3$. The dashed lines show f^n and act as a guide.

of the approximation. That is, the energy splitting between the $q = 0$ and $q = 1$ sectors, calculated from $H^{\text{eff}(n)}$, is less than f^n. In general we expect that the maximum difference between q-dependent matrix elements of the effective Hamiltonians decay as f^n. How these matrix elements affect the energy splitting between q-sectors is not completely clear. However it is reasonable to expect that these corrections should in general decay faster than f^n, since the number of q-dependent matrix elements is relatively small and the dimension of the effective Hamiltonians grows with L. This

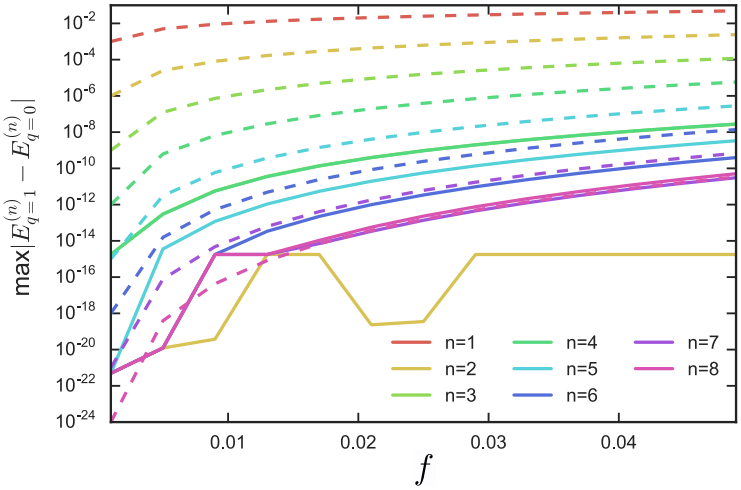

Figure 6.4: The maximum differences between $q = 0$ and $q = 1$ sectors of the estimates from nth order degenerate perturbation theory for a range of values of the perturbing parameter f. This is for the second and third excited bands for a chain of length $L = 8$ with $N = 3$ and with the chiral parameter set to the prominent resonance point at $\theta = \frac{\pi}{6}$. The dashed lines show f^n and act as a guide.

behaviour is observed for all bands as long as θ is not resonant and f is sufficiently small. For short chains, when $n \geq L$ a non-vanishing splitting between q-sectors can be observed which is always less than f^L.

The same qualitative behaviour is also shown at resonance points where the total domain wall parity is conserved. In figure 6.2.1 we show the difference between the perturbative energy estimates for states in the $q = 0$ and $q = 1$ sectors for the most prominent of such resonance points, $\theta = \frac{\pi}{6}$.
We should mention here that the perturbation theory and exact diagonalisation give the same qualitative results regardless of the value chosen for the other chiral parameter ϕ. This suggests that strong zero-modes exist all along the $\theta = \frac{\pi}{6}$ line. Note that their existence is not dependent on the super-integrability as this occurs only at the point $(\theta, \phi) = (\frac{\pi}{6}, \frac{\pi}{6})$.

Showing the behaviour illustrated above directly in the degenerate perturbation series for all cases is a formidable task. However we can intuitively argue why we expect it to be true. For a process to lead to q-dependent energy splitting it must include at least one q-dependent term acting at the end of the chain. Since these terms change the total domain-wall angle, such a process must also include a term acting at the start of the chain to connect back to the original band. This means that at orders lower than L any process that contributes will contain disconnected sets of operators acting on opposite ends of the chain. We may intuitively expect that contributions to the energy arising from operators acting on spatially disconnected parts of the chain that depend on q should vanish. General arguments in this direction can be made starting from extensive energy scaling: if a system consists of independent subsystems the total energy should equal the sum of the energies of the subsystems and one would expect cross terms in the perturbation series to vanish, or at least the energy per site due to such terms should vanish in the thermodynamic limit $L \to \infty$ (see e.g. Ref. [86]). These considerations are closely related to the existence of linked-cluster-theorems for degenerate systems, where non-local terms corresponding to un-linked diagrams cancel [87, 88, 89].

6.3 The case $N = 4$

In the next chapter we will address the existence of strong zero modes in full generality. Before undertaking this task it is worth to consider more closely the case of $N = 4$, as in this case the model is exactly solvable for $\theta = 0$ and all ϕ. It can be therefore used to identify some of the general features of the problem.

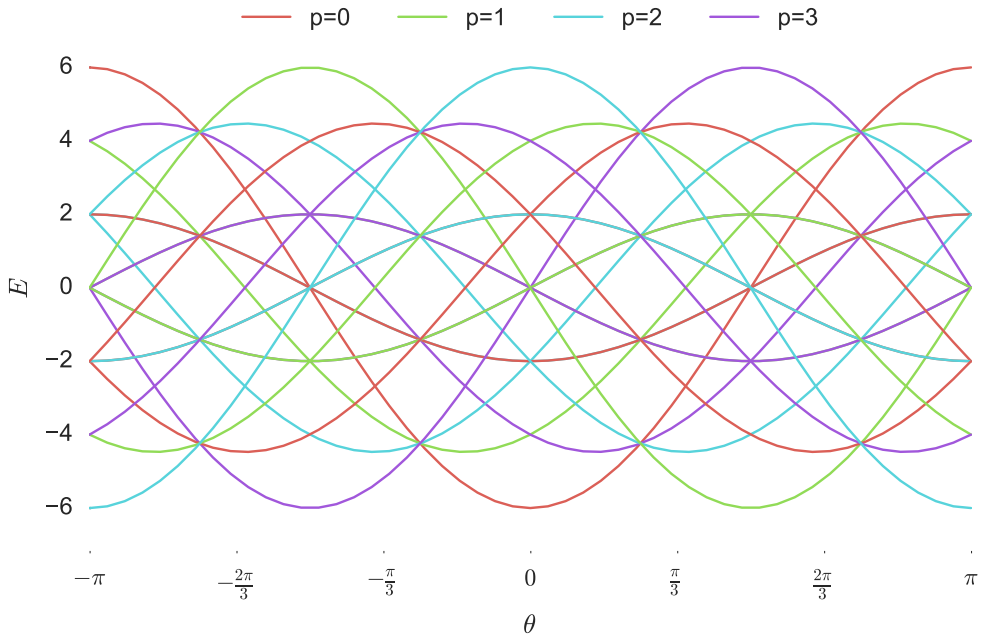

Figure 6.5: Full spectrum of H_0 for $N = 4$ and $L = 4$ the different colors represent different domain wall parities.

We consider a Hamiltonian as in (5.1) with σ, τ given by

$$\sigma = \begin{pmatrix} 1 & 0 & 0 & 0 \\ 0 & i & 0 & 0 \\ 0 & 0 & -1 & 0 \\ 0 & 0 & 0 & -i \end{pmatrix} \qquad \tau = \begin{pmatrix} 0 & 1 & 0 & 0 \\ 0 & 0 & 1 & 0 \\ 0 & 0 & 0 & 1 \\ 1 & 0 & 0 & 0 \end{pmatrix} \tag{6.21}$$

In figure 6.5 we show the spectrum for the free Hamiltonian H_0 for a chain of length 4 as a function of θ.

Consider now the operator ζ defined as

$$\zeta = \frac{1}{2}(\mathbb{1} + \sigma_d^x - \sigma_u^z \sigma_d^x + \sigma_u^z) = \begin{pmatrix} 1 & 0 & 0 & 0 \\ 0 & 1 & 0 & 0 \\ 0 & 0 & 0 & 1 \\ 0 & 0 & 1 & 0 \end{pmatrix} \tag{6.22}$$

where

$$\begin{aligned} \sigma_u^z &= \sigma^z \otimes \mathbb{1} & \sigma_u^x &= \sigma^x \otimes \mathbb{1} \\ \sigma_d^z &= \mathbb{1} \otimes \sigma^z & \sigma_d^x &= \mathbb{1} \otimes \sigma^x \end{aligned} \tag{6.23}$$

with σ^z, σ^x Pauli matrices. The meaning of the subscript d (down) and u (up) will

become clear later. It can be seen by direct computation that

$$\zeta\sigma\zeta^\dagger = \frac{1}{\sqrt{2}}\left(e^{i\frac{\pi}{4}}\sigma_u^z + e^{-i\frac{\pi}{4}}\sigma_d^z\right) = \begin{pmatrix} 1 & 0 & 0 & 0 \\ 0 & i & 0 & 0 \\ 0 & 0 & -i & 0 \\ 0 & 0 & 0 & -1 \end{pmatrix} \tag{6.24}$$

$$\zeta\tau\zeta^\dagger = \frac{1}{2}(\sigma_u^x + \sigma_d^x) + \frac{i}{2}(\sigma_u^z\sigma_d^y - \sigma_u^y\sigma_d^z) = \begin{pmatrix} 0 & 1 & 0 & 0 \\ 0 & 0 & 0 & 1 \\ 1 & 0 & 0 & 0 \\ 0 & 0 & 1 & 0 \end{pmatrix} \tag{6.25}$$

and

$$\zeta^2 = \mathbb{1} \tag{6.26}$$

We can define ζ operators for every site of the chain and set

$$Z = \prod_{i=1}^{L} \zeta_i \ . \tag{6.27}$$

Since ζ_i are unitary operators, Z is also unitary. We can therefore act with it on the Hamiltonian $H = H_0 + fV$ without changing the spectrum. In particular we have

$$ZH_0Z^\dagger = -\cos(\theta)\sum_{i=1}^{L-1}\left[\sigma_{i,u}^z\sigma_{i+1,u}^z + \sigma_{i,d}^z\sigma_{i+1,d}^z\right] - \sin(\theta)\sum_{i=1}^{L-1}[\sigma_{i,u}^z\sigma_{i+1,d}^z - \sigma_{i,d}^z\sigma_{i+1,u}^z]$$
$$ZVZ^\dagger = -\cos(\phi)\sum_{i=1}^{L}\left[\sigma_{i,u}^x + \sigma_{i,d}^x\right] - \sin(\phi)\sum_{i=1}^{L}[\sigma_{i,u}^y\sigma_{i,d}^z - \sigma_{i,u}^z\sigma_{i,d}^y]$$

and this shows that we can think of the clock model for $N = 4$ as two coupled chains of spins $\frac{1}{2}$. This justifies the use of the up and down indexes.
Setting $\theta = \frac{n\pi}{2}$ and $\phi = m\pi$, we see that many of the terms in H_0, V vanish and we end up with two decoupled chains. For $\theta = n\pi$, these are transverse Ising chains on the legs of the ladder, whereas for $\theta = n\pi + \frac{\pi}{2}$ they are zig-zag chains with alternating ferromagnetic and anti-ferromagnetic couplings. This structure is shown in figure 6.6. The same transformation can be also directly be applied in terms of fermionic variables and this leads to the same results see for example [90].

When the system can be written as decoupled spin-$\frac{1}{2}$ chains (for $\theta = \frac{n\pi}{2}$ and $\phi = m\pi$), there is an exact four fold degeneracy that results from the $\mathbb{Z}_2$ degeneracies of the two Ising chains. Note that the existence of a $\mathbb{Z}_2 \times \mathbb{Z}_2$ is a result of the dihedral symmetry discussed before, as $D_4 \supset \mathbb{Z}_2 \times \mathbb{Z}_2$.
To better understand how the original $\mathbb{Z}_4$ symmetry and the two copies of $\mathbb{Z}_2$ are

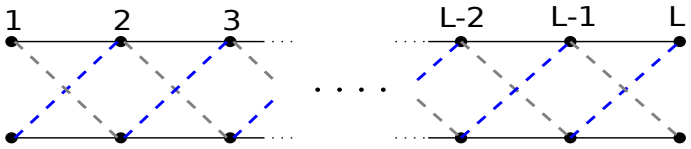

Figure 6.6: The $\mathbb{Z}_4$ model decouples into two decoupled spin-$\frac{1}{2}$ chains when $\theta = \frac{n\pi}{2}$ and $\phi = m\pi$. For $\theta = n\pi$ these are transverse Ising chains defined on the legs (solid black lines), whereas for $\theta = n\pi + \frac{\pi}{2}$ these are zig-zag chains which opposite signs, depicted here with blue and grey dashed lines.

related, we can directly write down Q_4 in terms of the Ising variables. We have

$$ZQ_4Z^\dagger = TQ_2^d = Q_2^u T \tag{6.28}$$

where $Q_2^{u(d)}$ are the operators relative to the $\mathbb{Z}_2$ symmetry of the up (down) chain. With T we have indicated the operator that exchanges the up and down chains

$$T\sigma^z_{i,u}T^\dagger = \sigma^z_{i,d} \qquad T\sigma^x_{i,u}T^\dagger = \sigma^x_{i,d}\ . \tag{6.29}$$

This operator can be written as

$$T = \frac{1}{2}\prod_{i=1}^{L}(\mathbb{1} + \sigma^z_{i,u}\sigma^z_{i,d} + \sigma^x_{i,u}\sigma^x_{i,d} + \sigma^y_{i,u}\sigma^y_{i,d}), \tag{6.30}$$

as can be checked by noting that

$$\frac{1}{2}(\mathbb{1} + \sigma^z_u\sigma^z_d + \sigma^x_u\sigma^x_d + \sigma^y_u\sigma^y_d) = \begin{pmatrix} 1 & 0 & 0 & 0 \\ 0 & 0 & 1 & 0 \\ 0 & 1 & 0 & 0 \\ 0 & 0 & 0 & 1 \end{pmatrix}. \tag{6.31}$$

To simplify the notation, from now on, we will omit the presence of the Z operator. Anyhow it has to be kept in mind that every equation relating parafermionic variables and Ising ones needs the presence of Z to be rigorously true.

Since for $\theta = \frac{n\pi}{2}$ and $\phi = m\pi$ the two chains are decoupled and each of them has strong zero modes living on the edges, we can expect that a parafermionic zero mode exists as well. This is indeed the case, as we will now show.
To fix the ideas consider $\theta = 0$ and the limit $f = 0$. From our discussion of Section 5.1 we know that in the free case the strong zero modes are given by

$$\gamma_1 = \sigma_1 \qquad \gamma_{2L} = i\sigma_L Q_4. \tag{6.32}$$

we can rewrite these operators in terms of the Ising variables, using (6.24,6.25) and

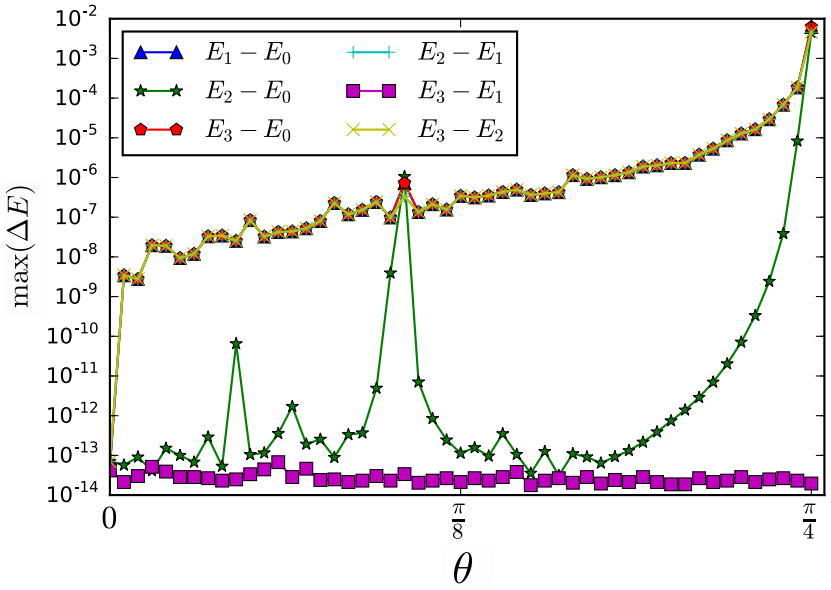

Figure 6.7: Maximal energy splitting between q-sectors at $N = 4$, as a function of θ (for $\phi = 0$). The maximum is taken over the entire spectrum (obtained by exact diagonalisation), for an $L = 8$ chain with $f = 0.01$.

(6.28). We have

$$\begin{aligned} \gamma_1 &= \frac{1}{\sqrt{2}} \left(e^{i\frac{\pi}{4}} \sigma^z_{1,u} + e^{-i\frac{\pi}{4}} \sigma^z_{1,d} \right) \\ \gamma_{2L} &= \frac{i}{\sqrt{2}} \left(e^{i\frac{\pi}{4}} \sigma^z_{L,u} Q^u_2 + e^{-i\frac{\pi}{4}} \sigma^z_{L,d} Q^u_2 \right) T \ . \end{aligned} \tag{6.33}$$

In this form, we can now recognize the presence in γ_1, γ_{2L} of the first orders of the expansions (2.23) for Majorana zero modes of the upper chain and the lower one. When the two chains are decoupled we can use the same method employed in Section 2.2 separately for the two chains and thus find the zero modes of the interacting model, i. e. for all $f = 0$ and $\theta = 0$. This leads to

$$\begin{aligned} \gamma_1 &= \frac{1}{\sqrt{2}} \left(e^{i\frac{\pi}{4}} \psi^u_{left} + e^{-i\frac{\pi}{4}} \psi^d_{left} \right) \\ \gamma_{2L} &= -\frac{i}{\sqrt{2}} \left(e^{i\frac{\pi}{4}} \psi^u_{right} + e^{-i\frac{\pi}{4}} \psi^d_{right} Q^u_2 Q^d_2 \right) T \end{aligned} \tag{6.34}$$

where $\psi^{u(d)}_{left}$, $\psi^{u(d)}_{right}$ are as in (2.23), but relative to the up (down) chain degrees of freedom. We already saw that these operators are localised on the edges by construction and therefore also their combination is.

We can now consider what happens to the zero mode once we move away from $\theta = 0$. As noted in Section 5.1.2, when N is composite (and $N = 4$ is), there are bands which are everywhere degenerate and from our previous discussion we expect that this should allow them to be split in a q-dependent fashion for generic θ. The special points above are an exception to this, but once we move away from these we

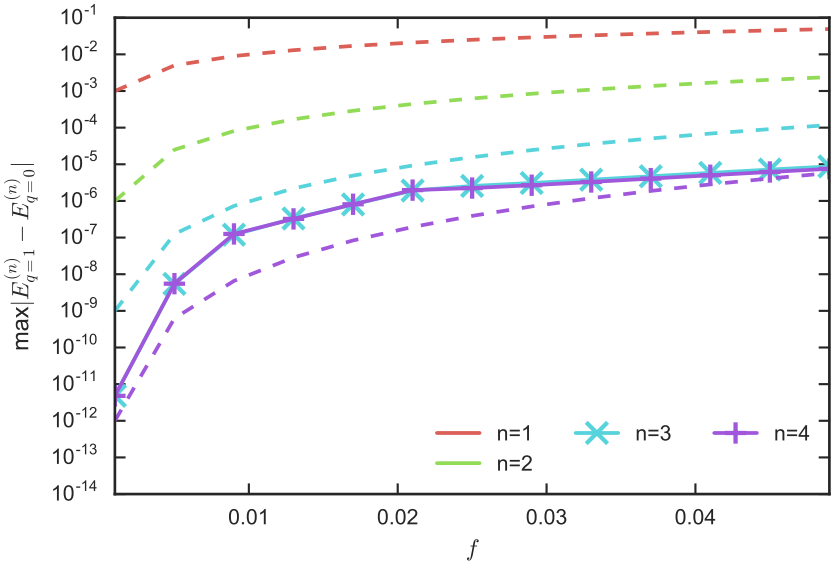

Figure 6.8: The maximum differences between $q = 1$ and $q = 0$ sectors of the estimates from nth order degenerate perturbation theory for a range of values of the perturbing parameter f. This is for the eighth and ninth excited bands for a chain of length $L = 7$ with $N = 4$ and with chiral parameter $\theta = 0.2$. The dashed lines show f^n and act as a guide. The degenerate space from which we perturb here has dimension 90.

expect to rapidly lose the strong zero-mode protection. This is clear from figure 6.3, where we show the maximal energy splitting between q-sectors for all energy levels as a function of θ, for a small finite system. Away from the $\theta = 0$ there is generically splitting between all q-sectors which differ by 1 or 3. Figure 6.3 shows the splitting as a function of f at each order of perturbation theory for two such everywhere degenerate bands of a seven site system. This figure clearly demonstrates that there are third order processes which split the degeneracy between q-sectors and that this splitting does not disappear as higher order terms are added.

For q-sectors which differ by 2, there is no splitting observed at generic θ. The absence of splitting between the $q = 1$ and $q = 3$ sectors is explained by the dihedral symmetry discussed in Section 5.2 (which is present since we set $\phi = 0$). However between the $q = 0$ and $q = 2$ sectors there is splitting around the most prominent resonance points (cf. Fig. 6.5), but behaviour consistent with exact degeneracy away from these points.

The fact that the sectors with $\Delta q = 2$ do not generally split is connected to the survival of order two zero-mode operators related to γ_1^2 and γ_{2L}^2. To see this note that whenever we have a $\mathbb{Z}_N$ parafermionic zero-mode Ψ such that N is even, then the operator $\Phi = \Psi^{(N/2)}$ is a zero-mode with

$$\Phi^2 = 1 \qquad \Phi Q_N = -Q_N \Phi.$$

Considering the two zero modes at the end of the chain Φ_{left}, Φ_{right}, we also note that

$$\Phi_{left}\Phi_{right} = (-1)^{N/2}\Phi_{right}\Phi_{left},$$

so Φ is a fermionic mode if $N/2$ is odd. If $N/2$ is even, as is the case we are considering, Φ is bosonic. Nevertheless its existence implies order two degeneracy throughout the spectrum, as it anti-commutes with Q_N. At $\theta = 0$ we can immediately write

$$\begin{aligned}\Phi_{left} &= (\gamma_1)^2 = \psi^u_{left}\psi^d_{left} \\ \Phi_{right} &= (\gamma_{2L})^2 = i\psi^u_{right}\psi^d_{right}\end{aligned} \tag{6.35}$$

and we stress that these operators exist for any f. Away from $\theta = 0$, the parafermionic zero-modes no longer exist but the mode $\Phi_{left/right}$ may survive. We can attempt to construct it using an iterative technique similar to the one employed in Section 2.2 to find the Majorana zero modes. In the next chapter we will define a general scheme to carry on such iterative construction of the zero modes. We will therefore delay the explanation on how this is done and only state the result here. To first order in f we have

$$\begin{aligned}\Phi_{left} = \sigma^z_{1,u}\sigma^z_{1,d} &+ f\frac{\sigma^x_{1,u}}{\cos(2\theta)}\left(\cos(\theta)\sigma^z_{d,1}\sigma^z_{u,2} - \sin(\theta)\sigma^z_{d,1}\sigma^z_{d,2}\right) \\ &+ f\frac{\sigma^x_{1,d}}{\cos(2\theta)}\left(\cos(\theta)\sigma^z_{u,1}\sigma^z_{d,2} + \sin(\theta)\sigma^z_{u,1}\sigma^z_{u,2}\right)\end{aligned} \tag{6.36}$$

The number of terms on the right hand side grows fast with the order of approximation. For example, the second order involves terms with products of the operators $\sigma^x_{u/d,1/2}$ and $\sigma^z_{u/d,1/2/3}$ and we spare the reader the explicit expression. We will see in the next chapter that such operators are generically normalizable.

There are some features that are worth noting. It is clear that, even at first order, there are singularities in the expansion. The factor $1/\cos(2\theta)$ in the of $\Phi^{(1)}_{left}$ diverges precisely at the resonance point $\theta = \pi/4$ where there is indeed q-dependent splitting of the degeneracy at first order in f (this is prominently visible in Fig.6.3). This is true also for the next order, where we see that the next resonance point appear at $\theta = \frac{1}{2}\arccos\left(\frac{4}{5}\right)$, exactly where we see splittings appears in Fig. 6.3. The reason for the emergence of this structure will be clarified in the next chapter.

Chapter 7

Construction of the Zero Mode

In this chapter we will explain how to explicitly construct the zero mode. The method developed here constitutes a generalization of the one used in [21]. We will describe this construction for parafermionic clock models, but it can be employed to find zero modes of other spin models as well. The material contained in this chapter is based upon [28].

7.1 Iterative method and super-operators

The previous analysis shows, through a perturbative approach, that the perturbation V can destroy the zero mode for values of θ where bands with different values of the total domain wall parity cross. The same perturbative analysis hints that the band degeneracy is left unbroken whenever the total domain wall parity is conserved. Even though the persistence of this degeneracy strongly suggests the presence of zero modes there is no guarantee that *localised* and *normalizable* zero modes exist. Our aim is therefore to build up a recursive method, along the lines of [21], that would allow the explicit construction of such operators. To keep the exposition simple in the following, except when explicitly specified, we will consider quantum clock models as in (5.1) for $N = 3$.

To fix the ideas let's consider the left edge. It is reasonable to expect that if a localised zero mode ψ exists, when we introduce the transverse field, this will reduce to γ_1 in the limit $f \to 0$. In other words, we suppose that the zero mode admits an expansion

$$\psi = \psi^{(0)} + f\psi^{(1)} + \ldots + f^L\psi^{(L)} = \sum_{i=0}^{L} f^i\psi^{(i)} \tag{7.1}$$

Where $\psi^{(0)} = \gamma_1 = \sigma_1$. As we saw, the defining relations of the zero mode ψ are similar to those satisfied by $\psi^{(0)}$

$$[H, \psi] = O(e^{-\frac{L}{\xi}}) \tag{7.2}$$

with $\xi > 0$, some constant length scale that can also be $+\infty$. Moreover

$$Q\psi = \omega\psi Q \tag{7.3}$$

which, as we saw, implies that the splitting between bands with the same (n_0, n_1, n_2), in different Q sectors, vanishes exponentially with the length of the system. For the normalization, as we said, we will mainly be concerned with the conditions

$$\psi^3 = 1 + O(e^{-\frac{L}{\xi}}) \tag{7.4}$$

and

$$\psi^2 = \psi^\dagger + O(e^{-\frac{L}{\xi}}) \ . \tag{7.5}$$

Together, they imply that the zero mode is normalized on a finite chain and, in fact, we see that

$$\psi^\dagger\psi = 1 + O(e^{-\frac{L}{\xi}}) \ . \tag{7.6}$$

Despite this, the norm of ψ may still diverge if the limit $L \to \infty$ is taken at fixed f, because the coefficient in front of the Lth term may grow quickly with L, similarly to what happens in [23] for spin chains. We will consider this further in Section 7.5. We stress that we will be interested in zero modes localised at the edge of the system. As we saw, for finite systems, this property is ensured if matrix elements acting on longer chains of sites also appear at higher order in f. However in the limit $L \mapsto \infty$ this may not be enough to guarantee that the mode is localised as the matrix elements themselves could grow faster than f^L. This is closely connected to the normalization issue.

Let's now consider the commutator $[H, \psi]$. Because of (7.1) we have

$$[H, \psi] = \sum_{k=1}^{L} f^k \left(\left[H_0, \psi^{(k)} \right] + \left[V, \psi^{(k-1)} \right] \right) \ , \tag{7.7}$$

which means that in order for (7.2) to be true (for all f) we must have

$$\left[H_0, \psi^{(k)} \right] = - \left[V, \psi^{(k-1)} \right] \qquad k = 1, 2, \ \ldots, \ L-1 \ . \tag{7.8}$$

The commutators with H_0, and V are linear operators acting on a Hilbert space of operators. Therefore, in principle, each of (7.8) gives a linear system that can be solved recursively once we fix $\psi^{(0)}$. In reality this method still presents certain ambiguities, related to the fact that the commutators with H_0, and V are not invertible operators. We will address these in detail in the following.

To understand the point it is better to rewrite the operators $\mathcal{H}_0 = [H_0, \cdot\,]$ and $\mathcal{V} = [V, \cdot\,]$ in a nicer form.

The Hilbert space on which these commutators act is isomorphic to the Hilbert

space for two copies of the original model. This can be established by using the so called Choi-Jamiolkowski isomorphism [91, 92], which can be defined by linearly extending its definition on the basis elements:

$$|i_1, i_2, \ldots, i_L\rangle|j_1, j_2, \ldots, j_L\rangle := |i_1, i_2, \ldots, i_L\rangle\langle j_1, j_2, \ldots, j_L| \tag{7.9}$$

with $|i_1, i_2, \ldots, i_L\rangle$ and $|j_1, j_2, \ldots, j_L\rangle$ as in (5.3). On each site this basis simply corresponds to the canonical basis for matrices. For example we have

$$\begin{aligned} \sigma &= \begin{pmatrix} 1 & 0 & 0 \\ 0 & \omega & 0 \\ 0 & 0 & \omega^2 \end{pmatrix} = |0\rangle|0\rangle + \omega|1\rangle|1\rangle + \omega^2|2\rangle|2\rangle \\ \tau &= \begin{pmatrix} 0 & 1 & 0 \\ 0 & 0 & 1 \\ 1 & 0 & 0 \end{pmatrix} = |0\rangle|1\rangle + |1\rangle|2\rangle + |2\rangle|0\rangle \ . \end{aligned} \tag{7.10}$$

It can be easily seen that, given any operator O, in this basis the commutator with O takes the form

$$[O, \cdot\,] = O \otimes \mathbb{1} - \mathbb{1} \otimes O^T \tag{7.11}$$

where O^T is the transpose of the operator O. In the following we will usually name these operators after their action on the Left and Right sectors of (7.9)

$$O^L = O \otimes \mathbb{1} \qquad O^R = \mathbb{1} \otimes O \tag{7.12}$$

Since H_0 and V are hermitian, because of (7.11), we have

$$\begin{aligned} \mathcal{H}_0 &= [H_0, \cdot\,] = H_0^L - H_0^{R^T} = H_0^L - H_0^{R^*} \\ \mathcal{V} &= [V, \cdot\,] = V^L - V^{R^T} = V^L - V^{R^*} \ . \end{aligned} \tag{7.13}$$

The basis that we chose is precisely the one in which $\mathcal{H}_0$ is diagonal and we can write

$$\begin{aligned} \mathcal{H}_0 &= -\sum_{i=1}^{L-1} e^{i\theta} {\sigma_{i+1}^L}^\dagger \sigma_i^L - e^{i\theta} {\sigma_{i+1}^R}^\dagger \sigma_i^R + h.c. \\ \mathcal{V} &= -\sum_{i=1}^{L} e^{i\phi} \tau_i^L - e^{-i\phi} \tau_i^R + h.c. \ . \end{aligned} \tag{7.14}$$

Since $\mathcal{H}_0$ is diagonal we can easily find its eigenvalues, which we will indicate as

$$E^{i_1, i_2, \ldots, i_L}_{j_1, j_2 \ldots, j_L} = E_{j_1, j_2, \ldots, j_L} - E_{i_1, i_2, \ldots, i_L} \tag{7.15}$$

with $E_{j_1, j_2, \ldots, j_L}$, $E_{i_1, i_2, \ldots, i_L}$ as in (5.12).

As we saw the free energies of H_0 depend only on the domain walls along the chain. This means that when the left and right chain have the same domain walls at the end, they will cancel out

$$E^{i_1,i_2,\ldots,j_{L-1},i_L}_{j_1,j_2\ldots,j_{L-1},i_L} = E^{i_1,i_2,\ldots,j_{L-1}}_{j_1,j_2\ldots,j_{L-1}} \qquad \forall\ i_L, j_{L-1} = 0,1,2\ . \tag{7.16}$$

It will be useful for the following to isolate the local structure of $\mathcal{V}$, therefore we set

$$\mathcal{V}_k = -e^{i\phi}\tau^L_k + e^{-i\phi}\tau^R_k + h.c. \tag{7.17}$$

and $\mathcal{V}$ can be written as the sum of its local terms

$$\mathcal{V} = \sum_{k=1}^{L} \mathcal{V}_k\ . \tag{7.18}$$

Using a nomenclature coming from the study of open quantum systems, we will refer to operators acting on the space of operators as *super-operators* [93] (note that in literature the definition of right operators usually differs from our own by a transposition, that is $O^R = \mathbb{1} \otimes O^T$).
Written in terms of the basis (7.9) the operator $\psi^{(0)}$ takes the form

$$\psi^{(0)} = \sigma_1 = \sum_{i_1} \omega^{i_1} |i_1\rangle|i_1\rangle \otimes I_{L-1} \tag{7.19}$$

where I_k is the identity operator acting on a chain of length k:

$$I_k = \sum_{i_1,\ldots,i_k} |i_1, i_2, \ldots, i_k\rangle|i_1, i_2, \ldots, i_k\rangle \tag{7.20}$$

In order to simplify the notation, we will often write (7.9) as

$$|\mathbf{i}_k\rangle|\mathbf{j}_k\rangle\ ,$$

where $\mathbf{i}_k$, $\mathbf{j}_k$ represents the collection of the k indices $i_1, i_2, \ldots, i_k$ and $j_1, j_2, \ldots, j_k$. If $k < L$ it will be implicitly left for understood that there is a I_{L-k} tensored at the end of the chain. For example we will write (7.19) as

$$\psi^{(0)} = \sum_{i_1} \omega^{i_1} |i_1\rangle|i_1\rangle\ . \tag{7.21}$$

When we will need to highlight relations between specific indices we will often write terms like

$$|\mathbf{i}_{t-1}, i_t, \mathbf{i}_{k-t}\rangle|\mathbf{j}_{t-1}, j_t, \mathbf{j}_{k-t}\rangle\ .$$

As a final remark, we write down the form taken in the super-operator basis by

the equations (7.8), which define the zero mode expansion:

$$\mathcal{H}_0\psi^{(k+1)} = -\mathcal{V}\psi^{(k)} \qquad k = 1, 2, \ldots, L-1 \ . \tag{7.22}$$

7.1.1 Restrictions on the solutions

In this section we will consider super-operator symmetries of $\mathcal{H}_0$ and $\mathcal{V}$. These can be used to reduce the dimension of the space where we need to look for a solution of the problem. The first symmetry we will describe can be given in terms of the super-operator

$$\mathcal{Q} = \prod_{i=1}^{L} \tau_i^L \prod_{i=1}^{L} \tau_i^R. \tag{7.23}$$

Note that in ordinary operator language, given an operator O, with this definition we have

$$\mathcal{Q}O = QOQ^T \ . \tag{7.24}$$

The use of $\mathcal{Q}$ allows us to rewrite condition (7.3) as [1]

$$\mathcal{Q}\psi = \omega\psi \ . \tag{7.25}$$

Since $\mathcal{Q}\psi^{(0)} = \omega\psi^{(0)}$ and since $\mathcal{H}_0$ and $\mathcal{V}$ commute with $\mathcal{Q}$ we can impose this condition also at higher orders.

The two super-operators $\mathcal{H}_0$ and $\mathcal{V}$ also have a chiral symmetry that reflects the commutator structure of their definition

$$\begin{aligned} (\mathcal{T}\mathcal{K})\mathcal{H}_0(\mathcal{T}\mathcal{K})^{-1} &= -\mathcal{H}_0 \\ (\mathcal{T}\mathcal{K})\mathcal{V}(\mathcal{T}\mathcal{K})^{-1} &= -\mathcal{V} \end{aligned} \tag{7.26}$$

where $\mathcal{T}$ is the super-operator which exchanges the left and right sectors,

$$\mathcal{T}|\mathbf{i}_L\rangle|\mathbf{j}_L\rangle = |\mathbf{j}_L\rangle|\mathbf{i}_L\rangle. \tag{7.27}$$

and $\mathcal{K}$ is the complex conjugation

$$\mathcal{K}(i\mathbb{1})\mathcal{K}^{-1} = -i\mathbb{1} \ . \tag{7.28}$$

Therefore $\mathcal{T}\mathcal{K}$ simply corresponds to the conjugate transposition of operators. As in the previous case, since

$$\mathcal{T}\mathcal{K}(\psi^{(0)}) = (\mathcal{K}\psi^{(0)}) \tag{7.29}$$

[1] From our definitions we have that (7.3) can be given as

$$Q^L\psi = \omega {Q^R}^T\psi \ .$$

Since in our basis Q is orthogonal, equation (7.25) follows.

we can impose this condition, by induction, also at higher orders. By this we mean that the expansion obtained starting from $\mathcal{K}(\psi^{(0)})$, denoted as $(\mathcal{K}\psi)^{(k)}$, can be obtained as

$$(\mathcal{K}\psi)^{(k)} = \mathcal{T}\mathcal{K}(\psi^{(k)}) \ . \tag{7.30}$$

Note that in the case $\phi = 0$, both $\mathcal{H}_0$ and $\mathcal{V}$ are *real* super-operators, and (7.30) reduces to

$$\psi^{(k)} = \mathcal{T}\psi^{(k)} \ , \tag{7.31}$$

which can be used to diminish the dimensionality of the Hilbert space where we need to look for a solution.

7.1.2 General considerations on $Null(\mathcal{H}_0)$

Consider now a vector belonging to $Null(\mathcal{H}_0)$, which is non trivial only up to some site $k \leq L-1$ (locality). Explicitly,

$$|i_1, i_2, \ldots, i_{k-1}, i_k\rangle |j_1, j_2, \ldots, j_{k-1}, j_k\rangle \otimes I_{L-k} \ . \tag{7.32}$$

if this vector belongs to $Null(\mathcal{H}_0)$, because of (7.15), we are forced to have

$$E_{i_1,i_2,\ldots,i_k,l} = E_{j_1,j_2,\ldots,j_k,l} \qquad l = 0, 1, 2 \ . \tag{7.33}$$

Since l is arbitrary, we can subtract two copies of the above equation with different values of the final clocks l and l'. Using (5.13) we get

$$E_{i_k,l} - E_{i_k,l'} = E_{j_k,l} - E_{j_k,l'}$$

and, after simple trigonometric manipulation, we end up with the condition

$$\sin\left((l + l' - 2i_k)\frac{\pi}{3} + \theta\right) = \sin\left((l + l' - 2j_k)\frac{\pi}{3} + \theta\right) \ . \tag{7.34}$$

Since l, l' are arbitrary this equation can be true if and only if $i_k = j_k$ [2]. Concretely this means that operators that commute with H_0 cannot have τs on the last site where they act non-trivially[3]. We remark that this has to be true independently of θ.

Suppose now that θ is such that the total domain wall parity, as defined in (5.28), is conserved, in the sense that two vectors with the same energy also have the same

[2]The same conclusion could be obtained also by considering directly in the commutator picture without the need to consider super-operators.

[3]Note that we are still supposing that these operators do not act non-trivially on the whole the chain, since we will be interested in the large L limit.

total domain wall parity[4]. This means that

$$i_k - i_1 = j_k - j_1 \ . \tag{7.35}$$

Since we just saw that, for operators in $Null(\mathcal{H}_0)$, $i_k = j_k$, we are forced to have

$$i_1 = j_1 \ . \tag{7.36}$$

We can therefore sum up these observations by the following statement

Property 1. *A basis for the operators belonging to $Null(\mathcal{H}_0)$ and acting non trivially only up to some site k is given by*

$$|\mathbf{i}_{k-1}, i_k\rangle|\mathbf{j}_{k-1}, i_k\rangle \qquad s.t. \qquad E^{\mathbf{i}_{k-1},i_k}_{\mathbf{j}_{k-1},i_k} = 0$$

if additionally θ is such that the total domain wall parity is conserved, then the basis is given by

$$|i_1, \mathbf{i}_{k-2}, i_k\rangle|i_1, \mathbf{j}_{k-1}, i_k\rangle \qquad E^{i_1,\mathbf{i}_{k-1},i_k}_{i_1,\mathbf{j}_{k-1},i_k} = 0$$

As we will see this simple characterization of the vectors in $Null(\mathcal{H}_0)$ will be crucial when we will consider the existence of zero modes.

7.2 Super-operators and perturbation theory

As seen above, in order to find the zero mode, we need to solve the system of equations

$$\mathcal{H}_0\psi^{(k+1)} = -\mathcal{V}\psi^{(k)} \qquad k = 1, \ldots, L-1 \ . \tag{7.37}$$

We will now show that this problem configures as a perturbation expansion of the super-Hamiltonian

$$\mathcal{H} = \mathcal{H}_0 + f\mathcal{V} \ . \tag{7.38}$$

Consider in fact an operator ψ as in (7.1) and such that

$$\mathcal{H}\psi = E\psi \tag{7.39}$$

with

$$E = E^{(0)} + fE^{(1)} + f^2E^{(2)} + \ldots + f^LE^{(L)} \ . \tag{7.40}$$

If we call $\mathcal{P}_0$ the projector into $Null(\mathcal{H}_0)$ and $\mathcal{Q}_0 = 1 - \mathcal{P}_0$, we can project (7.39) into $Null(\mathcal{H}_0)$ and its orthogonal space. Using that $\mathcal{P}_0\mathcal{H}_0 = 0$ and $\mathcal{P}_0 + \mathcal{Q}_0 = 1$ we

[4]As explained in Section 5.1.2 resonance points appear because there are two different combinations of domain walls with the same energy. Given a resonance point that does (does not) conserve the total domain wall parity at some energy, it is not possible to have another resonance, at higher energy, that does not (does) conserve the total domain wall parity.

have

$$\begin{aligned} f\mathcal{P}_0\mathcal{V}\psi &= E\mathcal{P}_0\psi \\ \mathcal{H}_0\mathcal{Q}_0\psi + f\mathcal{Q}_0\mathcal{V}\psi &= E\mathcal{Q}_0\psi \ . \end{aligned} \tag{7.41}$$

Order by order this set of equations gives

$$\begin{aligned} \mathcal{P}_0\mathcal{V}\psi_p^{(k)} &= -\mathcal{P}_0\mathcal{V}\psi_q^{(k)} + \sum_{i=0}^{k+1} E^{(k+1-i)}\psi_p^{(i)} \\ \mathcal{H}_0\psi_q^{(k+1)} &= -\mathcal{Q}_0\mathcal{V}\left(\psi_q^{(k)} + \psi_p^{(k)}\right) + \sum_{i=0}^{k+1} E^{(k+1-i)}\psi_q^{(i)} \ , \end{aligned} \tag{7.42}$$

where $\psi_p^{(k)} = \mathcal{P}_0\psi^{(k)}$, $\psi_q^{(k)} = \mathcal{Q}_0\psi^{(k)}$ and these are the defining equations of any degenerate perturbation theory.
We can now see that finding the zero mode is equivalent to solving the perturbation theory problem when we impose the conditions

$$E^{(j)} = 0 \qquad \forall\ j \leq L-1 \ , \tag{7.43}$$

which concretely means that we are asking our perturbation to not split the degeneracy up to order $L-1$.
Equation (7.42) thus reduces to

$$\mathcal{P}_0\mathcal{V}\psi_p^{(k)} = -\mathcal{P}_0\mathcal{V}\psi_q^{(k)} \tag{7.44}$$

$$\mathcal{H}_0\psi_q^{(k+1)} = -\mathcal{Q}_0\mathcal{V}\left(\psi_q^{(k)} + \psi_p^{(k)}\right) \tag{7.45}$$

which in turn is equivalent to (7.22).

Usually in degenerate perturbation theory one looks for solutions that split the energy at some order. This is therefore quite a strange perturbation expansion, as we are specifically looking for a solution of the perturbative problem that does not split the energy at any order less than L. Moreover we explicitly require that $\psi^{(0)} = \sigma_1$, while generally the starting point of the perturbation, inside the degenerate space is, to some extent, undetermined.
This makes the existence of a solution of (7.44) and (7.45) highly non trivial. In particular we know from [27] and our previous discussion, that if we are at resonance points where the total domain wall parity is not conserved, the system will develop energy splitting at order strictly less than L and this means that a solution of (7.44, 7.45) will in general be not possible.

To understand the structure of the possible solution let's now consider the action of $\mathcal{H}_0$ and $\mathcal{V}$. The terms of the operator $\mathcal{V}$ can act at most on one element of the chains, while the terms of $\mathcal{H}_0$ can act on two elements. This means that, if as in (7.19) we start with an operator that is localised on the edge, and a solution of

(7.22) exists, the next order will be made of operators different from the identity for at most one site more than the previous order.
For this reason, from now on we will consider each $\psi^{(k)}$ to be operators acting non-trivially on a chain of length $k+1$. In this sense (7.22) can be rewritten as

$$\mathcal{H}_0\psi^{(k+1)} = -\mathcal{V}\psi^{(k)} \otimes I_1 \tag{7.46}$$

With this notation, we can rewrite (7.44, 7.45) as

$$\mathcal{P}_0(\mathcal{V}\psi_p^{(k)} \otimes I_1) = -\mathcal{P}_0\mathcal{V}(\psi_q^{(k)} \otimes I_1) \tag{7.47}$$

$$\mathcal{H}_0\psi_q^{(k+1)} = -\mathcal{Q}_0\mathcal{V}\left(\psi_q^{(k)} + \psi_p^{(k)}\right) \otimes I_1 \ . \tag{7.48}$$

If a solution exists, equation (7.47) implies that

$$\mathcal{V}\left(\psi_p^{(k)} + \psi_q^{(k)}\right) \otimes I_1 \in Null(\mathcal{H}_0)^{\perp} \ , \tag{7.49}$$

where the inner product entering into the definition of the orthogonal space is the canonical one (in the space of operators). If this condition is satisfied we can then easily find a solution for $\psi_q^{(k+1)}$, by inverting $\mathcal{H}_0$

$$\psi_q^{(k+1)} = -\frac{1}{\mathcal{H}_0}\mathcal{V}\left(\psi_p^{(k)} + \psi_q^{(k)}\right) \otimes I_1 \ , \tag{7.50}$$

where we can omit the $\mathcal{Q}_0$ because of (7.49).
Hence, starting with $\psi_q^{(k)}$, given a $\psi_p^{(k)}$ such that (7.47) holds, we can always find a $\psi_q^{(k+1)}$ which makes the iterative construction work and if $\psi_p^{(k)}$ acts on chains only up to order $k+1$ then $\psi_q^{(k+1)}$ will still be localised on the edge by construction. Note however that nothing prevents $\mathcal{P}_0\mathcal{V}\psi_q^{(k)} \otimes I_1$ to contain terms living on chains of length $k+2$[5]. We will see that if this is the case, then a "local" solution for $\psi_p^{(k)}$ will generally not exist (see Section 7.3.2).
This treatment clarifies the importance of $\psi_p^{(k)}$ and equation (7.50) shows that the problem of finding zero modes is essentially a problem of finding $\psi_p^{(k)}$.

In the following we will carefully consider the situations in which such a "local" $\psi_p^{(k)}$ exists and in which it does not.

7.2.1 Some restrictions on ψ_p

In this section we will consider some general properties of the solution $\psi_p^{(k)}$. Let's therefore start by considering a generalization of (7.47)

$$\mathcal{P}_0\mathcal{V}(\alpha_p \otimes I_1) = \beta_p \otimes I_1 \tag{7.51}$$

[5] $\psi_q^{(k)}$ lives on a chain of length $k+1$

with arbitrary $\beta_p \in Null(\mathcal{H}_0)$ and $\alpha_p \in Null(\mathcal{H}_0)$.
Suppose β_p to be an operator that acts non trivially only up to some site t

$$\beta_p = \sum_{i,j} \beta^{\mathbf{i}_{t-1},i_t}_{\mathbf{j}_{t-1},i_t} |\mathbf{i}_{t-1}, i_t\rangle|\mathbf{j}_{t-1}, i_t\rangle \tag{7.52}$$

for some coefficients $\beta^{\mathbf{j}_{t-1},i_t}_{\mathbf{i}_{t-1},i_t}$. Note that the equality between the last left-right coefficients comes from Property 1. In the same way we can suppose that α_p is an operator that acts non trivially only up to some site t'

$$\alpha_p = \sum_{i,j} \alpha^{\mathbf{i}_{t'-1},i_{t'}}_{\mathbf{j}_{t-1},i_{t'}} |\mathbf{i}_{t'-1}, i_{t'}\rangle|\mathbf{j}_{t'-1}, i_{t'}\rangle \ . \tag{7.53}$$

The action of $\mathcal{V}$ on α_p is given by

$$\mathcal{V}\alpha_p = \sum_{k=1}^{t'-1} \mathcal{V}_k\alpha_p + \mathcal{V}_{t'}\alpha_p \ . \tag{7.54}$$

Since the last two left and right indices in (7.53) are the same for all the terms in the sum, we can easily write down the action of $\mathcal{V}_{t'}$ on α_p. That is

$$\begin{aligned}\mathcal{V}_{t'}\alpha_p = &\sum_{i,j} \left(\alpha^{\mathbf{i}_{t'-1},i_{t'}+1}_{\mathbf{j}_{t'-1},i_{t'}+1} - \alpha^{\mathbf{i}_{t'-1},i_{t'}}_{\mathbf{j}_{t'-1},i_{t'}}\right) e^{-i\phi}|\mathbf{i}_{t'-1}, i_{t'}+1\rangle|\mathbf{j}_{t'-1}, i_{t'}\rangle \\ &+ \sum_{i,j} \left(\alpha^{\mathbf{i}_{t'-1},i_{t'}-1}_{\mathbf{j}_{t'-1},i_{t'}-1} - \alpha^{\mathbf{i}_{t'-1},i_{t'}}_{\mathbf{j}_{t'-1},i_{t'}}\right) e^{i\phi}|\mathbf{i}_{t'-1}, i_{t'}-1\rangle|\mathbf{j}_{t'-1}, i_{t'}\rangle \ .\end{aligned} \tag{7.55}$$

In order to consider solutions of (7.51) we now need to project down these terms in $Null(\mathcal{H}_0)$. As we saw, since the terms in $\mathcal{H}_0$ can act on two neighbouring sites, we need to consider the addition of an identity operator at the end of the chain. This means that we need to consider operators of the type

$$|\mathbf{i}_{t'-1}, i_{t'} \pm 1, i_{t'+1}\rangle|\mathbf{j}_{t'-1}, i_{t'}, i_{t'+1}\rangle \ . \tag{7.56}$$

Projecting down into $Null(\mathcal{H}_0)$ consists in finding those values $i_{t'+1} \in \mathbb{Z}_3$ such that $E^{\mathbf{i}_{t'-1},i_{t'}\pm1,i_{t'+1}}_{\mathbf{j}_{t'-1},\ \ i_{t'}\ ,i_{t'+1}} = 0$. To simplify the problem we can write $E^{\mathbf{i}_{t'-1},i_{t'}\pm1,i_{t'+1}}_{\mathbf{j}_{t'-1},\ \ i_{t'}\ ,i_{t'+1}}$ as

$$E^{\mathbf{i}_{t'-1},i_{t'}\pm1,i_{t'+1}}_{\mathbf{j}_{t'-1},\ \ i_{t'}\ ,i_{t'+1}} = E^{\mathbf{i}_{t'-1},i_{t'}}_{\mathbf{j}_{t'-1},i_{t'}} + E^{i_{t'-1},i_{t'}\pm1,i_{t'+1}}_{i_{t'-1},\ \ i_{t'}\ ,i_{t'+1}} \ ,$$

where we have gathered all the final domain walls in the second term. Since by hypothesis $E^{\mathbf{i}_{t'-1},i_{t'}}_{\mathbf{j}_{t'-1},i_{t'}} = 0$, we are left with

$$E^{\mathbf{i}_{t'-1},i_{t'}\pm1,i_{t'+1}}_{\mathbf{j}_{t'-1},\ \ i_{t'}\ ,i_{t'+1}} = E^{i_{t'-1},i_{t'}\pm1,i_{t'+1}}_{i_{t'-1},\ \ i_{t'}\ ,i_{t'+1}} \ .$$

Consider now $E^{i_{t'-1},i_{t'}\pm 1,i_{t'+1}}_{i_{t'-1},\ i_{t'}\ ,i_{t'+1}}$. In terms of domain wall energies we have

$$E^{\mathbf{i}_{t'-1},i_{t'}\pm 1,i_{t'+1}}_{\mathbf{j}_{t'-1},\ i_{t'}\ ,i_{t'+1}} = \epsilon_{i_{t'+1}-i_{t'}} + \epsilon_{i_{t'}-i_{t'-1}} - \epsilon_{i_{t'+1}-i_{t'}\mp 1} - \epsilon_{i_{t'}\pm 1-i_{t'-1}} \ ,$$

with ϵ_m as in (5.13). If we now set

$$i_{t'+1} = 2i_{t'} \pm 1 - i_{t'-1} \mod 3 \tag{7.57}$$

we get

$$E^{\mathbf{i}_{t'-1},i_{t'}\pm 1,i_{t'+1}}_{\mathbf{j}_{t'-1},\ i_{t'}\ ,i_{t'+1}} = 0 \tag{7.58}$$

This means that all the terms in (7.55) will always produce operators that belong to the $Null(\mathcal{H}_0)$ when we tensor them out with I_1 [6]. Therefore the operator $\mathcal{P}_0\mathcal{V}_t\alpha_p\otimes I_1$ will always contain terms of the form

$$|\mathbf{i}_{t'-1}, i_{t'}, i_{t'+1}\rangle|\mathbf{j}_{t'-1}, j_{t'}, i_{t'+1}\rangle \qquad i_{t'} \neq j_{t'} \ . \tag{7.59}$$

Imposing that α_p constitutes a solution of (7.51), with β_p as in (7.52) then implies that $t = t'$ and

$$\mathcal{V}_t\alpha_p = 0 \ , \tag{7.60}$$

since in β_p all the terms have the same left-right indices at site t, while we saw that if (7.60) is not satisfied then $\mathcal{V}_t$ invariably produces terms of the form (7.59) when it acts on α_p.
Condition (7.60), in turn means that

$$\alpha_p = \sum_{i,j} \alpha^{\mathbf{i}_{t-2},i_{t-1}}_{\mathbf{j}_{t-2},i_{t-1}} |\mathbf{i}_{t-2}, i_{t-1}\rangle|\mathbf{j}_{t-2}, i_{t-1}\rangle \otimes I_1 \ , \tag{7.61}$$

where, as before, the identity between the left-right indices at site $t-1$ comes from Property 1. The presence of I_1 at the end comes from (7.60) and was made explicit. In the context of finding zero modes, we can sum up the previous discussion into the following statement

Property 2. *Suppose that a local solution of the zero mode exists up to some order k. If $\mathcal{P}_0\mathcal{V}\psi^{(k)}_q$ acts on a chain of length $k+1$, then $\psi^{(k)}_p$ acts on a chain that is not longer than k.*

[6] To get a feeling of what this property means consider the state

$$|0,2,0\rangle|0,1,0\rangle \ ,$$

which belongs to $Null(\mathcal{H}_0)$ for a system of length 3 and general θ, as can be easily checked. The above property means that we can be sure the states

$$|0,2,1,2\rangle|0,1,0,2\rangle \qquad |0,2,2,0\rangle|0,1,0,0\rangle$$

belong to $Null(\mathcal{H}_0)$ for a system of length 4 and general θ without the need to compute their energies.

The above discussion also allows us to find the solutions of the equation

$$\mathcal{P}_0 \mathcal{V} \alpha_p \otimes I_1 = 0 \ . \tag{7.62}$$

In fact, by repeating the previous argument by induction, we can argue that α_p has to be of the form

$$\alpha_p = \sum_{i_1} \alpha_{i_1}^{i_1} |i_1\rangle |i_1\rangle \ . \tag{7.63}$$

This means that all the solutions are given by the linear combination of the operators

$$|0\rangle|0\rangle \qquad |1\rangle|1\rangle \qquad |2\rangle|2\rangle \ , \tag{7.64}$$

except when $\theta = 0, \frac{\pi}{3}, \frac{2\pi}{3}$, in which cases the unique solution is given[7] by $\alpha = I_1$. This last remark imposes restrictions on the possible local starting points for the zero mode expansion. In fact equation (7.47), in the case of $k = 0$, reduces to

$$\mathcal{P}_0 \mathcal{V} \psi_p^{(0)} \otimes I_1 = 0 \tag{7.65}$$

(as by assumption $\psi_q^{(0)} = 0$). This property, together with the condition

$$\mathcal{Q} \psi_p^{(0)} = \omega \psi_p^{(0)} \ , \tag{7.66}$$

implies that the following holds

Property 3. *When $\theta \neq 0, \frac{\pi}{3}, \frac{2\pi}{3}$, the unique possible local starting point of the zero mode expansion is given by*

$$\psi_p^{(0)} = \sigma_1 \ . \tag{7.67}$$

When $\theta = 0, \frac{\pi}{3}, \frac{2\pi}{3}$ a local zero mode does not exist.

As a last remark we note that in the above discussion a fundamental role was played by the fact that we have identities I_1 at the end of our operators. This means that the existence of solutions of (7.51) that act non-trivially on the whole chain is in principle not excluded.

[7] This can be easily seen by considering that at these resonance points there are additional states present in $Null(\mathcal{H}_0)$. For example consider $\theta = 0$, we have

$$\begin{aligned}
\mathcal{P}_0 \mathcal{V} |0\rangle|0\rangle \otimes I_1 &= -e^{-i\phi}|1,2\rangle|0,2\rangle - e^{i\phi}|2,1\rangle|0,1\rangle + e^{i\phi}|0,2\rangle|1,2\rangle + e^{-i\phi}|0,1\rangle|2,1\rangle \\
\mathcal{P}_0 \mathcal{V} |1\rangle|1\rangle \otimes I_1 &= -e^{-i\phi}|2,0\rangle|1,0\rangle - e^{i\phi}|0,2\rangle|1,2\rangle + e^{i\phi}|1,0\rangle|2,0\rangle + e^{-i\phi}|1,2\rangle|0,2\rangle \\
\mathcal{P}_0 \mathcal{V} |2\rangle|2\rangle \otimes I_1 &= -e^{-i\phi}|0,1\rangle|2,1\rangle - e^{i\phi}|1,0\rangle|2,0\rangle + e^{i\phi}|2,0\rangle|1,0\rangle + e^{-i\phi}|2,1\rangle|0,1\rangle
\end{aligned}$$

and similarly for the other θs. Note that normally we would get zero out of this, but in the case $\theta = 0$ two domain walls have the same energy, so $\mathcal{P}_0$ does not project to zero. It can be easily seen that the unique solution of (7.51) that gives 0 is

$$I_1 = |0\rangle|0\rangle + |1\rangle|1\rangle + |2\rangle|2\rangle \ .$$

7.3 Locality and total domain wall parity

In this section we will prove that, if total domain wall parity is conserved, then

$$\mathcal{P}_0(\mathcal{V}\psi_q^{(k)} \otimes I_1) = \beta_p^{(k)} \otimes I_1 \ , \tag{7.68}$$

with $\beta_p^{(k)} \in Null(\mathcal{H}_0)$. We will see that this condition is the main factor that allows a formal expansion of the zero mode to exist at each order k.
This equation imposes that the terms in $Null(\mathcal{H}_0)$ coming from the action of $\mathcal{V}$ on $\psi_q^{(k)}$ are not living on chains longer than the one on which $\psi_q^{(k)}$ lives, and it is therefore a condition imposed upon the locality of the terms of $\mathcal{V}\psi_q^{(k)}$.

In this section we will prove that this condition is fulfilled whenever the total domain wall parity is conserved and that it is generally not satisfied otherwise. We will also prove that when (7.68) does not hold it is not possible to find local solutions for $\psi_p^{(k)}$.
Let's therefore separately consider the two cases.

7.3.1 Conserved total domain wall parity

We will now show that when the total domain wall parity is conserved, condition (7.68) is satisfied. This is related to the general structure taken by the solution $\psi_q^{(k)}$. Suppose therefore that a solution exists up to some order k, then the following statement holds

Property 4. *If the total domain wall parity is conserved the solution $\psi^{(k)}$, with $k \geq 1$, is composed of operators that act non trivially on a chain of length $k+1$ and in particular*

- *The operators $\psi_q^{(k)}$ can be written as*

$$\psi_q^{(k)} = \eta_q^{(k)} + \rho_q^{(k)}$$

where $\eta_q^{(k)}$ is a linear combination of operators of the form

$$|i_1, i_2, \ldots, i_k, i_{k+1}\rangle|j_1, j_2, \ldots, j_k, i_{k+1}\rangle \qquad i_l \neq j_l \qquad \forall\ l = 1, 2 \ldots, k \tag{7.69}$$

while $\rho_q^{(k)}$ acts trivially on site k and it is a linear combination of operators of the form

$$|\mathbf{i}_{k-1}, i_k\rangle|\mathbf{j}_{k-1}, i_k\rangle \otimes I_1 \qquad E^{\mathbf{i}_{k-1}, i_k}_{\mathbf{j}_{k-1}, i_k} \neq 0 \ .$$

- *$\psi_p^{(k)}$ is made of operators that act non-trivially on chains that are no longer than k. This means that $\psi_p^{(k)}$ is a linear combination of operators of the form*

$$|i_1, \mathbf{i}_{k-2}, i_k\rangle|i_1, \mathbf{j}_{k-2}, i_k\rangle \otimes I_1 \qquad E^{i_1, \mathbf{i}_{k-2}, i_k}_{i_1, \mathbf{j}_{k-2}, i_k} = 0 \ .$$

The proof of the first part of Property 4 is given in Appendix C, while the second part, related to the structure of $\psi_p^{(k)}$ follows from Property 2. In the next part of this section we will content ourselves with showing that Property 4 implies (7.68). Suppose therefore that a solution exists up to some order k and that total domain wall parity is conserved, as in Property 4.
First of all we recall equation (7.16), which states that whenever we have the same domain walls on the left and on the right sector at end of the chain, they cancel out when computing the energy

$$E^{\mathbf{j}_{k-1},i_k,i_{k+1}}_{\mathbf{i}_{k-1},i_k,i_{k+1}} = E^{\mathbf{j}_{k-1},i_k}_{\mathbf{i}_{k-1},i_k} \qquad \forall\ i_k = 0,1,2\ . \tag{7.70}$$

This means in particular that

$$\mathcal{P}_0(\mathcal{V}|\mathbf{i}_{k-1},i_k\rangle|\mathbf{j}_{k-1},i_k\rangle \otimes I_2) = \mathcal{P}_0(\mathcal{V}|\mathbf{i}_{k-1},i_k\rangle|\mathbf{j}_{k-1},i_k\rangle \otimes I_1) \otimes I_1\ , \tag{7.71}$$

As can be explicitly checked. Therefore, extending by linearity, we have

$$\begin{aligned} \mathcal{P}_0(\mathcal{V}\rho_q^{(k)} \otimes I_1) &= \mathcal{P}_0(\mathcal{V}\rho_q^{(k)}) \otimes I_1 \\ \mathcal{P}_0(\mathcal{V}\psi_p^{(k)} \otimes I_1) &= \mathcal{P}_0(\mathcal{V}\psi_p^{(k)}) \otimes I_1 \end{aligned} \tag{7.72}$$

Thus the only problems when we consider (7.68), may arise from $\eta_q^{(k)}$. If the total domain wall parity is conserved, however, this can never happen. In (7.69), in fact, $i_1 \neq j_1$ and we know that operators in $Null(\mathcal{H}_0)$ need to have $i_1 = j_1$ because of Property 1. This means that the action of $\mathcal{V}_1$ is the only one that can survive after the projection into $Null(\mathcal{H}_0)$:

$$\mathcal{P}_0(\mathcal{V}\eta_q^{(k)} \otimes I_1) = \mathcal{P}_0(\mathcal{V}_1\eta_q^{(k)} \otimes I_1) + \mathcal{P}_0(\sum_{l=2}^{k+1} \mathcal{V}_l\eta_q^{(k)} \otimes I_1) = \mathcal{P}_0(\mathcal{V}_1\eta_q^{(k)} \otimes I_1)\ .$$

Since the action $\mathcal{V}_{k+1}$ does not survive the projection, the last indices in the constituent (7.69) of $\eta_q^{(k)}$ are still the same. Therefore, using again (7.70), we have

$$\mathcal{P}_0(\mathcal{V}\eta_q^{(k)} \otimes I_1) = \beta_p^{(k)} \otimes I_1\ . \tag{7.73}$$

with $\beta_p^{(k)} \in Null(\mathcal{H}_0)$ and this proves (7.68).

7.3.2 Broken total domain wall parity

We will now consider what happens when total domain wall parity is not conserved. We already saw what are the problems arising when $\theta = 0, \frac{\pi}{3}, \frac{2\pi}{3}$ in Section 7.2.1, when we considered solutions of equation (7.65). For higher order resonance points something similar happens and, in general, it is not possible to find a local solution for the zero mode expansion. Suppose therefore that $\mathcal{P}_0(\mathcal{V}\psi_q^{(k)} \otimes I_1)$ contains vectors

that do not conserve total domain wall parity.
As we saw in Section 6.2.1 resonance points appear when we consider chains of increasing length. Suppose therefore that θ is such that total domain wall parity is not conserved on chains of length $k+2$.
Using Property 1 we know that the operators $\mathcal{P}_0(\mathcal{V}\psi_q^{(k)}\otimes I_1)$ are a linear combination of operators of the form

$$|i_1, \mathbf{i}_{k-1}, i_k, i_{k+2}\rangle|j_1, \mathbf{j}_{k-1}, j_k, i_{k+2}\rangle \qquad i_1 \neq j_1 \qquad E^{i_1,\mathbf{i}_{k-1},i_k,i_{k+2}}_{j_1,\mathbf{j}_{k-1},j_k,i_{k+2}} = 0 \ . \tag{7.74}$$

We stress that the existence of this type of terms is the same as saying that condition (7.68) is not fulfilled (otherwise we would have an identity at the end). Note also that these terms are bound to stem out from the $\eta_q^{(k)}$ of Property 4.

Using Property 2 we know that the solution $\psi_p^{(k)}$ has to live on a chain of length $k+1$, but for chains of smaller length the total domain wall parity is still conserved, which means, using Property 1, that $\psi_p^{(k)}$ has to be the linear combination of vectors of the type

$$|i_1, \mathbf{i}_{k-1}, i_k\rangle|i_1, \mathbf{j}_{k-1} i_k\rangle \otimes I_1 \ . \tag{7.75}$$

Given the local structure of $\mathcal{V}$ this is impossible unless, $i_k = j_k$ in (7.74)[8]. This means that

$$E^{i_1,\mathbf{i}_{k-1},i_k,i_{k+2}}_{j_1,\mathbf{j}_{k-1},i_k,i_{k+2}} = E^{i_1,\mathbf{i}_{k-1},i_k}_{j_1,\mathbf{j}_{k-1},i_k} = 0 \ , \tag{7.76}$$

but this is not possible since by hypothesis for chains of length $k+1$ the total domain wall parity is conserved and $i_1 \neq j_1$. This means that a local solution of (7.47) cannot exist at resonance points where total domain wall parity is broken.

7.3.3 General form of the solution

We will now present a method that allows constructing a general solution for the recursive problem. Unfortunately we do not have a complete proof of the method, but we were able to check our ansatz using symbolic calculation with Mathematica[9] up to 7th order. We stress that our approach can be used to consider the solution of similar problems in other spin chain models, which we explored to some extent, as we will discuss later in the section. This makes us believe in the existence of some general principle that allows the machinery to work, although we were not able to completely demonstrate it so far.

As we said, the problem of finding a zero mode at some order k is essentially a problem of finding $\psi_p^{(k)}$. We repeat for clarity, that once we find a $\psi_p^{(k)}$ such that

$$\mathcal{P}_0(\psi_p^{(k)} + \psi_q^{(k)}) \otimes I_1 = 0 \ , \tag{7.77}$$

[8] $\mathcal{V}$ in fact has to act through $\mathcal{V}_1$ to make $i_1 \neq j_1$ in (7.74).

[9] The set of codes used for the computation and a collection of the results that we obtained can be found at: `https://github.com/Domenico89/clock-models-zero-modes.git` .

we can readily find $\psi_q^{(k+1)}$, by inverting $\mathcal{H}_0$

$$\psi_q^{(k+1)} = -\frac{\mathcal{Q}_0}{\mathcal{H}_0}(\psi_p^{(k)} + \psi_q^{(k)}) \otimes I_1 \tag{7.78}$$

and this inversion is straightforward when everything is written in the basis that we chose, as $\mathcal{H}_0$ is in diagonal form.
As we said, the problems related to finding $\psi_p^{(k)}$, seem to be connected to the locality of the operator $\mathcal{P}_0\mathcal{V}\psi_q^{(k)} \otimes I_1$, as described by condition (7.68).
If condition (7.68) is satisfied, then we find that a solution of the problem can always be written in the form

$$\psi_p^{(k)} = \sum_{l_1+l_2+\ldots+l_{k-1}=k} \Gamma_{l_1,l_2,\ldots,l_{k-1}} \mathcal{P}_0\mathcal{V}\mathcal{S}^{l_1}\mathcal{V}\mathcal{S}^{l_2}\cdots\mathcal{S}^{l_{k-1}}\mathcal{V}\psi_p^{(0)} \tag{7.79}$$

with $\Gamma_{l_1,l_2,\ldots,l_{k-1}} \in \mathbb{Q}$ and

$$\mathcal{S}^l = \begin{cases} \mathcal{P}_0 & l = 0 \\ \left(\frac{\mathcal{Q}_0}{\mathcal{H}_0}\right)^l & l \neq 0 \end{cases} \tag{7.80}$$

In the case of the $N = 3$ parafermionic clock model we have, for example

$$\begin{aligned}
\psi_p^{(0)} &= \sigma_1 \ , \\
\psi_p^{(1)} &= 0 \ , \\
\psi_p^{(2)} &= -\frac{1}{2}\mathcal{P}_0\mathcal{V}\left(\frac{\mathcal{Q}_0}{\mathcal{H}_0}\right)^2\mathcal{V}\psi_p^{(0)} \ , \\
\psi_p^{(3)} &= \frac{1}{2}\mathcal{P}_0\mathcal{V}\left(\frac{\mathcal{Q}_0}{\mathcal{H}_0}\right)^2\mathcal{V}\left(\frac{\mathcal{Q}_0}{\mathcal{H}_0}\right)\mathcal{V}\psi_p^{(0)} + \frac{1}{2}\mathcal{P}_0\mathcal{V}\left(\frac{\mathcal{Q}_0}{\mathcal{H}_0}\right)\mathcal{V}\left(\frac{\mathcal{Q}_0}{\mathcal{H}_0}\right)^2\mathcal{V}\psi_p^{(0)} \ , \\
\psi_p^{(4)} &= \frac{3}{8}\mathcal{P}_0\mathcal{V}\left(\frac{\mathcal{Q}_0}{\mathcal{H}_0}\right)^2\mathcal{V}\mathcal{P}_0\mathcal{V}\left(\frac{\mathcal{Q}_0}{\mathcal{H}_0}\right)^2\mathcal{V}\psi_p^{(0)} - \frac{3}{4}\mathcal{P}_0\mathcal{V}\left(\frac{\mathcal{Q}_0}{\mathcal{H}_0}\right)^2\mathcal{V}\left(\frac{\mathcal{Q}_0}{\mathcal{H}_0}\right)\mathcal{V}\left(\frac{\mathcal{Q}_0}{\mathcal{H}_0}\right)\mathcal{V}\psi_p^{(0)} + \\
&\quad - \frac{1}{2}\mathcal{P}_0\mathcal{V}\left(\frac{\mathcal{Q}_0}{\mathcal{H}_0}\right)\mathcal{V}\left(\frac{\mathcal{Q}_0}{\mathcal{H}_0}\right)^2\mathcal{V}\left(\frac{\mathcal{Q}_0}{\mathcal{H}_0}\right)\mathcal{V}\psi_p^{(0)} - \frac{1}{4}\mathcal{P}_0\mathcal{V}\left(\frac{\mathcal{Q}_0}{\mathcal{H}_0}\right)\mathcal{V}\left(\frac{\mathcal{Q}_0}{\mathcal{H}_0}\right)\mathcal{V}\left(\frac{\mathcal{Q}_0}{\mathcal{H}_0}\right)^2\mathcal{V}\psi_p^{(0)} + \\
&\quad + \frac{1}{4}\mathcal{P}_0\mathcal{V}\mathcal{P}_0\mathcal{V}\left(\frac{\mathcal{Q}_0}{\mathcal{H}_0}\right)\mathcal{V}\left(\frac{\mathcal{Q}_0}{\mathcal{H}_0}\right)^3\mathcal{V}\psi_p^{(0)} + \frac{3}{4}\mathcal{P}_0\mathcal{V}\mathcal{P}_0\mathcal{V}\left(\frac{\mathcal{Q}_0}{\mathcal{H}_0}\right)^2\mathcal{V}\left(\frac{\mathcal{Q}_0}{\mathcal{H}_0}\right)^2\mathcal{V}\psi_p^{(0)} \ .
\end{aligned}$$

The coefficients for $\psi_p^{(5)}$ are given in Appendix D. As far as we could check with our Mathematica code, the solutions always follow this structure. Note that the coefficients do not depend on θ and ϕ and that all the terms in the sums act trivially on the last site of the chain, as imposed by Property 2. The fact that the coefficients Γ for the solution does not depend on θ gives another hint of the fact that when θ is such that the total domain wall parity is not conserved, the zero mode operator cannot be constructed. In particular the presence of $\frac{\mathcal{Q}_0}{\mathcal{H}_0}$ accounts for the divergences that we witnessed when we found the zero mode for $N = 4$ in Section 6.3. In Appendix B we will present a proof for the solutions of $\psi_p^{(1)}$, $\psi_p^{(2)}$ .The solutions for the next orders were found by symbolic computation using Mathematica.

Note that the existence of this type of solutions is related to the exact cancellation

of a very large number of terms, as we will illustrate in Section 7.3.4. It is therefore hard to believe that the above structure is simply the result of chance and this becomes even more apparent when we try to apply the same method to other spin models.

As a final remark, we note that this ansatz is quite reminiscent of the formulas obtained for effective hamiltonians in the framework of degenerate perturbation theory [94, 95]. In particular, the first two orders agree with known formulas for effective hamiltonians, while the rest disagree.

The iterative method in other models

In order to understand the structure of the solution we tried to apply our method to spin models where the existence of a zero mode is already known, like the XYZ model [16] or the models considered in [23]. In every case we studied, we found that the known solutions for the zero modes follow our description.

Strangely enough the existence of these formal expressions for the zero modes hold even when there is no underlying symmetry, as for example in the case of the Hamiltonian

$$H' = -\sum_{i=1}^{L-1} \sigma_i^z \sigma_{i+1}^z + f \sum_{i}^{L} (\sigma_i^x + \sigma_i^z) \ . \tag{7.81}$$

with f, the perturbing parameter. This Hamiltonian, in fact, does not commute with Q_2 (or any other symmetry as far as we know), nonetheless our construction can still be carried out, starting with $\psi_p^{(0)} = \sigma_1^z$ (the free model still possess a local zero mode on the left edge)[10]. The resulting zero mode is in general not normalizable, which means that we do not expect it to survive in the thermodynamic limit, but surprisingly a formal expression for the zero mode can still be written out for any order we could check (up to 8th order). Note that this Hamiltonian is non-integrable and, if written in terms of fermions via Jordan-Wigner transformation, it is highly interacting.

By considering different models, we also see that in general the coefficients Γs are model dependent. For example, if we consider the Hamiltonian

$$H' = -\sum_{i=1}^{L-1} \sigma_i^z \sigma_{i+1}^z + f \sum_{i} \sigma_{i+1}^x \sigma_i^x + \sigma_{i+1}^y \sigma_i^y = H'_0 + fV' \tag{7.82}$$

the first orders of the projections of the zero mode, $psi'_p \in Null(\mathcal{H}'_0)$, constructed

[10]The different phases of this Hamiltonian have been studied in several works see e.g. [96, 97].

with our method, are given by

$$
\begin{aligned}
&psi'^{(0)}_p = \sigma^z_1 \ , \\
&psi'^{(1)}_p = 0 \ , \\
&psi'^{(2)}_p = -\frac{1}{2}\mathcal{P}'_0\mathcal{V}'\left(\frac{\mathcal{Q}'_0}{\mathcal{H}'_0}\right)^2\mathcal{V}'psi'^{(0)}_p \ , \\
&psi'^{(3)}_p = -\frac{2}{3}\mathcal{P}'_0\mathcal{V}'\left(\frac{\mathcal{Q}'_0}{\mathcal{H}'_0}\right)^2\mathcal{V}'\left(\frac{\mathcal{Q}'_0}{\mathcal{H}'_0}\right)\mathcal{V}'\psi^{(0)}_p - \frac{1}{3}\mathcal{P}'_0\mathcal{V}'\left(\frac{\mathcal{Q}'_0}{\mathcal{H}'_0}\right)\mathcal{V}'\left(\frac{\mathcal{Q}'_0}{\mathcal{H}'_0}\right)^2\mathcal{V}'psi'^{(0)}_p \ .
\end{aligned}
$$

We have reasons to believe that the existence of these expressions has to do with the chiral symmetry $\mathcal{TK}$ introduced in Section 7.1.1, but we were not able to figure out how so far.

We tried to apply the same method also to non-hermitian models and the same general structure holds. Notably to the case of free parafermions [81], which can be described through the Hamiltonian $H' = H'_0 + fV'$, with

$$
H' = -\sum_{i=1}^{L-1}\sigma^\dagger_{i+1}\sigma_i - f\sum_{i=1}^{L}\tau_i \ . \tag{7.83}
$$

This is the same as the spin clock model (5.1) for $\theta = 0$, except for the addition of the hermitian conjugated term. In this case, to each order k, we find

$$
psi'^{(k)}_q = \left(-\frac{\mathcal{Q}_0}{\mathcal{H}'_0}\mathcal{V}'\right)^k\psi^{(0)}_p \qquad psi'^{(k)}_p = 0 \ . \tag{7.84}
$$

These are formally the same expressions that one obtains in the case of the transverse Ising model, which we believe provides further evidence that these types of models, rather than (5.1), constitute a closer generalization, even if not hermitian, of the transverse Ising model [81].

7.3.4 Algorithmic solution for ψ_p

The above ansatz for the solution lends itself well to direct checking. Nevertheless the problem of finding the constants Γs of (7.79) is generally not an easy task, especially for large k. However, if we are not interested in the values taken by the Γs, it is possible to design algorithms that would allow finding the $\psi^{(k)}_p$ at any given order (with limitations due to computational power). Strictly speaking, we cannot prove that this algorithm work at all orders, as we need to assume our ansatz (7.79) to hold true in order for it to work. If this is the case we can employ some of the symmetries of the problem, and some of the remarkable cancellations of terms that have to take place for such a solution to exist, in order to simplify the determination of $\psi^{(k)}_p$. As such the recipes that we will present in this section never failed us when we applied them at all the orders that we could check.

Consider therefore a solution for $\psi^{(k)}_p$ as in (7.79). It can be seen by induction,

using repeatedly property (7.16) and the local structure of $\mathcal{V}$, that

$$\psi_p^{(k)} = \psi_{p,k} + \psi_{p,k-1} \otimes I_1 + \ldots + \psi_{p,1} \otimes I_{k-1} \tag{7.85}$$

where $\psi_{p,l}$ are operators acting on chains of length l:

$$\psi_{p,l} = \sum_{j,i} (\chi_l)^{i_1,\mathbf{i}_{l-2},i_l}_{i_1,\mathbf{j}_{l-2},i_l} |i_1,\mathbf{i}_{l-2},i_l\rangle|i_1,\mathbf{j}_{l-2},i_l\rangle \quad \text{with} \quad E^{i_1,\mathbf{i}_{l-2},i_l}_{i_1,\mathbf{j}_{l-2},i_l} = 0 \ . \tag{7.86}$$

With $\mathbf{i}_{l-2}$ and $\mathbf{j}_{l-2}$ not necessarily different from each other. The equation satisfied by the solution $\psi_p^{(k)}$ is given by

$$\mathcal{P}_0(\mathcal{V}\psi_p^{(k)} \otimes I_1) = \beta_p^{(k)} \tag{7.87}$$

with $\beta_p^{(k)} = -\mathcal{P}_0(\mathcal{V}\psi_q^{(k)})$ and

$$\beta_p^{(k)} = \sum_{j,i} (\beta)^{i_1,\mathbf{i}_{k-1},i_{k+1}}_{i_1,\mathbf{j}_{k-1},i_{k+1}} |i_1,\mathbf{i}_{k-1},i_{k+1}\rangle|i_1,\mathbf{j}_{k-1},i_{k+1}\rangle \quad \text{with } E^{i_1,\mathbf{i}_{k-1},i_{k+1}}_{i_1,\mathbf{j}_{k-1},i_{k+1}} = 0 \ . \tag{7.88}$$

The idea behind how to find a solution is now to determine one by one all the $\psi_{p,l}$ that constitute $\psi_p^{(k)}$, starting from $\psi_{p,k}$. Doing this will reduce at each step the dimensionality of the problem. Suppose in fact, to fix the ideas, that we are able to find $\psi_{p,k}$, then we can write

$$\mathcal{P}_0(\mathcal{V}\psi_p^{(k,1)} \otimes I_2) = \beta_p^{(k)} - \mathcal{P}_0(\mathcal{V}\psi_{p,k} \otimes I_1) \tag{7.89}$$

with

$$\psi_p^{(k,1)} = \psi_{p,k-1} + \psi_{p,k-2} \otimes I_1 + \ldots + \psi_{p,1} \otimes I_{k-2} \tag{7.90}$$

If a solution exists and follows (7.85), because of the locality structure of $\mathcal{V}$ and because of condition (7.16) then, necessarily, we need to have

$$\mathcal{P}_0(\mathcal{V}\psi_p^{(k,1)} \otimes I_2) = \beta_p^{(k,1)} \otimes I_1 \tag{7.91}$$

with $\beta_p^{(k,1)} \otimes I_1 = \beta_p^{(k)} - \mathcal{P}_0(\mathcal{V}\psi_{p,k} \otimes I_1)$ and

$$\beta_p^{(k,1)} = \sum_{j,i} (\beta_1)^{i_1,\mathbf{i}_{k-2},i_k}_{i_1,\mathbf{j}_{k-2},i_k} |i_1,\mathbf{i}_{k-2},i_k\rangle|i_1,\mathbf{j}_{k-2},i_k\rangle \quad \text{with} \quad E^{i_1,\mathbf{i}_{k-2},i_k}_{i_1,\mathbf{j}_{k-2},i_k} = 0 \ . \tag{7.92}$$

Therefore $\beta_p^{(k,1)}$ acts on a chain that is one site smaller than the one on which $\beta^{(k)}$ acts. This means that we can reduce the problem to

$$\mathcal{P}_0(\mathcal{V}\psi_p^{(k,1)} \otimes I_1) = \beta_p^{(k,1)} \ , \tag{7.93}$$

which is equivalent to solve the initial problem on a smaller chain and this is com-

putationally very convenient, as the Hilbert spaces involved in the process are of smaller dimensions. This process can be repeated now for $\psi_{p,k-1}$, $\psi_{p,k-2}$, etc... until we exhaust all the terms.

We now need to describe how to determine the various $\psi_{p,l}$. Note however that the fact that it is always possible to go from $\beta_p^{(k,l)}$ living on a chain of length $k+1-l$ to a $\beta_p^{(k,l+1)}$ living on a chain of length $k-l$ is not trivial. It is a consequence of the existence of a solution of the form (7.85) and this implies the equality and the cancellation of a large number of terms in $\beta_p^{(k)}$ when we remove $\psi_{p,l}$ as described above. The presence of this structure can be traced back to the general form of the solution described in Section 7.3.3 and is part of the reason that makes us believe that this form holds in general.

We will now describe how to determine the various $\psi_{p,l}$ terms. This is simpler than it may look, as we do not need to consider the action of the whole $\mathcal{V}$ on $\psi_{p,l}$, but only the action of $\mathcal{V}_l$. Given in fact the structure of (7.85) this super-operator can act non-trivially only on $\psi_{p,l}$ and its action is particularly simple, as all the terms appearing in $\psi_{p,l}$ have $i_l = j_l$. This means that, in order to deduce the form of $\psi_{p,l}$, we only need to consider those terms in $\beta_p^{(k,k-l)}$ such that $i_l \neq j_l$.
For the sake of clarity, we will describe the method for a specific example. We will hence consider the case for $\theta = \frac{\pi}{12}$ and $\phi = 0$, where no resonance occurs. In general, the analysis for any given resonance point (where total domain wall parity is conserved), will depend upon the particular combinations of domain walls that happen to have the same energy. The following analysis needs therefore to be changed accordingly on a case by case basis and works only when we are not at a resonant point. Our purpose is to present a general approach to constructing solutions for $\psi_{p,l}$. There is no real difference in considering solutions for $\psi_{p,l}$ for different ls.

Consider therefore, as an example, the case of $\psi_p^{(5)}$, and suppose that we already know the solution for $\psi_{p,5}$. As we described we can find $\beta_p^{(5,1)}$ from $\beta_p^{(5)}$ and $\psi_{p,4}$ will be given as

$$\psi_{p,4} = \sum_{i,j} (\chi_4)^{i_1,i_2,i_3,i_4}_{i_1,j_2,j_3,i_4} |i_1,i_2,i_3,i_4\rangle |i_1,j_2,j_3,i_4\rangle \quad E^{i_1,j_2,j_3,i_4}_{i_1,j_2,j_3,i_4} = 0 \tag{7.94}$$

and

$$\beta_p^{(4,1)} = \sum_{j,i} (\beta_1)^{i_1,i_2,i_3,i_4,i_5}_{i_1,j_2,j_3,j_4,i_5} |i_1,j_2,j_3,j_4,i_5\rangle |i_1,i_2,i_3,i_4,i_5\rangle \quad E^{i_1,i_2,i_3,i_4,i_5}_{i_1,j_2,j_3,j_4,i_5} = 0 \tag{7.95}$$

As we said we can reconstruct $\psi_{p,4}$ from $\beta_p^{(4,1)}$ by considering the action of $\mathcal{V}_4$ only. This means that we need to look at the elements of $\beta_p^{(4,1)}$ such that $i_4 \neq j_4$. We have to distinguish two subcases with respect of the values taken by i_3 and j_3.

Case $i_3 \neq j_3$

To explain the strategy in this situation we consider a specific example. Consider therefore the terms

$$(\beta_1)^{0,0,2,0,1}_{0,1,0,1,1} \quad (\beta_1)^{0,0,2,0,2}_{0,1,0,2,2} \quad (\beta_1)^{0,0,2,1,2}_{0,1,0,2,2} \quad (\beta_1)^{0,0,2,2,0}_{0,1,0,0,0} \ ,$$

that is, vectors that agree up to the third indices. Using Mathematica it can be checked that

$$\begin{aligned} \beta^{0,0,2,0,1}_{0,1,0,1,1} = \beta^{0,0,2,0,1}_{0,1,0,2,2} &= -\left(\frac{62+71i-(5+60i)\sqrt{3}}{16\sqrt{2+\sqrt{3}}}\right) \\ \beta^{0,0,2,1,2}_{0,1,0,0,2} = \beta^{0,0,2,2,0}_{0,1,0,0,0} &= \left(\frac{62+71i-(5+60i)\sqrt{3}}{16\sqrt{2+\sqrt{3}}}\right) \ . \end{aligned}$$

Note that all the coefficients are the same up to a sign. This is in agreement with the fact that they stem from the action of $\mathcal{V}_4$ on a single operator. In order to find what it is, it suffices to consider the operators that we obtain when we make the fourth indices agree by changing only one of them and discarding the fifth indices. For example for the first vector, $|0,0,2,0,1\rangle|0,1,0,1,1\rangle$, we would get the two terms

$$|0,0,2,1\rangle|0,1,0,1\rangle \quad |0,0,2,0\rangle|0,1,0,0\rangle \tag{7.96}$$

It can be checked that only $|0,0,2,0\rangle|0,1,0,0\rangle$ belongs to $Null(\mathcal{H}_0)$ and therefore is the only vector that can belong to $\psi_{p,4}$. With some effort it can be shown that when $i_3 \neq j_3$ and we are not at a resonance there is always one and only one vector that belongs to $Null(\mathcal{H}_0)$ for any given combination of indexes i_1, j_1, etc... that are not involved[11]. Therefore all these vectors can be obtained from the action of $\mathcal{P}_0\mathcal{V}_4$ on

$$-\left(\frac{62+71i-(5+60i)\sqrt{3}}{16\sqrt{2+\sqrt{3}}}\right)|0,0,2,0\rangle|0,1,0,0\rangle \otimes I_1 \ . \tag{7.97}$$

In other words $(\chi_4)^{0,0,2,0}_{0,1,0,0} = -\left(\frac{62+71i-(5+60i)\sqrt{3}}{16\sqrt{2+\sqrt{3}}}\right)$. Note that all this is possible because the coefficients for β follow the symmetries that we have highlighted above, this means that we are using the assumption that a solution exists. This procedure can then be repeated for all the terms in $\beta^{(4,1)}$ such that $i_4 \neq j_4$ and $i_3 \neq j_3$.
We can now consider the case of $i_3 = j_3$.

[11]Note that there are vectors such that by making the 4th indices agree and discarding the last ones, none of the resulting operators belong to $Null(\mathcal{H}_0)$. Consider for example $|0,2,2,2,0\rangle|0,1,1,1,0\rangle$. It can be easily checked then both $|0,2,2,1\rangle|0,1,1,1\rangle$ and $|0,2,2,2\rangle|0,1,1,2\rangle$ are not part of $Null(\mathcal{H}_0)$.
This means that $(\beta_1)^{0,2,2,2,0}_{0,1,1,1,0} = 0$, otherwise it would not possible to find a solution. This is part of the peculiar cancellations that take place when solving these systems.

Case $i_3 = j_3$

Also in this case, to understand the point, it is better to consider a specific case. Take therefore the terms

$$\begin{array}{ccc} (\beta_1)^{0,0,2,2,0}_{0,2,2,0,0} & (\beta_1)^{0,0,2,1,1}_{0,2,2,2,1} & (\beta_1)^{0,0,2,0,2}_{0,2,2,1,2} \\ (\beta_1)^{0,0,2,1,2}_{0,2,2,0,2} & (\beta_1)^{0,0,2,0,0}_{0,2,2,2,0} & (\beta_1)^{0,0,2,2,1}_{0,2,2,1,1} \end{array}$$

It can be checked with Mathematica that

$$(\beta_1)^{0,0,2,2,1}_{0,2,2,1,1} = -(\beta_1)^{0,0,2,1,1}_{0,2,2,2,1} \quad (\beta_1)^{0,0,2,0,0}_{0,2,2,2,0} = -(\beta_1)^{0,0,2,2,0}_{0,2,2,0,0} \quad (\beta_1)^{0,0,2,1,2}_{0,2,2,0,2} = -(\beta_1)^{0,0,2,0,1}_{0,2,2,1,0}$$

and

$$\begin{aligned} (\beta_1)^{0,0,2,2,0}_{0,2,2,0,0} &= -\frac{-276+117i+217\sqrt{3}}{8\sqrt{2+\sqrt{3}}(-37-14i+(20+3i)\sqrt{3}))} + \frac{1}{52}\sqrt{1980-2337i} \\ (\beta_1)^{0,0,2,1,1}_{0,2,2,2,1} &= -\frac{1}{52}\sqrt{1980-2337i} \\ (\beta_1)^{0,0,2,0,2}_{0,2,2,1,2} &= \frac{-276+117i+217\sqrt{3}}{8\sqrt{2+\sqrt{3}}(-37-14i+(20+3i)\sqrt{3}))} \end{aligned} \tag{7.98}$$

Note that

$$(\beta_1)^{0,0,2,2,0}_{0,2,2,0,0} + (\beta_1)^{0,0,2,1,1}_{0,2,2,2,1} + (\beta_1)^{0,0,2,0,2}_{0,2,2,1,2} = 0 \ . \tag{7.99}$$

Again we need to consider the action of $\mathcal{P}_0\mathcal{V}_4$ on vectors of length 4. Consider therefore

$$(\chi_4)^{0,0,2,0}_{0,2,2,0}|0,0,2,0\rangle|0,2,2,0\rangle + (\chi_4)^{0,0,2,1}_{0,2,2,1}|0,0,2,1\rangle|0,2,2,1\rangle + (\chi_4)^{0,0,2,2}_{0,2,2,2}|0,0,2,2\rangle|0,2,2,2\rangle \ .$$

Taking $\mathcal{P}_0\mathcal{V}_4$ on this vector (tensored with I_1) and equating it with the terms in $\beta^{(4,1)}_p$ that we are interested in, yields the system of equations

$$\begin{cases} (\chi_4)^{0,0,2,2}_{0,2,2,2} - (\chi_4)^{0,0,2,0}_{0,2,2,0} = (\beta_1)^{0,0,2,2,0}_{0,2,2,0,0} \\ (\chi_4)^{0,0,2,1}_{0,2,2,1} - (\chi_4)^{0,0,2,2}_{0,2,2,2} = (\beta_1)^{0,0,2,1,1}_{0,2,2,2,1} \\ (\chi_4)^{0,0,2,0}_{0,2,2,0} - (\chi_4)^{0,0,2,1}_{0,2,2,1} = (\beta_1)^{0,0,2,0,2}_{0,2,2,1,2} \ . \end{cases} \tag{7.100}$$

Since condition (7.99) holds, this system of equation admits solutions and we can set

$$\begin{aligned} (\chi_4)^{0,0,2,0}_{0,2,2,0} &= \frac{\beta^{0,0,2,0,2}_{0,2,2,1,2} - \beta^{0,0,2,2,0}_{0,2,2,0,0}}{3} + \lambda \\ (\chi_4)^{0,0,2,1}_{0,2,2,1} &= \frac{\beta^{0,0,2,1,1}_{0,2,2,2,1} - \beta^{0,0,2,0,2}_{0,2,2,1,2}}{3} + \lambda \\ (\chi_4)^{0,0,2,2}_{0,2,2,2} &= \frac{\beta^{0,0,2,2,0}_{0,2,2,0,0} - \beta^{0,0,2,1,1}_{0,2,2,2,1}}{3} + \lambda \end{aligned} \tag{7.101}$$

with some arbitrary constant λ that we can take to be 0. The value that we chose for this constant is not important, from our discussion in Section 7.2.1 we in fact know that a basis for the solution of

$$\mathcal{P}_0\mathcal{V}(\psi_p^{(5)} \otimes I_1) = 0 \tag{7.102}$$

is given by σ_1. This means that at the end of this process, after we determined all the $\psi_{p,l}$, the various arbitrary constants that we fix during the solution will reduce to some multiple of σ_1 (always assuming that the algorithm will produce a legitimate solution for the problem)[12].

Repeating this procedure for all terms of $\beta_p^{(4,1)}$ such that $i_3 = j_3$ we can exhaust all of them and then we can continue to the next step and consider $\beta_p^{(4,2)}$ as we described. The process can now be repeated in the same way again by considering terms with $i_3 \neq j_3$, consider the subcases $i_2 \neq j_2$, $i_2 = j_2$ and so on until we find all the terms in $\psi_p^{(k)}$.

This concludes our explanation on how to find solutions for ψ_p. Obviously, the fact that we can formally construct these operators, does not generally mean that in the limit $L \to \infty$ the zero modes exists, as the perturbation series could fail to converge. This problem is the subject of the next section.

7.4 The problem of normalization

We will now address the problem of normalization. As we said, in order for the zero mode to describe parafermionic degrees of freedom sitting on the edges of the system, we need to have

$$\psi^3 = I_L + O\left(f^{-L}\right) \tag{7.103}$$

moreover we would like the zero mode to be normalizable

$$\psi^\dagger\psi = I_L + O\left(f^{-L}\right) \ , \tag{7.104}$$

in this section we will show that these two conditions are equivalent and that once we find a formal solution for the zero mode they can always be fulfilled. Let's therefore consider these cases in full generality.

7.4.1 Expansions of ψ^3

Let's consider ψ^3 first. Since ψ admits an expansion in f, so does ψ^3:

$$\psi^3 = I_L + f(\psi^3)^{(1)} + f^2(\psi^3)^{(2)} + \dots \tag{7.105}$$

[12]As we will see in Section 7.4, we can exploit the addition of linear combinations of σ_1 to fix the normalization of the zero mode. So, at this level, it does not really matter which constant multiplies σ_1.

and we have

$$(\psi^3)^{(k)} = \sum_{k_1+k_2+k_3=k} \psi^{(k_1)}\psi^{(k_2)}\psi^{(k_3)} \ . \tag{7.106}$$

Since every $\psi^{(k)}$ satisfies the equation $[H_0, \psi^{(k)}] = -[V, \psi^{(k-1)}]$ so does $(\psi^3)^{(k)}$, in fact

$$\begin{aligned} &\left[H_0, (\psi^3)^{(k)}\right] = \\ &= \sum_{k_1+k_2+k_3=k} \left[H_0, \psi^{(k_1)}\right] \psi^{(k_2)}\psi^{(k_3)} + \psi^{(k_1)} \left[H_0, \psi^{(k_2)}\right] \psi^{(k_3)} + \psi^{(k_1)}\psi^{(k_2)} \left[H_0, \psi^{(k_3)}\right] \end{aligned}$$

using that $\left[H_0, \psi^{(l)}\right] = -\left[V, \psi^{(l-1)}\right]$ for all $l \leq k$

$$\begin{aligned} &\left[H_0, (\psi^3)^{(k)}\right] = \\ &= -\sum_{k_1+k_2+k_3=k} \left[V, \psi^{(k_1-1)}\right] \psi^{(k_2)}\psi^{(k_3)} + \psi^{(k_1)} \left[V, \psi^{(k_2-1)}\right] \psi^{(k_3)} + \psi^{(k_1)}\psi^{(k_2)} \left[V, \psi^{(k_3-1)}\right] \ . \end{aligned}$$

Since $\psi^{(-1)} = 0$ we see that

$$\left[H_0, (\psi^3)^{(k)}\right] = -\left[V, (\psi^3)^{(k-1)}\right] \tag{7.107}$$

or, written in the super-operator formalism

$$\mathcal{H}_0(\psi^3)^{(k)} \otimes I_1 = -\mathcal{V}(\psi^3)^{(k-1)} \otimes I_1 \ . \tag{7.108}$$

In line with what we have done in the previous sections, we can project this equation down to $Null(\mathcal{H}_0)$ and its orthogonal space. Equation (7.108) is therefore equivalent to

$$\begin{aligned} &\mathcal{H}_0(\psi^3)^{(k)}_q \otimes I_1 = -\mathcal{Q}_0\mathcal{V}\left((\psi^3)^{(k-1)}_q + (\psi^3)^{(k-1)}_p\right) \otimes I_1 \\ &\mathcal{P}_0\mathcal{V}(\psi^3)^{(k)}_p \otimes I_1 = -\mathcal{P}_0\mathcal{V}(\psi^3)^{(k)}_q \otimes I_1 \end{aligned} \tag{7.109}$$

with $(\psi^3)^{(k)}_q = \mathcal{Q}_0(\psi^3)^{(k)}$ and $(\psi^3)^{(k)}_p = \mathcal{P}_0(\psi^3)^{(k)}$.

We can now see that the following property holds

Property 5. *If a solution for the zero mode exists up to some order k then*

$$(\psi^3)^{(j)}_q = 0 \qquad (\psi^3)^{(j)}_p = \lambda_j I_{j+1} \qquad \forall j = 1, 2 \ldots, k \tag{7.110}$$

with constants $\lambda_j \in \mathbb{C}$.

This property can be easily proved by induction. It is true for $j = 0$, as

$$\sigma_1^3 = I_1 \ .$$

Since

$$\mathcal{Q}(\psi^3)^{(0)} = (\psi^3)^{(0)}$$

and since the super-operator $\mathcal{Q}$ commutes with $\mathcal{H}_0$ and $\mathcal{V}$, we can assume that

$$\mathcal{Q}(\psi^3)^{(j)} = (\psi^3)^{(j)} \qquad \forall j = 1, 2, \ldots, k \ . \tag{7.111}$$

Suppose therefore that Property 5 is true for $j-1$, that is

$$(\psi^3)_q^{(j-1)} = 0 \qquad (\psi^3)_p^{(j-1)} = \lambda_{j-1} I_j \ . \tag{7.112}$$

Since $\mathcal{V} I_j = 0$ we have

$$\mathcal{H}_0(\psi^3)_q^{(j)} \otimes I_1 = -\mathcal{Q}_0 \mathcal{V}(\psi^3)_p^{(j-1)} \otimes I_1 = 0 \ ,$$

which in turn means

$$(\psi^3)_q^{(j)} = 0 \ ,$$

and hence we are left with

$$\mathcal{P}_0 \mathcal{V}(\psi^3)_p^{(j)} \otimes I_1 = -\mathcal{P}_0 \mathcal{V}(\psi^3)_q^{(j)} \otimes I_1 = 0 \ .$$

We already encountered this equation in Section 7.2.1 and we know that its solutions are the linear combinations of the operators

$$|0\rangle|0\rangle \otimes I_j \qquad |1\rangle|1\rangle \otimes I_j \qquad |2\rangle|2\rangle \otimes I_j \ .$$

Since we are supposing that a solution exists and because of (7.111), we have that the unique solution is given by

$$(\psi^3)_p^{(j)} = \lambda_j I_L \ . \tag{7.113}$$

for some constant $\lambda_j \in \mathbb{C}$.

7.4.2 Expansion of $\psi^\dagger \psi$

We can now consider what happens to $\psi^\dagger \psi$. Also in this case, since ψ admits an expansion in f, so does $\psi^\dagger \psi$

$$\psi^\dagger \psi = I_L + f(\psi^\dagger \psi)^{(1)} + f^2(\psi^\dagger \psi)^{(2)} + \ldots \tag{7.114}$$

and we have

$$(\psi^\dagger \psi)^{(k)} = \sum_{k_1 + k_2 = k} {\psi^{(k_1)}}^\dagger \psi^{(k_2)} \ . \tag{7.115}$$

Now the discussion goes exactly as it went for ψ^3 and we have that $(\psi^\dagger\psi)^{(k)}$ satisfies the equations

$$\begin{aligned}&\mathcal{H}_0(\psi^\dagger\psi)^{(k)}_q = -\mathcal{Q}_0\mathcal{V}\left((\psi^\dagger\psi)^{(k-1)}_q + (\psi^\dagger\psi)^{(k-1)}_p\right)\otimes I_1\\&\mathcal{P}_0\mathcal{V}(\psi^\dagger\psi)^{(k)}_p\otimes I_1 = -\mathcal{P}_0\mathcal{V}(\psi^\dagger\psi)^{(k)}_q\otimes I_1\ .\end{aligned} \tag{7.116}$$

In the same way as before, the following property can be proved

Property 6. *If a solution for the zero mode exists up to some order k then*

$$(\psi^\dagger\psi)^{(j)}_q = 0 \qquad (\psi^\dagger\psi)^{(j)}_p = \lambda'_j I_L \qquad \forall j = 1, 2\ldots, k \tag{7.117}$$

with constants $\lambda'_j \in \mathbb{R}$.

7.4.3 Expansions of ψ^2 and $\psi^\dagger$

We will now consider the expansions of ψ^2 and $\psi^\dagger$ [13] and we will see how we can choose the normalization by considering the relation between them.

To understand the point suppose that

$$\psi^2 = \psi^\dagger + O(f^L)\ . \tag{7.118}$$

then this would imply that

$$(\psi^3)^{(j)} = (\psi^\dagger)^{(j)} \qquad \forall\ j = 1, 2, \ldots, L-1 \tag{7.119}$$

and therefore:

$$\lambda_j = \lambda'_j \qquad \forall\ j = 1, 2, \ldots, L-1\ . \tag{7.120}$$

If this condition is satisfied then we can always make sure that (7.103,7.104) are satisfied by renormalizing ψ.
This, therefore, raises the question: can we make sure that at each order j

$$(\psi^2)^{(j)} = (\psi^{(j)})^\dagger\ ,$$

or use our freedom in choosing a solution to make sure that this is true?
We can start to answer this question by establishing the following

Property 7. *Suppose that*

$$(\psi^2)^{(j)} = (\psi^{(j)})^\dagger \tag{7.121}$$

[13] Note that in the super-operator basis (7.9) $\psi^\dagger$ is given by

$$\psi^\dagger = \mathcal{T}\mathcal{K}\psi$$

with $j = 1, 2, \ldots, k-1$. *Then we have*

$$(\psi^2)^{(k)} - (\psi^\dagger)^{(k)} = \lambda''_k \sigma_1^\dagger \otimes I_{L-1} \tag{7.122}$$

with $\lambda''_k \in \mathbb{C}$.

The proof of this property goes exactly in the same way as the proofs for Property 5 and Property 6. Although note that for it to be true we need to assume that we are able, somehow, to make sure that (7.121) holds at each order $j < k$. The only difference is that

$$\mathcal{Q}((\psi^2)^{(0)} - (\psi^\dagger)^{(0)}) = \omega^2((\psi^2)^{(0)} - (\psi^\dagger)^{(0)})$$

which means that a solution to

$$\mathcal{P}_0 \mathcal{V}((\psi^2)^{(k)} - (\psi^\dagger)^{(k)}) \otimes I_1 = 0 \ .$$

is given by $\lambda''_k \sigma_1^2 \otimes I_{L-1}$.
We are finally in the position to consider how to fix the normalization.

Choice of the normalization

As we already pointed out, whenever we find a solution for the expansion of the zero mode, it is not unique. In fact, given a solution of order k, we can always add to it a solution of the equation

$$\mathcal{P}_0 \mathcal{V} \xi_p^{(k)} \otimes I_1 = 0 \ , \tag{7.123}$$

with $\xi_p^{(k)} \in Null(\mathcal{H}_0)$ and we would still get a zero mode, in fact

$$\mathcal{P}_0 \mathcal{V}(\psi_p^{(k)} + \xi_p^{(k)}) \otimes I_1 = \mathcal{P}_0 \mathcal{V} \psi_p^{(k)} \otimes I_1 = -\mathcal{P}_0 \mathcal{V} \psi_q^{(k)} \otimes I_1 \ .$$

By now we should be acquainted with the fact that if we are looking for solutions such that $\mathcal{Q}\psi = \omega\psi$, the only possible choice for $\xi_p^{(k)}$ is given by

$$\xi_p^{(k)} = \xi_k \sigma_1 \otimes I_k \tag{7.124}$$

with $\xi_k \in \mathbb{C}$. This freedom can be used to fix the normalization and in particular we can use it to enforce the condition

$$(\psi^2)^{(j)} = (\psi^\dagger)^{(j)}. \tag{7.125}$$

Doing this at every order will guarantee that

$$\psi^2 = \psi^\dagger + O(f^L) \ . \tag{7.126}$$

First of all note that

$$(\psi^2)^{(k)} = \sum_{k_1+k_2=k} \psi^{(k_1)}\psi^{(k_2)} \ . \tag{7.127}$$

It is therefore not difficult to prove that if we use our freedom to add operators of the form $\xi_p^{(k)}$ to $\psi^{(k)}$

$$\psi^{(k)} \to \psi^{(k)} + \xi_p^{(k)} \tag{7.128}$$

$(\psi^2)^{(k)} - (\psi^\dagger)^{(k)}$ will transform as

$$(\psi^2)^{(k)} - (\psi^\dagger)^{(k)} \to (\psi^2)^{(k)} - (\psi^\dagger)^{(k)} + (2\xi_k - \xi_k^*)\sigma_1^\dagger \tag{7.129}$$

Using induction and Property 7, we therefore see that if at every order $j \leq L-1$ we set

$$\xi_j = -\mathrm{Re}(\lambda_j'') - \frac{i}{3}\mathrm{Im}(\lambda_j'') \ , \tag{7.130}$$

then

$$\psi^2 = \psi^\dagger + O\left(f^L\right) \ . \tag{7.131}$$

As we already noted, because of Property 5 and Property 6 this condition entail

$$(\psi^3)^{(j)} = \lambda_j I_L \qquad (\psi^\dagger\psi)^{(j)} = \lambda_j I_L \qquad \forall j = 1, 2, \ldots, k \tag{7.132}$$

and $\lambda_j \in \mathbb{R}$ as in Property 6. Therefore, up to a normalization factor, equations (7.103) and (7.104) are true. Note however that in general λ_j will depend on θ and ϕ.

7.5 Convergence of the formal series

Even though the method outlined above seems to work at every order, divergences may still arise, as the coefficients of the truncated series constituting the zero mode for a chain of length L could grow faster than f^L . In this sense the above expansions for the zero mode have to be to considered as formal expressions that we can write whenever θ is such that the total domain wall parity is conserved.
The next problem we need to address is therefore about the radius of convergence of these formal series in f.
To this end, we first need to define what is the error that we make when we truncate the expressions for the zero modes. Hence we define

$$\mathcal{N}^2 = \left| \frac{1}{3^L}\mathrm{Tr}\left(\psi^\dagger\psi\right) - 1 \right| \ , \tag{7.133}$$

where the normalization factor $1/3^L$ is such that I_L has norm 1 and ψ is obtained

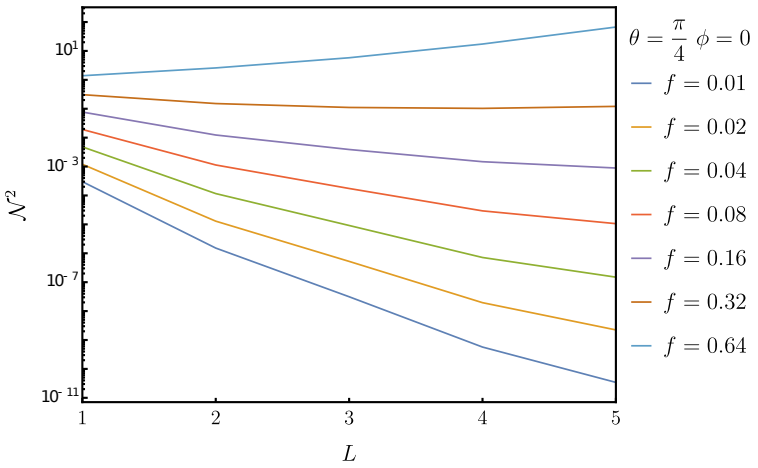

Figure 7.1: The norm of the truncated expansion for different chain lengths L and $\theta = \frac{\pi}{4}$, $\phi = 0$.

by truncating the expansion at order L

$$\psi = \psi^{(0)} + f\psi^{(1)} + \ldots + f^{L-1}\psi^{(L-1)} + f^{L}\psi^{(L)} \ . \tag{7.134}$$

$\mathcal{N}^2$ is therefore simply the Frobenius norm of ψ [98]. As we said, even though we can always satisfy

$$\psi^{\dagger}\psi = I_L + O\left(f^L\right) \tag{7.135}$$

the sum of all terms of order f^L could still diverge for $L \to \infty$. The expansion converges if and only if $\mathcal{N}^2 \to 0$. In Figure 7.5 and Figure 7.5 we show the plots of $\mathcal{N}^2$ for $\theta = \frac{\pi}{4}$ and $\frac{\pi}{6}$, in both cases we chose $\phi = 0$.
From these graphs we see that there seems to be a finite radius of convergence, even though the information we can get from this kind of plot is obviously limited.

Another related, but different problem, regards the convergence of the commu-

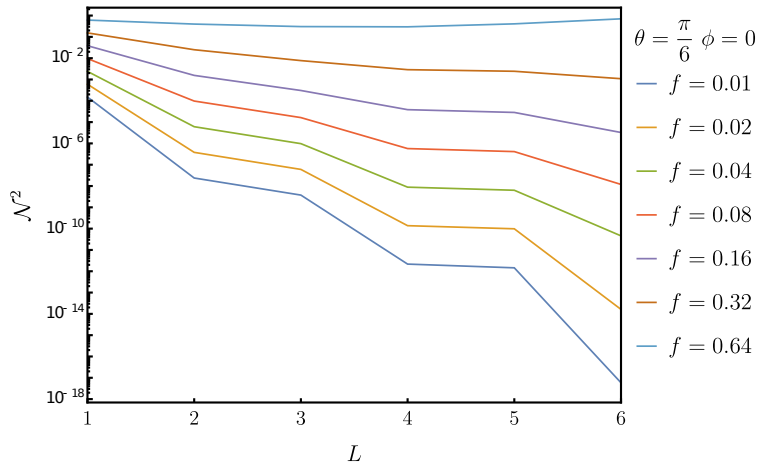

Figure 7.2: The norm of the truncated expansion for different chain lengths L and $\theta = \frac{\pi}{6}$, $\phi = 0$.

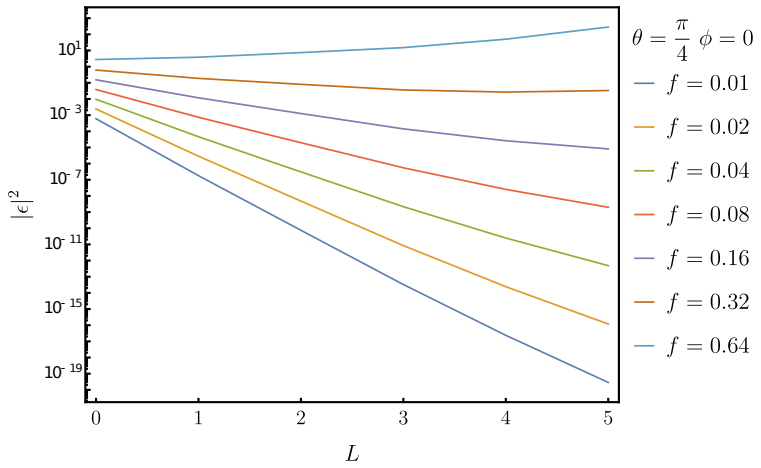

Figure 7.3: The norm of ϵ as in (7.136) for different chain lengths L and $\theta = \frac{\pi}{4}$, $\phi = 0$.

tator between the total Hamiltonian H and the truncated zero mode

$$\epsilon = (\mathcal{H}_0 + f\mathcal{V})\psi = \mathcal{V}\psi^{(L)} \ . \tag{7.136}$$

In Figure 7.5 and Figure 7.5 we show plots for the norm[14] of ϵ in the cases of $\theta = \frac{\pi}{6}$, $\theta = \frac{\pi}{4}$ and $\phi = 0$. In this case as well, we have strong suggestion that a finite radius of convergence exists, but further analysis is needed in order to have a definitive answer on the subject. In particular, in order to give an estimate of the radius of convergence, we need more information about the constants $\Gamma_{l_1,l_2,\ldots,l_{k-1}}$ appearing in (7.79) and at the moment we lack a proper understanding of these constants.

[14] As before we consider the normalization constant to be $\frac{1}{3^L}$.

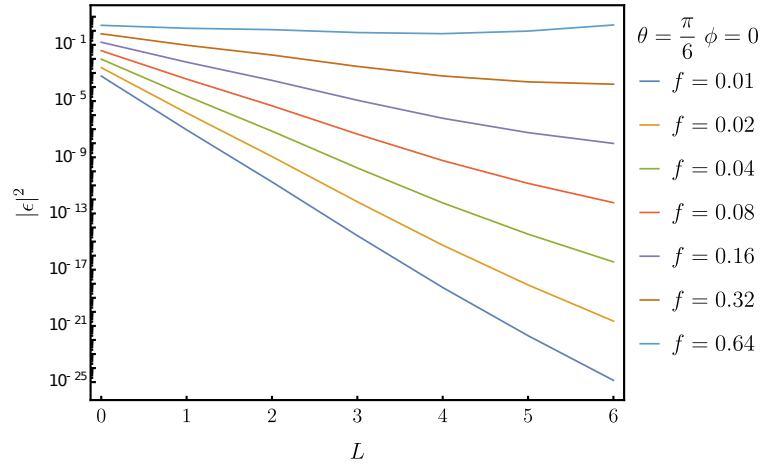

Figure 7.4: The norm of ϵ for different chain lengths L and $\theta = \frac{\pi}{6}$, $\phi = 0$.

Chapter 8

Conclusions

In this thesis we have considered different topological systems and problems related to the existence of zero modes.

In the context of Kitaev chains and p-wave superconductors, we have investigated possible sources of errors in a toy model of a topological qubit. Our motivation was to understand how error processes could arise due to the non-adiabatic variation of system parameters. As such, our analysis excludes errors due to interaction with an external environment, and therefore the results only incorporate a subset of possible error processes. Likewise, our analysis does not attempt to incorporate details of specific physical realisations of Majorana based qubits. However, the simplicity of the p-wave model should make it relevant to some degree, to more realistic device designs (e.g. the tetron and hexon proposals of [99, 100]) and scalable architectures built from them [101].

As we have stated throughout Chapter 4, we take the viewpoint that the topological qubit consists of two ground states of the Hamiltonian. Our perspective aligns with the original schemes for 2D topological computers [1], in which measurement of the fusion channels of the anyons occur as a projection to the many-body ground-states of the system. In this context then, our results specifically show how errors can arise in an isolated topological memory, assuming we have a perfect readout protocol. While this approach may not fully reflect the state of current devices, it is what allows us to resolve how errors propagate in time and to see how initial qubit-loss error can eventually lead to more damaging errors. These errors, even with perfect resolution of the fusion channels, cannot be detected without some conventional error correction protocols and the associated computational overhead. For bit-flip error we have shown that this must necessarily involve some tunneling from one wire to another, but for phase error we demonstrated how this could in principle happen via some local process within one wire. For non-interacting models, we argue that this result is due to finite size splitting, in addition to the qubit rotation that can be taken into account using a moving reference frame [55].

In Chapter 5 and 6 we considered generalized spin chains and in particular we

looked into the existence of strong zero modes in $\mathbb{Z}_N$ parafermionic chain models. We did this through a detailed study of topological degeneracies in the entire energy spectra of these models, a necessary condition for strong zero modes. When $N > 2$ is prime, and in particular when $N = 3$, the introduction of a chiral parameter θ can lead to regions where the necessary degeneracy exists, that is, splitting between near degenerate states is of order f^L. However, in the thermodynamic limit, resonance points where bands of the unperturbed model cross, become dense on the θ-axis and break the degeneracy at a lower order, at least in states which are nearby in energy. However not all resonance points result in splitting of the energy and we find points where no such splitting occurs. These are found where bands with the same total domain wall parity cross. A prominent example of this, for $N = 3$, is at $\theta = \frac{\pi}{6}$, which also corresponds to the super-integrable point of the theory when $\phi = \frac{\pi}{6}$.

For $N = 4$ we showed that at $\theta = 0$ the model is exactly solvable and expressions for the parafermionic zero modes were derived. We also showed that in this case and more generally when N is not prime, there is qualitatively different behaviour resulting from pairs of bands which remain degenerate for all values of θ. This causes energy splitting at fixed order over the entire θ axis (bar some exceptional points like $\theta = 0$). Hence there are generically no strong parafermionic zero modes when N is not prime. However at special values of N and θ, strong parafermionic zero modes do occur. In particular this is the case at $N = 4$ and $\theta = \frac{m\pi}{2}$.

The $N = 4$ model also has interesting features away from the special θ values. For example, despite its lack of parafermionic zero modes it does feature a bosonic zero mode, which again has convergence issues at resonance points, but only at those resonance points which involve pairs of bands which are not everywhere degenerate.

Another aspect of this work is the analysis of symmetries from Chapter 5. When θ is a multiple of $\frac{\pi}{N}$ and $\phi = 0$, the models have both a conjugation (time reversal) and a spatial parity symmetry. For general θ, but still at $\phi = 0$, these are no longer symmetries individually but their product is still a symmetry, which does not commute with Q. This gives us the non-Abelian dihedral group as a symmetry. From the representation theory of this group we can determine that (at $\phi = 0$), the q and $N - q$ sectors are exactly degenerate for each N.

In Chapter 7, we further investigated the existence of parafermionic zero modes when total domain wall angle is conserved and we iteratively built these operators, generalizing upon existing similar constructions [21, 16, 23].

We connected the existence of zero modes to the perturbation theory at the level of super-operators; we showed that the existence of zero modes is connected to the perturbative problem in the degenerate null space of the commutator with the free Hamiltonian.

We have shown that at resonance points where the total domain wall parity is not conserved, local zero modes cannot exist and we have shown that the conservation of

total domain wall parity is a condition regarding the locality of the terms appearing in the iterative expansion. We have provided a general ansatz for the shape taken by the solution of the perturbative expansion, which we could not directly prove, but have checked up to 6th order using symbolic calculations.
We find that this construction agrees with other known iterative constructions of strong zero modes in a variety of models [16, 23, 25]. Our approach allows an unifying view upon all these methods, through the use of degenerate perturbation theory at the level of super-operators; and allows us to identify the problematic aspects of all these types of constructions. This raises questions about the symmetries that allow such methods and some remarkable cancellations to work. Further developments in this direction are needed in order to fully understand this point.

At the end of the chapter we addressed the problem of normalization of the zero mode in the thermodynamic limit and we have shown that the properties of the zero mode existing in the unperturbed model are induced in the perturbed case as well, but the problem of convergence of the expansion is still largely unanswered. However we provided evidence that a finite radius of convergence may exist.

Closely connected with the problem of normalization of the zero mode is the problem of the long coherence time for the spin edge of the system as discussed in [23] and [24]. In this sense, it would be interesting to repeat the analysis shown there for the parafermionc model that we described here. This would possibly allow determining if the zero mode is to be considered a strong zero mode or rather an *almost* strong one. More generally it would be interesting to consider how the structure of the solution for the zero mode expansion is connected to the problem of prethermalization [25], where certain physical quantities take a long time to reach thermal equilibrium because of the existence of *almost* conservation laws. These problems are connected to the Eigenstate Thermalization Hypotesis [18, 19] and to the eigenstate phase transition [102], it would be of great interest to investigate how (and if at all) they relate with what we showed.

We note that the same analysis conducted in this thesis, could in principle be extended to consider more general energy modes. It is therefore worth considering if the same general structure of the zero mode expansion, applies to the formal expansions of the higher energy modes as well. In this sense the connection between strong zero modes and integrability is still not well understood and hopefully our framework could be employed in this direction. In this regard, it might be of interest to look specifically at the superintegrable point of the $\mathbb{Z}_3$.

It is known that some of the spin systems that we analysed here possess topological protection. A possible additional outlook for future work might hence consist in considering how the present framework changes/extends when we introduce disorder in the system and how this connects to the problem of Many Body Localisation [103]. From what we have seen, it seems in fact, that the iterative algorithm could

adjust to any local variation in the perturbing term.

Appendix A

Bloch's Perturbation Theory

In this appendix we will review a method to solve degenerate perturbation theory due to Bloch [83, 84, 85]. Consider therefore a Hamiltonian

$$H = H_0 + fV \tag{A.1}$$

where V is the perturbation and f is the perturbing parameter. Suppose we are considering some degenerate d-dimensional eigenspace of H_0, that we will denote by $\mathcal{E}^{(0)}$. It is not restrictive to consider the eigenvalue of H_0 in the space $\mathcal{E}^{(0)}$ to be $E_0 = 0$, and therefore

$$\mathcal{E}^{(0)} = Null(H_0) \ . \tag{A.2}$$

The general case $E_0 \neq 0$, can be easily got from this by considering the substitution $H_0 \to H_0 - E_0$.

Let $|\psi_1\rangle, |\psi_2\rangle, \ldots, |\psi_d\rangle$ be the perturbed eigenstates arising from the perturbation on the ground space and let $E_1, E_2, \ldots, E_d$ be their perturbed eigenvalues. If we call P_0 the projector onto $\mathcal{E}^{(0)}$ we can consider the states

$$|\alpha_j\rangle = P_0|\psi_j\rangle \ . \tag{A.3}$$

Note that these states are in general not orthogonal, but, if the perturbation is small enough, we can expect these states to be linear independent. In the following we will refer to the projector into ${\mathcal{E}^{(0)}}^{\perp}$ as

$$Q_0 = 1 - P_0 \ . \tag{A.4}$$

The idea behind Bloch's perturbation theory is to find the operator $\mathcal{U}$ such that

$$|\psi_j\rangle = \mathcal{U}|\alpha_j\rangle \tag{A.5}$$

and

$$\mathcal{U}Q_0 = 0 \ . \tag{A.6}$$

Therefore we look for a sort of "inverse" of P_0. Note that as a consequence of this definition

$$\begin{aligned} \mathcal{U} &= \mathcal{U}(P_0 + Q_0) = \mathcal{U}P_0 \\ P_0\mathcal{U} &= P_0\mathcal{U}P_0 = P_0 \ , \end{aligned} \tag{A.7}$$

where the latter follows by applying $P_0\mathcal{U}P_0$ to $|\alpha_j\rangle$ and from the fact that $|\alpha_j\rangle$ are linear independent. From the former of these properties, it follows that

$$\mathcal{U}|\psi_j\rangle = |\psi_j\rangle \ . \tag{A.8}$$

Consider now the operator H^{eff} defined as

$$H^{eff} = fP_0V\mathcal{U} \ . \tag{A.9}$$

which we named in this way for reasons that will become clear soon. In general we have

$$fP_0V = P_0(H_0 + fV) = P_0H \tag{A.10}$$

and therefore, by applying H^{eff} to $|\alpha_j\rangle$, we get

$$H^{eff}|\alpha_j\rangle = P_0H\mathcal{U}|\alpha_j\rangle = P_0H|\psi_j\rangle = E_j|\alpha_j\rangle \ .$$

This means that $|\alpha_j\rangle$ constitute eigenvectors of the operator H^{eff} with eigenvalues E_j. Since

$$H^{eff}Q_0 = 0 \tag{A.11}$$

this operator is a d-dimensional matrix with eigenvalues equal to the perturbed eigenvalues and eigenvectors equal to the projections of the perturbed eigenvectors into $\mathcal{E}^{(0)}$. It therefore constitutes an effective Hamiltonian that acts on the unperturbed eigenspace. The idea is therefore to diagonalize the simpler Hamiltonian H^{eff}, find the right eigenvectors $|\alpha_j\rangle$ and eigenvalues of E_j and then get $|\psi_j\rangle$ by using $\mathcal{U}$.

We note that the effective Hamiltonian has real eigenvalues, but it is in general not hermitian; this means that if we replace $\mathcal{U}$ with approximated expressions we might get eigenvalues that are not reals. There are other schemes following the same framework, in which the effective Hamiltonian can be chosen to be hermitian (see e.g. [94]).

We will now see how to approximate the operator $\mathcal{U}$ and, consequently H^{eff}. Consider therefore

$$fP_0V|\psi_j\rangle = E_j|\alpha_j\rangle \ . \tag{A.12}$$

Multiplying this equation by $\mathcal{U}$, and using (A.7) yields

$$(H - f\mathcal{U}V)\mathcal{U}|\alpha_j\rangle = 0 \tag{A.13}$$

Since $\mathcal{U}\mathcal{E}^{(0)\perp} = 0$ and the $|\alpha_j\rangle$ constitute a basis of $\mathcal{E}^{(0)}$ we have

$$(H_0 + fV - f\mathcal{U}V)\mathcal{U} = 0 \tag{A.14}$$

therefore

$$H_0 Q_0 \mathcal{U} = -f(V\mathcal{U} - \mathcal{U}V\mathcal{U}) \tag{A.15}$$

This gives a recursive equation for $\mathcal{U}$ that can be conveniently exploited to find approximated expressions for $\mathcal{U}$, namely

$$\mathcal{U} = P_0\mathcal{U} - f\frac{Q_0}{H_0}(V\mathcal{U} - \mathcal{U}V\mathcal{U}) \ , \tag{A.16}$$

where we used that $P_0 + Q_0 = 1$. Note that the operator Q_0/H_0 is perfectly well defined, while $1/H_0$ is not.

The operator $\mathcal{U}$ can be expanded in powers of f as

$$\mathcal{U} = \mathcal{U}^{(0)} + \sum_{m=1}^{\infty} f^m \mathcal{U}^{(m)} \ . \tag{A.17}$$

Substituting this expansion in (A.16) we get

$$\begin{aligned} &\mathcal{U}^{(0)} = P_0 \\ &\mathcal{U}^{(m)} = -\frac{Q_0}{H_0}\left(V\mathcal{U}^{(m-1)} - \sum_{p=1}^{m-1} \mathcal{U}^{(p)} V \mathcal{U}^{m-p-1}\right) \qquad m \geq 1 \end{aligned} \tag{A.18}$$

It can be proved by induction [83, 85] that the solutions for these equations are given by

$$\mathcal{U}^{(m)} = \sum{}' S^{l_1} V S^{l_2} V \ldots V S^{l_m} V P_0 \ , \tag{A.19}$$

where the sum $\sum'$ is over non-negative integers $l_1, l_2, \ldots, l_m$ such that[1]

$$\begin{cases} l_1 + l_2 + \ldots + l_m = m \\ l_1 + l_2 + \ldots + l_p \geq p \qquad p = 1, 2, \ldots, m-1 \end{cases} \tag{A.20}$$

and S^l is defined as

$$S^l = \begin{cases} \frac{Q_0}{(-H_0)^l} & l > 0 \\ P_0 & l = 0 \ . \end{cases} \tag{A.21}$$

Bringing back the dependence on E_0, we have that the first few orders of the effective

[1]For example, for m=3 the set of values $(l_1, l_2, l_3) = (1, 0, 2)$ is excluded from the sum.

Hamiltonian are given by

$$
\begin{aligned}
H^{eff(0)} &= E_0 \\
H^{eff(1)} &= E_0 + fP_0VP_0 \\
H^{eff(2)} &= E_0 + fP_0VP_0 + f^2P_0V\frac{Q_0}{E_0 - H_0}VP_0 \\
H^{eff(3)} &= E_0 + fP_0VP_0 + f^2P_0V\frac{Q_0}{E_0 - H_0}VP_0 + \\
&\quad + f^3P_0V\frac{Q_0}{E_0 - H_0}V\frac{Q_0}{E_0 - H_0}VP_0 - f^3P_0V\frac{Q_0}{(E_0 - H_0)^2}VP_0VP_0 \ .
\end{aligned}
\tag{A.22}
$$

Appendix B

Proof of the solution for $\psi_p^{(2)}$

In this appendix we will provide a proof of the formula for the solution of $\psi_p^{(1)}$ and $\psi_p^{(2)}$ seen in Section 7.3.3.

B.1 Solution for $\psi^{(0)}$

We start by considering $\psi^{(0)}$. We have

$$\psi^{(0)} = \psi_p^{(0)} = \sum_i \omega^i |i\rangle|i\rangle \ . \tag{B.1}$$

As we saw in Chapter 7, if the total domain wall parity is conserved (which for chains of length 1 means $\theta \neq 0, \frac{\pi}{3}, \frac{2\pi}{3}$), then

$$\mathcal{P}_0(\mathcal{V}\psi_p^{(0)} \otimes I_1) = 0 \ . \tag{B.2}$$

We have in fact

$$(\mathcal{V}\psi_p^{(0)}) \otimes I_1 = (-\tau_1^L + \tau_1^R + h.c)\psi_p^{(0)} \otimes I_1 \ .$$

To compute this expression consider

$$(\tau_1^L - \tau_1^R + h.c)|0\rangle|0\rangle = -|2\rangle|0\rangle + |0\rangle|2\rangle - |1\rangle|0\rangle + |0\rangle|1\rangle \ .$$

Considering the action of $\mathcal{V}$ on the other terms of $\psi_p^{(0)}$ yields, after some algebra and renaming of indexes

$$\mathcal{V}\psi_p^{(0)} \otimes I_1 = -\sum_{i_1 \neq j_1, i_2} (\omega^{j_1} - \omega^{i_1}) e^{i(j_1 - i_1)\phi} |i_1, i_2\rangle|j_1, i_2\rangle \ . \tag{B.3}$$

The difference between the two indexes $j_1 - i_1$ has been introduced for notation convenience and has to be intended as taking values in $\{-1, 1\}$. Note that, as we saw in Section 7.1.1, we could equivalently use the symmetry under $\mathcal{Q}$ and $\mathcal{TK}$ to build the complete action of $\mathcal{V}$ on $\psi^{(0)}$. From the point of view of numerical analysis

this is more convenient than direct computation.
Since we are supposing that total domain wall parity is conserved then (B.2) follows, because $i_1 \neq j_1$ in (B.3), while operators in $Null(\mathcal{H}_0)$ have $i_1 = j_1$ (Property 1).

B.2 Solution for $\psi^{(1)}$

In order to find $\psi^{(1)}$ we now need to use equations (7.47), which in the present case are given by

$$\begin{aligned} \mathcal{H}_0\psi_q^{(1)} &= -\mathcal{Q}_0\mathcal{V}(\psi_q^{(0)} \otimes I_1) \\ \mathcal{P}_0\mathcal{V}(\psi_p^{(1)} \otimes I_1) &= -\mathcal{P}_0\mathcal{V}(\psi_q^{(1)} \otimes I_1) \ . \end{aligned} \tag{B.4}$$

As we saw, the first of these equations is easily solved:

$$\psi_q^{(1)} = -\frac{\mathcal{Q}_0}{\mathcal{H}_0}\mathcal{V}(\psi_p^{(0)} \otimes I_1) = \sum_{i_1 \neq j_1, i_2} (\omega^{j_1} - \omega^{i_1}) \frac{e^{i(j_1 - i_1)\phi}}{E^{i_1,i_2}_{j_1,i_2}} |i_1, i_2\rangle |j_1, i_2\rangle \ .$$

In order to find a solution for $\psi_p^{(1)}$ we need to repeat what we did for $\psi^{(0)}$. After some algebra we get:

$$\begin{aligned} &\mathcal{V}\psi_q^{(1)} \otimes I_1 = \\ &- \sum_{i_1 \neq j_1, i_2 \neq j_2, i_3} (\omega^{j_1} - \omega^{i_1}) \left(\frac{1}{E^{i_1,j_2}_{j_1,j_2}} - \frac{1}{E^{i_1,i_2}_{j_1,i_2}} \right) e^{i(j_1 - i_1)\phi} e^{i(j_2 - i_2)\phi} |i_1, i_2, i_3\rangle |j_1, j_2, i_3\rangle \\ &- \sum_{i_1 \neq j_1, i_2, i_3} (\omega^{j_1} - \omega^{i_1}) \left(\frac{e^{2i(j_1 - i_1)\phi}}{E^{2i_1 - j_1, i_2}_{j_1 \ \ , i_2}} - \frac{e^{-2i(j_1 - i_1)\phi}}{E^{\ \ i_1 \ \ , i_2}_{2j_1 - i_1, i_2}} \right) e^{i(i_1 - j_1)\phi} |i_1, i_2, i_3\rangle |j_1, i_2, i_3\rangle \ . \end{aligned}$$

Where the terms with $i_1 = j_1$ cancel identically and are therefore excluded by the sum. Alternatively, this can also be understood by considering the symmetry under $\mathcal{TK}$. Again, since all terms in the sum have $i_1 \neq j_1$, if total domain wall parity is conserved[1], we have

$$\mathcal{P}_0\mathcal{V}(\psi_q^{(1)} \otimes I_1) = 0 \ . \tag{B.5}$$

Note that in this case

$$\mathcal{P}_0\mathcal{V}(\psi_q^{(1)} \otimes I_1) = (\mathcal{P}_0\mathcal{V}\psi_q^{(1)}) \otimes I_1 \ , \tag{B.6}$$

in agreement with our discussion in Section 7.3. We therefore see that $\psi_p^{(1)} = 0$ constitutes a solution of (B.4); so

$$\psi^{(1)} = \psi_q^{(1)} \ . \tag{B.7}$$

[1]For chains of length $L = 3$ the resonance points are given by $\theta = 0,\ \frac{\pi}{3},\ \frac{2\pi}{3}$ and $\theta = \frac{\pi}{6}$. Since the resonance at $\theta = \frac{\pi}{6}$ conserves total domain wall parity the only problematic phases are $\theta = 0,\ \frac{\pi}{3},\ \frac{2\pi}{3}$, the same as for chains of length $L = 2$.

B.2.1 Normalization

We can now consider the problem of normalization. Since (B.5) holds, we have

$$\mathcal{P}_0\mathcal{V}(\psi_p^{(1)} \otimes I_1) = 0 \ .$$

From our discussion in Section 7.4, we know that all the solutions of this equation are given by

$$\psi_p^{(1)} = \xi_1 \sigma_1 \tag{B.8}$$

and the value of ξ_1 is determined by the condition

$$(\psi^2)^{(1)} = (\psi^\dagger)^{(1)} \ . \tag{B.9}$$

The operator $(\psi^2)^{(1)}$ can be computed as

$$\begin{aligned}(\psi^2)^{(1)} =& \psi^{(0)}\psi^{(1)} + \psi^{(1)}\psi^{(0)} = \sum_{i_1 \neq j_1, i_2} (\omega^{j_1} - \omega^{i_1}) \frac{\omega^{i_1} e^{i(j_1 - i_1)\phi}}{E^{i_1,i_2}_{j_1,i_2}} |i_1, i_2\rangle |j_1, i_2\rangle + \\ &+ \sum_{i_1 \neq j_1, i_2} (\omega^{j_1} - \omega^{i_1}) \frac{\omega^{j_1} e^{i(j_1 - i_1)\phi}}{E^{i_1,i_2}_{j_1,i_2}} |i_1, i_2\rangle |j_1, i_2\rangle + \xi_1 \sigma_1^2 = \\ &= \sum_{i_1 \neq j_1, i_2} (\omega^{2j_1} - \omega^{2i_1}) \frac{\omega^{i_1} e^{i(j_1 - i_1)\phi}}{E^{i_1,i_2}_{j_1,i_2}} |i_1, i_2\rangle |j_1, i_2\rangle + \xi_1 \sigma_1^2 \ ,\end{aligned}$$

where we used that $\psi^{(0)} = \sum_{i_1,i_2} \omega^{i_1} |i_1, i_2\rangle |i_1, i_2\rangle$ and the scalar product as given by the definition

$$|i_1, i_2\rangle |j_1, i_2\rangle := |i_1, i_2\rangle \langle j_1, i_2| \ . \tag{B.10}$$

On the other hand, considering $(\psi^\dagger)^{(1)}$ yields

$$\begin{aligned}(\psi^\dagger)^{(1)} &= \sum_{i_1 \neq j_1, i_2} (\omega^{-j_1} - \omega^{-i_1}) \frac{e^{-i(j_1 - i_1)\phi}}{E^{i_1,i_2}_{j_1,i_2}} |j_1, i_2\rangle |i_1, i_2\rangle + \xi_1^* \sigma_1^2 = \\ &= \sum_{i_1 \neq j_1, i_2} (\omega^{2j_1} - \omega^{2i_1}) \frac{e^{i(j_1 - i_1)\phi}}{E^{i_1,i_2}_{j_1,i_2}} |i_1, i_2\rangle |j_1, i_2\rangle + \xi_1^* \sigma_1^2 \ ,\end{aligned}$$

where we used that $E^{i_1,i_2}_{j_1,i_2} = -E^{j_1,i_2}_{i_1,i_2}$. Therefore if we pick $\xi_1 = 0$, condition (B.9) is satisfied.

Consider now

$$(\psi^3)^{(1)} = \psi^{(0)}\psi^{(0)}\psi^{(1)} + \psi^{(0)}\psi^{(1)}\psi^{(0)} + \psi^{(1)}\psi^{(0)}\psi^{(0)} \tag{B.11}$$

All the terms in $\psi_q^{(1)}$ have $i_1 \neq j_1$. This means that, as operators, all the terms in $\psi^{(1)}$ have either a τ_1 or a τ_1^2. Since $\psi^{(0)} = \sigma_1$, using that $\tau_1\sigma_1 = \omega\sigma_1\tau_1$ and $1 + \omega + \omega^2 = 0$, gives

$$\psi^{3(1)} = 3\xi_1 I_L = 0 \ . \tag{B.12}$$

Therefore, to recap, the solution to the first order can be given as

$$\psi^{(1)} = \psi_q^{(1)} = \sum_{i_1 \neq j_1, i_2} (\omega^{j_1} - \omega^{i_1}) \frac{e^{i(j_1 - i_1)\phi}}{E_{j_1,i_2}^{i_1,i_2}} |i_1, i_2\rangle |j_1, i_2\rangle \ . \tag{B.13}$$

It can be checked that in terms of the operators σ and τ this operator can be written as

$$\begin{aligned} \psi^{(1)} = & \frac{9}{2} e^{-i(\phi - \frac{\pi}{6})} \frac{1}{\sin 3\theta} \left(\tau_1 \sigma_1 + \omega^2 e^{-2i\theta} \tau_1 \sigma_2 + \omega \ e^{2i\theta} \tau_1 \sigma_1^2 \sigma_2^2 \right) \\ & + \frac{9}{2} e^{\ i(\phi + \frac{\pi}{6})} \frac{1}{\sin 3\theta} \left(\tau_1^2 \sigma_1 + \omega \ e^{-2i\theta} \tau_1^2 \sigma_2 + \omega^2 e^{2i\theta} \tau_1^2 \sigma_1^2 \sigma_2^2 \right) \ . \end{aligned} \tag{B.14}$$

B.3 Solution for $\psi^{(2)}$

We will now find the solution for $\psi^{(2)} = \psi_q^{(2)} + \psi_p^{(2)}$. To simplify the notation we will consider the case $\phi = 0$. The general case can be considered in a similar way. As before we can solve for $\psi_q^{(2)}$ by simply inverting $\mathcal{H}_0$:

$$\begin{aligned} \psi_q^{(2)} = & \sum_{i_1 \neq j_1, i_2 \neq j_2, i_3} \frac{\omega^{j_1} - \omega^{i_1}}{E_{j_1,j_2,i_3}^{i_1,i_2,i_3}} \left(\frac{1}{E_{j_1,j_2}^{i_1,j_2}} - \frac{1}{E_{j_1,i_2}^{i_1,i_2}} \right) |i_1, i_2, i_3\rangle |j_1, j_2, i_3\rangle \\ & + \sum_{i_1 \neq j_1, i_2} \frac{\omega^{j_1} - \omega^{i_1}}{E_{j_1,i_2}^{i_1,i_2}} \left(\frac{1}{E^{2i_1 - j_1, j_2}_{\ \ j_1 \ \ , j_2}} - \frac{1}{E_{2j_1 - i_1, i_2}^{\ \ i_1 \ \ , i_2}} \right) |i_1, i_2\rangle |j_1, i_2\rangle \otimes I_1 \ . \end{aligned} \tag{B.15}$$

Note that (B.15) follows the structure outlined in Property 4. We are now in a position to prove that

$$\psi_p^{(2)} = -\frac{1}{2} \mathcal{P}_0 \mathcal{V} \left(\frac{\mathcal{Q}_0}{\mathcal{H}_0} \right)^2 \mathcal{V} (\psi_p^{(0)} \otimes I_2) \ . \tag{B.16}$$

First of all note that with this definition

$$\psi_p^{(2)} = -\frac{1}{2} \sum_{i_1 \neq j_1, i_2} (\omega^{j_1} - \omega^{i_1}) \left(\frac{1}{\left(E_{j_1,i_2}^{i_1,i_2}\right)^2} + \frac{1}{\left(E_{i_1,i_2}^{j_1,i_2}\right)^2} \right) |i_1, i_2\rangle |i_1, i_2\rangle \otimes I_1$$

and since $E_{i_1,i_2}^{j_1,i_2} = -E_{j_1,i_2}^{i_1,i_2}$ we have

$$\psi_p^{(2)} = -\sum_{i_1 \neq j_1, i_2} (\omega^{j_1} - \omega^{i_1}) \frac{1}{\left(E_{j_1,i_2}^{i_1,i_2}\right)^2} |i_1, i_2\rangle |i_1, i_2\rangle \otimes I_1 \ . \tag{B.17}$$

We can therefore now compute the action of $\mathcal{V}$ on $\psi_p^{(2)}$, that is

$$\mathcal{P}_0 \mathcal{V} \psi_p^{(2)} = -\sum_{\substack{i_1 \neq j_1 \\ i_2 \neq j_2, i_3}} (\omega^{j_1} - \omega^{i_1}) \left(\frac{1}{\left(E_{j_1,j_2}^{i_1,j_2}\right)^2} - \frac{1}{\left(E_{j_1,i_2}^{i_1,i_2}\right)^2} \right) |i_1, i_2, i_3\rangle |i_1, j_2, i_3\rangle \ . \tag{B.18}$$

We will now show that $\mathcal{P}_0(\mathcal{V}\psi_q^{(2)} \otimes I_1)$ yields the same expression. Since $\psi_q^{(2)}$ follows Property 4 we know that

$$\mathcal{P}_0(\mathcal{V}\psi_q^{(2)} \otimes I_1) = (\mathcal{P}_0\mathcal{V}\psi_q^{(2)}) \otimes I_1 \tag{B.19}$$

This simplifies the problem, as we do not need to consider chains of length 4 and the problem stays confined on a chain of length[2] 3.
Using Property 1, we can concentrate our attention on the terms obtained under the action of $\mathcal{V}$ with $i_1 = j_1$:

$$\begin{aligned}\mathcal{P}_0\mathcal{V}\psi_q^{(2)} = &\sum_{i_1\neq j_1, i_2\neq j_2, i_3} \frac{\omega^{j_1}-\omega^{i_1}}{E^{i_1,i_2,i_3}_{j_1,j_2,i_3}}\left(\frac{1}{E^{i_1,j_2}_{j_1,j_2}} - \frac{1}{E^{i_1,i_2}_{j_1,i_2}}\right)|i_1,i_2,i_3\rangle|i_1,j_2,i_3\rangle \\ &- \sum_{i_1\neq j_1, i_2\neq j_2, i_3} \frac{\omega^{i_1}-\omega^{j_1}}{E^{j_1,i_2,i_3}_{i_1,j_2,i_3}}\left(\frac{1}{E^{j_1,j_2}_{i_1,j_2}} - \frac{1}{E^{j_1,i_2}_{i_1,i_2}}\right)|i_1,i_2,i_3\rangle|i_1,j_2,i_3\rangle\end{aligned}$$

and all the operators in the sums are such that[3] $E^{i_1,i_2,i_3}_{i_1,j_2,i_3} = 0$.
Consider now the energies $E^{i_1,i_2,i_3}_{j_1,j_2,i_3}$, $E^{j_1,i_2,i_3}_{i_1,j_2,i_3}$ with $j_1 \neq i_1$ as in the sums. We have

$$\begin{aligned}E^{i_1,i_2,i_3}_{j_1,j_2,i_3} &= E^{i_1,i_2,i_3}_{i_1,j_2,i_3} + E^{i_1,j_2}_{j_1,j_2} = E^{i_1,j_2}_{j_1,j_2} \\ E^{j_1,i_2,i_3}_{i_1,j_2,i_3} &= E^{i_1,i_2,i_3}_{i_1,j_2,i_3} + E^{j_1,i_2}_{j_1,i_2} = E^{j_1,i_2}_{i_1,i_2}\ ,\end{aligned} \tag{B.20}$$

where we used that $E^{i_1,i_2,i_3}_{i_1,j_2,i_3} = 0$. Hence we get

$$\begin{aligned}\mathcal{P}_0\mathcal{V}\psi_q^{(2)} = &\sum_{i_1\neq j_1, i_2\neq j_2, i_3} (\omega^{j_1}-\omega^{i_1})\left(\frac{1}{(E^{i_1,j_2}_{j_1,j_2})^2} - \frac{1}{E^{i_1,j_2}_{j_1,j_2}E^{i_1,i_2}_{j_1,i_2}}\right)|i_1,i_2,i_3\rangle|j_1,j_2,i_3\rangle \\ &- \sum_{i_1\neq j_1, i_2\neq j_2, i_3} (\omega^{i_1}-\omega^{j_1})\left(\frac{1}{E^{j_1,i_2}_{i_1,i_2}E^{j_1,j_2}_{i_1,j_2}} - \frac{1}{(E^{j_1,i_2}_{i_1,i_2})^2}\right)|i_1,i_2,i_3\rangle|j_1,j_2,i_3\rangle\ .\end{aligned}$$

Now, since $E^{j_1,i_2}_{i_1,i_2} = -E^{i_1,i_2}_{j_1,i_2}$ and $E^{j_1,j_2}_{i_1,j_2} = -E^{i_1,j_2}_{j_1,j_2}$, we are left with

$$\mathcal{P}_0\mathcal{V}\psi_q^{(2)} = \sum_{i_1\neq j_1, i_2\neq j_2, i_3} (\omega^{j_1}-\omega^{i_1})\left(\frac{1}{(E^{i_1,j_2}_{j_1,j_2})^2} - \frac{1}{(E^{j_1,i_2}_{i_1,i_2})^2}\right)|i_1,i_2,i_3\rangle|j_1,j_2,i_3\rangle\ . \tag{B.21}$$

This is the same as (B.18). Therefore, to summarize, we have checked that a solution of

$$\mathcal{P}_0\mathcal{V}\psi_p^{(2)} = -\mathcal{P}_0\mathcal{V}\psi_q^{(2)} \tag{B.22}$$

[2]Again, this is true only in the case where the total domain wall parity is conserved. For chains of length 4 means $\theta \neq 0, \frac{\pi}{3}, \frac{2\pi}{3}, \arctan\frac{\sqrt{3}}{5}$.
[3]The terms with $i_2 = j_2$ are identically zero, as can be checked by direct computation.

for $\psi_p^{(2)}$ exists and is given by

$$\psi_p^{(2)} = -\frac{1}{2}\mathcal{P}_0\mathcal{V}\left(\frac{\mathcal{Q}_0}{\mathcal{H}_0}\right)^2\mathcal{V}(\psi_p^{(0)}\otimes I_2)\ . \tag{B.23}$$

B.3.1 Normalization

As we mentioned this solution is not unique and we can consider any linear combination of the form

$$\psi_p^{(2)} + \xi_2\sigma_1 \tag{B.24}$$

and we would still get a solution of (B.22), for any $\xi_2 \in \mathbb{C}$. As we already saw in this Appendix and in Section 7.4 the value of ξ_2 can be determined from the condition

$$(\psi^2)^{(2)} = (\psi^\dagger)^{(2)}\ . \tag{B.25}$$

Computing the value of ξ_2 directly is rather bothersome and the algebra quite involved, but we proved in Section 7.4 that we can always find a ξ_2 such that this condition is satisfied. By using Mathematica, for $\theta = \frac{\pi}{6}$, we get[4]

$$\xi_2 = 0\ . \tag{B.26}$$

The same analysis conducted with symbolic computation also shows that with this choice of ξ_2 we get

$$(\psi^3)^{(2)} = 0\ . \tag{B.27}$$

So, overall

$$\psi^{(2)} = \left(\left(\frac{\mathcal{Q}_0}{\mathcal{H}_0}\right)\mathcal{V}\left(\frac{\mathcal{Q}_0}{\mathcal{H}_0}\right)\mathcal{V} + \frac{1}{2}\mathcal{P}_0\mathcal{V}\left(\frac{\mathcal{Q}_0}{\mathcal{H}_0}\right)^2\mathcal{V}\right)\psi^{(0)}\ . \tag{B.28}$$

[4]Also in the case of $\theta = \frac{\pi}{4}$ we get

$$\xi_2 = 0\ .$$

Note however that in general these constants are different from 0 and depend on θ. For example in the case $\theta = \frac{\pi}{6}$ we get

$$\xi_3 = \frac{i}{6}\ ,$$

while in the case of $\theta = \frac{\pi}{4}$ we have

$$\xi_3 = \frac{i}{3\sqrt{2}}$$

Appendix C

Proof of Property 4

In this appendix we will prove Property 4 which we enunciated in Section 7.3.1 and that we recall here for convenience

Property 4. *Suppose that a solution for the zero mode exists up to some order $k \geq 1$. If the total domain wall parity is conserved the solution $\psi^{(k)}$ is composed of operators that act non trivially on a chain of length $k+1$ and in particular*

- *The operators $\psi_q^{(k)}$ can be written as*

$$\psi_q^{(k)} = \eta_q^{(k)} + \rho_q^{(k)}$$

where $\eta_q^{(k)}$ is a linear combination of operators of the form

$$|i_1, i_2, \ldots, i_k, i_{k+1}\rangle|j_1, j_2, \ldots, j_k, i_{k+1}\rangle \qquad i_l \neq j_l \qquad \forall\ l = 1, 2 \ldots, k \tag{C.1}$$

while $\rho_q^{(k)}$ acts trivially on site k and is a linear combination of operators of the form

$$|\mathbf{i}_{k-1}, i_k\rangle|\mathbf{j}_{k-1}, i_k\rangle \otimes I_1 \qquad E^{\mathbf{i}_{k-1}, i_k}_{\mathbf{j}_{k-1}, i_k} \neq 0\ .$$

- *$\psi_p^{(k)}$ is made of operators that act non-trivially on chains that are not longer than k. This means that $\psi_p^{(k)}$ is a linear combination of operators of the form*

$$|i_1, \mathbf{i}_{k-2}, i_k\rangle|i_1, \mathbf{j}_{k-2}, i_k\rangle \otimes I_1 \qquad E^{i_1, \mathbf{i}_{k-2}, i_k}_{i_1, \mathbf{j}_{k-2}, i_k} = 0\ .$$

As we saw in Section 7.3 the second part of this property follows from the first one using that

$$\mathcal{P}_0(\mathcal{V}\psi_q^{(k)} \otimes I_1) = \beta_p \otimes I_1 \quad \text{with} \quad \beta_p \in Null(\mathcal{H}_0) \tag{C.2}$$

and Property 2.

We will now prove that

$$\psi_q^{(k)} = \eta_q^{(k)} + \rho_q^{(k)} \tag{C.3}$$

by induction on $j \leq k$.

Case j=1

The case for $j = 1$ was already proved in Appendix B, where we have showed that

$$\begin{aligned} \psi_q^{(1)} &= \sum_{i_1 \neq j_1, i_2} (\omega^{j_1} - \omega^{i_1}) \frac{e^{i(j_1 - i_1)\phi}}{E_{j_1, i_2}^{i_1, i_2}} |i_1, i_2\rangle |j_1, i_2\rangle \\ \psi_p^{(1)} &= 0 \ . \end{aligned} \tag{C.4}$$

and therefore in this case

$$\psi_q^{(1)} = \eta_q^{(1)} \ . \tag{C.5}$$

Inductive step

Suppose therefore that Property 4 holds for $j - 1$. We have

$$\psi_q^{(j)} = -\frac{\mathcal{Q}_0}{\mathcal{H}_0} \mathcal{V} \psi^{(j-1)} \otimes I_1 = -\frac{1}{\mathcal{H}_0} \mathcal{V} \left(\eta_q^{(j-1)} + \rho_q^{(j-1)} + \psi_p^{(j-1)} \right) \otimes I_1$$

Consider now $\mathcal{V}$ as a sum of its local terms. Since $\psi^{(j-1)}$ lives on a chain of length j we can consider $\mathcal{V}$ only up to terms that act on site j on the chain

$$\mathcal{V} = \sum_{t=1}^{j-1} \mathcal{V}_t + \mathcal{V}_j = \widetilde{\mathcal{V}}_{j-1} + \mathcal{V}_j \tag{C.6}$$

where we defined

$$\widetilde{\mathcal{V}}_{j-1} = \sum_{t=1}^{j-1} \mathcal{V}_t \ . \tag{C.7}$$

Note that by hypothesis $\rho_q^{(j-1)}$, $\psi_p^{(j-1)}$ act non trivially only on a chain up to site $j - 1$, which means that $\mathcal{V}_j$ acts trivially on them:

$$\psi_q^{(j)} = -\frac{\mathcal{Q}_0}{\mathcal{H}_0} \left(\mathcal{V}_j \eta_q^{(j-1)} + \widetilde{\mathcal{V}}_{j-1} \left(\eta_q^{(j-1)} + \rho_q^{(j-1)} + \psi_p^{(j-1)} \right) \right) \otimes I_1 \ . \tag{C.8}$$

Suppose therefore that

$$\mathcal{Q}_0 \widetilde{\mathcal{V}}_{j-1} \left(\eta_q^{(j-1)} + \rho_q^{(j-1)} + \psi_p^{(j-1)} \right) \otimes I_1 = \sum \beta_{\mathbf{j}_{j-1}, i_j}^{\mathbf{i}_{k-1}, i_k} |\mathbf{i}_{j-1}, i_j\rangle |\mathbf{l}_{j-1}, i_j\rangle \otimes I_1 \ ,$$

where the operators in the sum have the same indexes at site k because $\widetilde{\mathcal{V}}_{j-1}$ acts trivially at site j. Therefore we have

$$\frac{\mathcal{Q}_0}{\mathcal{H}_0}\widetilde{\mathcal{V}}_{j-1}\left(\eta_q^{(j-1)}+\rho_q^{(j-1)}+\psi_p^{(j-1)}\right)\otimes I_1=\sum\frac{\beta^{\mathbf{i}_{j-1},i_j}_{\mathbf{l}_{j-1},i_j}}{E^{\mathbf{i}_{j-1},i_j,i_{j+1}}_{\mathbf{l}_{j-1},i_j,i_{j+1}}}|\mathbf{i}_{j-1},i_j,i_{j+1}\rangle|\mathbf{l}_{j-1},i_j,i_{j+1}\rangle\ ,$$

note that the dependence of the coefficients βs on i_j comes from $\eta_q^{(j-1)}$. Using that $E^{\mathbf{i}_{j-1},i_j,i_{j+1}}_{\mathbf{l}_{j-1},i_j,i_{j+1}}=E^{\mathbf{i}_{j-1},i_j}_{\mathbf{l}_{j-1},i_j}$ we get

$$\sum\frac{\beta^{\mathbf{i}_{j-1},i_j}_{\mathbf{l}_{j-1},i_j}}{E^{\mathbf{i}_{j-1},i_j}_{\mathbf{l}_{j-1},i_j}}|\mathbf{i}_{j-1},i_j,i_{j+1}\rangle|\mathbf{l}_{j-1},i_j,i_{j+1}\rangle=\sum\frac{\beta^{\mathbf{i}_{j-1},i_j}_{\mathbf{l}_{j-1},i_j}}{E^{\mathbf{i}_{j-1},i_j}_{\mathbf{l}_{j-1},i_j}}|\mathbf{i}_{j-1},i_j\rangle|\mathbf{l}_{j-1},i_j\rangle\otimes I_1\ ,$$

hence we can set

$$\rho_q^{(j)}=-\frac{\mathcal{Q}_0}{\mathcal{H}_0}\widetilde{\mathcal{V}}_{j-1}\left(\eta_q^{(j-1)}+\rho_q^{(j-1)}+\psi_p^{(j-1)}\right)\otimes I_1\ . \tag{C.9}$$

Suppose now that

$$\eta_q^{(j-1)}=\sum_{i_t\neq j_t}\eta^{i_1,i_2,\dots,i_{j-1},i_j}_{l_1,l_1,\dots,l_{j-1},i_j}|i_1,i_2,\dots,i_{j-1},i_j\rangle|l_1,l_2,\dots,l_{j-1},i_j\rangle\ . \tag{C.10}$$

the action of $\mathcal{V}_j$ is then given by:

$$\mathcal{V}_j\eta_q^{(j-1)}=\sum_{i_t\neq l_t}\left(\eta^{\mathbf{i}_{j-1},i_j}_{\mathbf{l}_{j-1},i_j}-\eta^{\mathbf{i}_{j-1},l_j}_{\mathbf{l}_{j-1},l_j}\right)e^{i(l_j-i_l)\phi}|i_1,i_2,\dots,i_{j-1},i_j\rangle|l_1,l_2,\dots,l_{j-1},l_j\rangle\ .$$

Since the left and right j indexes are all different from each other we can write

$$\eta_q^{(j)}=-\frac{\mathcal{Q}_0}{\mathcal{H}_0}(\mathcal{V}_j\eta_q^{(j-1)}\otimes I_1) \tag{C.11}$$

This proves the first part of the property and as we said the second part follows from it and Property 2.

From the proof of Property 4, we can find by induction an expansion for the coefficients $\eta^{i_1,i_2,\dots,i_j,i_{j+1}}_{l_1,l_2,\dots,l_j,i_{j+1}}$ of $\eta_q^{(j)}$ in terms of energies. After some algebra we get

$$\eta^{i_1,i_2,\dots,i_j,i_{j+1}}_{l_1,l_2,\dots,l_j,i_{j+1}}=-\frac{(\omega^{l_1}-\omega^{i_1})}{E^{i_1,i_2,\dots,i_j,i_{j+1}}_{l_1,l_2,\dots,l_j,l_{j+1}}}\prod_{t=2}^{l}e^{i(l_t-i_t)\phi}\left(\frac{1}{E^{i_1,i_2,\dots,i_{t-1},i_t}_{l_1,l_2,\dots,l_{t-1},i_t}}-\frac{1}{E^{i_1,i_2,\dots,i_{t-1},l_t}_{l_1,l_2,\dots,l_{t-1},l_t}}\right)\ . \tag{C.12}$$

Note that in principle, even if more involved, we could find formulas also for the other coefficients, but they would depend on the constants Γs that we introduced in Section 7.3.3, which are in general undetermined.

Appendix D

Coefficients for the solution $\psi_p^{(5)}$

In this appendix we will display, for completeness, the non-zero Γ_{i_1,i_2,i_3,i_4} introduced in Section 7.3.3, which appear in $\psi_p^{(5)}$ as found through the use of Mathematica. We have

$$\begin{array}{llll} \Gamma_{0,0,4,1} = -\frac{3}{35} & \Gamma_{0,0,3,2} = -\frac{2}{35} & \Gamma_{0,3,0,2} = -\frac{3}{14} & \Gamma_{0,1,1,3} = \frac{1}{35} \\ \Gamma_{0,1,3,1} = \frac{6}{35} & \Gamma_{1,0,3,1} = \frac{1}{5} & \Gamma_{0,3,1,1} = \frac{3}{7} & \Gamma_{0,1,2,2} = \frac{3}{35} \\ \Gamma_{1,0,2,2} = \frac{1}{5} & \Gamma_{0,2,1,2} = \frac{1}{7} & \Gamma_{2,0,1,2} = \frac{7}{20} & \Gamma_{1,2,0,2} = \frac{3}{10} \\ \Gamma_{2,1,0,2} = \frac{2}{5} & \Gamma_{0,2,2,1} = \frac{2}{7} & \Gamma_{2,0,2,1} = \frac{9}{20} & \Gamma_{1,1,1,2} = -\frac{1}{5} \\ \Gamma_{1,1,2,1} = -\frac{2}{5} & \Gamma_{1,2,1,1} = -\frac{3}{5} & \Gamma_{2,1,1,1} = -\frac{4}{5} \, . & \end{array} \tag{D.1}$$

Bibliography

[1] Chetan Nayak, Steven H. Simon, Ady Stern, Michael Freedman, and Sankar Das Sarma. Non-abelian anyons and topological quantum computation. *Reviews of Modern Physics*, 80:1083–1159, September 2008.

[2] A.Yu. Kitaev. Fault-tolerant quantum computation by anyons. *Annals of Physics*, 303(1):2 – 30, 2003.

[3] Andrew Resnick. Topological aspects of condensed matter physics: lecture notes of the les houches summer school: Volume 103, August 2014. *Contemporary Physics*, 59(3):320–321, 2018.

[4] B. Andrei Bernevig and Taylor L. Hughes. *Topological Insulators and Topological Superconductors*. Princeton University Press, 2013.

[5] X. G. Wen. Topological orders in rigid states. *International Journal of Modern Physics B*, 04(02):239–271, 1990.

[6] A. Kitaev. Anyons in an exactly solved model and beyond. *Annals of Physics*, 321(1):2 – 111, 2006. January Special Issue.

[7] Oroszlány L. Pályi A. Asbóth, J. K. *A Short Course on Topological Insulators*. Springer, 2016.

[8] Martin R. Zirnbauer. Riemannian symmetric superspaces and their origin in random-matrix theory. *Journal of Mathematical Physics*, 37(10):4986–5018, October 1996.

[9] Alexander Altland and Martin R. Zirnbauer. Nonstandard symmetry classes in mesoscopic normal-superconducting hybrid structures. *Physical Review B*, 55:1142–1161, January 1997.

[10] Alexei Kitaev. *Periodic table for topological insulators and superconductors*, volume 1134 of *American Institute of Physics Conference Series*. May 2009.

[11] Shinsei Ryu, Andreas P Schnyder, Akira Furusaki, and Andreas W W Ludwig. Topological insulators and superconductors: tenfold way and dimensional hierarchy. *New Journal of Physics*, 12(6):065010, June 2010.

[12] Lukasz Fidkowski and Alexei Kitaev. Topological phases of fermions in one dimension. *Physical Review B*, 83(7):075103, February 2011.

[13] Chong Wang and T. Senthil. Interacting fermionic topological insulators/superconductors in three dimensions. *Physical Review B*, 89(19):195124, May 2014.

[14] A. Y. Kitaev. Unpaired majorana fermions in quantum wires. *Phys. Usp.*, 44:131, October 2001.

[15] Sankar Das Sarma, Michael Freedman, and Chetan Nayak. Majorana zero modes and topological quantum computation. *Npj Quantum Information*, 1, January 2015.

[16] Paul Fendley. Strong zero modes and eigenstate phase transitions in the XYZ interacting Majorana chain. *Journal of Physics A: Mathematical and Theoretical*, 49(30):30LT01, June 2016.

[17] David A. Huse, Rahul Nandkishore, Vadim Oganesyan, Arijeet Pal, and S. L. Sondhi. Localization-protected quantum order. *Physical Review B*, 88(1):014206, July 2013.

[18] J. M. Deutsch. Quantum statistical mechanics in a closed system. *Physical Review A*, 43:2046–2049, February 1991.

[19] Mark Srednicki. Chaos and quantum thermalization. *Physical Review E*, 50(2):888–901, August 1994.

[20] Jason Alicea and Paul Fendley. Topological Phases with Parafermions: Theory and Blueprints. *Annual Review of Condensed Matter Physics*, 7:119–139, March 2016.

[21] P. Fendley. Parafermionic edge zero modes in Z_n-invariant spin chains. *J. Stat. Mech.*, 11:11020, November 2012.

[22] A. S. Jermyn, R. S. K. Mong, J. Alicea, and P. Fendley. Stability of zero modes in parafermion chains. *Physical Review B*, 90(16):165106, October 2014.

[23] Jack Kemp, Norman Y Yao, Christopher R Laumann, and Paul Fendley. Long coherence times for edge spins. *Journal of Statistical Mechanics: Theory and Experiment*, 2017(6):063105, June 2017.

[24] Loredana M. Vasiloiu, Federico Carollo, Matteo Marcuzzi, and Juan P. Garrahan. Strong zero modes in a class of generalised Ising spin ladders with plaquette interactions. *arXiv e-prints*, page arXiv:1901.10211, January 2019.

[25] Dominic V. Else, Paul Fendley, Jack Kemp, and Chetan Nayak. Prethermal strong zero modes and topological qubits. *Physical Review X*, 7(4):041062, October 2017.

[26] A. Conlon, D. Pellegrino, J. K. Slingerland, S. Dooley, and G. Kells. Error generation and propagation in majorana-based topological qubits. *Physical Review B*, 100:134307, October 2019.

[27] N. Moran, D. Pellegrino, J. K. Slingerland, and G. Kells. Parafermionic clock models and quantum resonance. *Physical Review B*, 95:235127, June 2017.

[28] D. Pellegrino, G. Kells, N. Moran, and J. K. Slingerland. Constructing edge zero modes through domain wall angle conservation. *arXiv e-prints*, page arXiv:1908.03459, August 2019.

[29] Ernst Ising. Contribution to the Theory of Ferromagnetism. *Zeitschrift für Physik*, 31:253–258, 1925.

[30] Subir Sachdev. *Quantum Phase Transitions*. Cambridge University Press, 2011.

[31] L.D. Landau, E.M. Lifshitz, and L.P. Pitaevskij. *Statistical Physics: Part 2 : Theory of Condensed State*. Landau and Lifshitz Course of theoretical physics. Oxford, 1980.

[32] T. D. Schultz, D. C. Mattis, and E. H. Lieb. Two-dimensional Ising model as a soluble problem of many fermions. *Rev. Mod. Phys.*, 36:856–871, July 1964.

[33] T. Senthil. Symmetry-Protected Topological Phases of Quantum Matter. *Annual Review of Condensed Matter Physics*, 6:299–324, March 2015.

[34] Jason Alicea, Yuval Oreg, Gil Refael, Felix von Oppen, and Matthew P. A. Fisher. Non-abelian statistics and topological quantum information processing in 1d wire networks. *Nature Physics*, 7:412, February 2011.

[35] Pientka F. Oppen Fv., Peng Y. *Topological superconducting phases in one dimension*, volume 103. Oxford University Press, August 2017.

[36] Yuval Oreg, Gil Refael, and Felix von Oppen. Helical liquids and Majorana bound states in quantum wires. *Physical Review Letters*, 105:177002, October 2010.

[37] Rasbha E. I. Bychkov Y. A. Oscillatory effects and the magnetic susceptibility of carriers in inversion layers. *Journal of Physics C: Solid State Physics*, 17, Nov 1984.

[38] M. V. Berry. Quantal phase factors accompanying adiabatic changes. *Proceedings of the Royal Society of London. Series A, Mathematical and Physical Sciences*, 392(1802):45–57, 1984.

[39] Frank Wilczek and A. Zee. Appearance of gauge structure in simple dynamical systems. *Physical Review Letters*, 52:2111–2114, June 1984.

[40] Michael A. Nielsen and Isaac L. Chuang. *Quantum Computation and Quantum Information: 10th Anniversary Edition*. Cambridge University Press, New York, NY, USA, 10th edition, 2011.

[41] Daniel Gottesman. The Heisenberg representation of quantum computers. In *Group theoretical methods in physics. Proceedings, 22nd International Colloquium, Group22, ICGTMP'98, Hobart, Australia, July 13-17, 1998*, pages 32–43, 1998.

[42] S. Bravyi. Universal quantum computation with the $\nu = 5/2$ fractional quantum Hall state. *Physical Review A*, 73, 04 2006.

[43] Ville Lahtinen and Jiannis Pachos. A Short Introduction to Topological Quantum Computation. *SciPost Physics*, 3:021, September 2017.

[44] V. Mourik, K. Zuo, S. M. Frolov, S. R. Plissard, E. P. A. M. Bakkers, and L. P. Kouwenhoven. Signatures of Majorana Fermions in Hybrid Superconductor-Semiconductor Nanowire Devices. *Science*, 336(6084):1003, May 2012.

[45] Anindya Das, Yuval Ronen, Yonatan Most, Yuval Oreg, Moty Heiblum, and Hadas Shtrikman. Zero-bias peaks and splitting in an Al-InAs nanowire topological superconductor as a signature of Majorana fermions. *Nature Physics*, 8(12):887–895, December 2012.

[46] A. D. K. Finck, D. J. Van Harlingen, P. K. Mohseni, K. Jung, and X. Li. Anomalous Modulation of a Zero-Bias Peak in a Hybrid Nanowire-Superconductor Device. *Physical Review Letters*, 110(12):126406, March 2013.

[47] Hao Zhang et al. Quantized Majorana conductance. *Nature*, 556(7699):74–79, April 2018.

[48] Roman M. Lutchyn, Jay D. Sau, and S. Das Sarma. Majorana fermions and a topological phase transition in semiconductor-superconductor heterostructures. *Physical Review Letters*, 105:077001, August 2010.

[49] Liang Fu and C. L. Kane. Josephson current and noise at a superconductor/quantum-spin-Hall-insulator/superconductor junction. *Physical Review B*, 79(16):161408, April 2009.

[50] H. J. Kwon, K. Sengupta, and V. M. Yakovenko. Fractional ac Josephson effect in p- and d-wave superconductors. *European Physical Journal B*, 37(3):349–361, February 2004.

[51] John M. Martinis and Kevin Osborne. Superconducting Qubits and the Physics of Josephson Junctions. *arXiv e-prints*, pages cond–mat/0402415, February 2004.

[52] Diego Rainis and Daniel Loss. Majorana qubit decoherence by quasiparticle poisoning. *Physical Review B*, 85:174533, May 2012.

[53] G. Goldstein and C. Chamon. Decay rates for topological memories encoded with Majorana fermions. *Physical Review B*, 84:205109, November 2011.

[54] Jan Carl Budich, Stefan Walter, and Björn Trauzettel. Failure of protection of Majorana based qubits against decoherence. *Physical Review B*, 85:121405, March 2012.

[55] M. S. Scheurer and A. Shnirman. Nonadiabatic processes in Majorana qubit systems. *Physical Review B*, 88:064515, August 2013.

[56] Torsten Karzig, Gil Refael, and Felix von Oppen. Boosting Majorana zero modes. *Physical Review X*, 3:041017, November 2013.

[57] Meng Cheng, Victor Galitski, and S. Das Sarma. Nonadiabatic effects in the braiding of non-abelian anyons in topological superconductors. *Physical Review B*, 84:104529, September 2011.

[58] P. Schuck P. Ring. *The Nuclear Many-Body Problem*. Springler-Verlag, 2004.

[59] Naoki Onishi and Shiro Yoshida. Generator coordinate method applied to nuclei in the transition region. *Nuclear Physics*, 80(2):367 – 376, 1966.

[60] David Aasen, Michael Hell, Ryan V. Mishmash, Andrew Higginbotham, Jeroen Danon, Martin Leijnse, Thomas S. Jespersen, Joshua A. Folk, Charles M. Marcus, Karsten Flensberg, and Jason Alicea. Milestones toward majorana-based quantum computing. *Physical Review X*, 6:031016, August 2016.

[61] Bela Bauer, Torsten Karzig, Ryan V. Mishmash, Andrey E. Antipov, and Jason Alicea. Dynamics of majorana-based qubits operated with an array of tunable gates. *SciPost Physics*, 5(1):004, July 2018.

[62] M. V. Berry. Quantum phase corrections from adiabatic iteration. *Proceedings of the Royal Society of London. Series A, Mathematical and Physical Sciences*, 414(1846), 1987.

[63] P. W. Brouwer, M. Duckheim, A. Romito, and F. von Oppen. Probability Distribution of Majorana End-State Energies in Disordered Wires. *Physical Review Letters*, 107(19):196804, November 2011.

[64] Piet W. Brouwer, Mathias Duckheim, Alessandro Romito, and Felix von Oppen. Topological superconducting phases in disordered quantum wires with strong spin-orbit coupling. *Physical Review B*, 84(14):144526, October 2011.

[65] Wade DeGottardi, Diptiman Sen, and Smitha Vishveshwara. Majorana fermions in superconducting 1d systems having periodic, quasiperiodic, and disordered potentials. *Physical Review Letters*, 110:146404, April 2013.

[66] Suhas Gangadharaiah, Bernd Braunecker, Pascal Simon, and Daniel Loss. Majorana edge states in interacting one-dimensional systems. *Physical Review Letters*, 107:036801, July 2011.

[67] G. Goldstein and C. Chamon. Exact zero modes in closed systems of interacting fermions. *Physical Review B*, 86:115122, September 2012.

[68] R. B. Potts. Some generalized order-disorder transformations. *Mathematical Proceedings of the Cambridge Philosophical Society*, 48(1):106–109, 1952.

[69] R. J. Baxter. *Exactly solved models in statistical mechanics*. Academic Press, 1982.

[70] G. von Gehlen and V. Rittenberg. Z_n-symmetric quantum chains with an infinite set of conserved charges and Z_n zero modes. *Nuclear Physics B*, 257:351 – 370, 1985.

[71] Steven Howes, Leo P. Kadanoff, and Marcel Den Nijs. Quantum model for commensurate-incommensurate transitions. *Nuclear Physics B*, 215(2):169 – 208, 1983.

[72] H. Au-Yang and J. H. H. Perk. The Many Faces of the Chiral Potts Model. *International Journal of Modern Physics B*, 11:11–26, 1997.

[73] H. N. V. Temperley and E. H. Lieb. Relations between the 'percolation' and 'colouring' problem and other graph-theoretical problems associated with regular planar lattices: Some exact results for the 'percolation' problem. *Proceedings of the Royal Society of London. Series A, Mathematical and Physical Sciences*, 322(1549):251–280, 1971.

[74] S. Ostlund. Incommensurate and commensurate phases in asymmetric clock models. *Physical Review B*, 24:398–405, July 1981.

[75] David A. Huse. Simple three-state model with infinitely many phases. *Physical Review B*, 24:5180–5194, November 1981.

[76] David A. Huse, Anthony M. Szpilka, and Michael E. Fisher. Melting and wetting transitions in the three-state chiral clock model. *Physica A: Statistical Mechanics and its Applications*, 121(3):363 – 398, 1983.

[77] Giuseppe Albertini, Barry M. McCoy, and Jacques H.H. Perk. Level crossing transitions and the massless phases of the superintegrable chiral Potts chain. *Physics Letters A*, 139(5):204 – 212, 1989.

[78] E. Fradkin and L. P. Kadanoff. Disorder variables and para-fermions in two-dimensional statistical mechanics. *Nucl. Phys. B*, 170(1):1–15, 1980.

[79] D. J. Clarke, J. Alicea, and K. Shtengel. Exotic non-Abelian anyons from conventional fractional quantum Hall states. *Nat. Comm.*, 4:1348, January 2013.

[80] J. Motruk, E. Berg, A. M. Turner, and F. Pollmann. Topological phases in gapped edges of fractionalized systems. *Physical Review B*, 88(8):085115, August 2013.

[81] P. Fendley. Free parafermions. *J. Phys. A Math. Theor.*, 47(7):075001, February 2014.

[82] E. Cobanera and G. Ortiz. Fock parafermions and self-dual representations of the braid group. *Physical Review A*, 89:012328, January 2014.

[83] Claude Bloch. Sur la théorie des perturbations des états liés. *Nucl. Phys.*, 6:329 – 347, 1958.

[84] A. Messiah. *Quantum Mechanics*. North Holland, Amsterdam, 1962. Chap. 16, Secs. 15-17.

[85] P. O. Löwdin. Studies in perturbation theory. iv. solution of eigenvalue problem by projection operator formalism. *J. Math. Phys.*, 3(5):969–982, 1962.

[86] Isaiah Shavitt and Rodney J Bartlett. *Many-body methods in chemistry and physics: MBPT and coupled-cluster theory*. Cambridge university press, 2009.

[87] P. O. Löwdin. A note on the quantum-mechanical perturbation theory. *J. Chem. Phys.*, 19(11):1396–1401, 1951.

[88] B. H. Brandow. Linked-Cluster Expansions for the Nuclear Many-Body Problem. *Rev. Mod. Phys.*, 39:771–828, October 1967.

[89] B. Tang, E. Khatami, and M. Rigol. A short introduction to numerical linked-cluster expansions. *Comp. Phys. Comm.*, 184:557–564, March 2013.

[90] Alessio Calzona, Tobias Meng, Maura Sassetti, and Thomas L. Schmidt. F_4 parafermions in one-dimensional fermionic lattices. *Physical Review B*, 98:201110, November 2018.

[91] Man-Duen Choi. Positive linear maps on C^*-algebras. *Canadian Journal of Mathematics*, 24(3):520–529, 1972.

[92] A. Jamiołkowski. Linear transformations which preserve trace and positive semidefiniteness of operators. *Reports on Mathematical Physics*, 3(4):275 – 278, 1972.

[93] Gernot Shaller. *Open Quantum Systems Far from Equilibrium*. Springer, 2014.

[94] C E Soliverez. An effective hamiltonian and time-independent perturbation theory. *Journal of Physics C: Solid State Physics*, 2(12):2161–2174, December 1969.

[95] D. J. Klein. Degenerate perturbation theory. *The Journal of Chemical Physics*, 61(3):786–798, 1974.

[96] A. A. Ovchinnikov, D. V. Dmitriev, V. Ya. Krivnov, and V. O. Cheranovskii. Antiferromagnetic Ising chain in a mixed transverse and longitudinal magnetic field. *Physical Review B*, 68(21):214406, December 2003.

[97] Amit Dutta, Gabriel Aeppli, Bikas K. Chakrabarti, Uma Divakaran, Thomas F. Rosenbaum, and Diptiman Sen. *Quantum Phase Transitions in Transverse Field Spin Models: From Statistical Physics to Quantum Information*. Cambridge University Press, 2015.

[98] Gene H. Golub and Charles F. Van Loan. *Matrix Computations (3rd Ed.)*. Johns Hopkins University Press, Baltimore, MD, USA, 1996.

[99] Stephan Plugge, Asbjørn Rasmussen, Reinhold Egger, and Karsten Flensberg. Majorana box qubits. *New Journal of Physics*, 19(1):012001, Jan 2017.

[100] Torsten Karzig et al. Scalable designs for quasiparticle-poisoning-protected topological quantum computation with Majorana zero modes. *Physical Review B*, 95:235305, June 2017.

[101] Daniel Litinski and Felix von Oppen. Quantum computing with Majorana fermion codes. *Physical Review B*, 97:205404, May 2018.

[102] S. A. Parameswaran, Andrew C. Potter, and Romain Vasseur. Eigenstate phase transitions and the emergence of universal dynamics in highly excited states. *Annalen der Physik*, 529(7):1600302, July 2017.

[103] Bela Bauer and Chetan Nayak. Area laws in a many-body localized state and its implications for topological order. *Journal of Statistical Mechanics: Theory and Experiment*, 2013(9):09005, September 2013.